The 7th International Workshop on Very High Energy Particle Astronomy: 19-20 March 2014, Kashiwa, Japan

X-ray and Gamma-ray Observations of Cosmic-Ray Accelerators

Yasunobu Uchiyama (Rikkyo University)

The 7th International Workshop on Very High Energy Particle Astronomy: 19-20 March 2014, Kashiwa, Japan

X-ray and Gamma-ray Observations of Galactic Cosmic-Ray Accelerators

Yasunobu Uchiyama (Rikkyo University)

X-ray Satellites in Orbit

ACIS: X-ray CCD camera
- energy range: 0.2 – 10 keV
- field of view: 16.9’ x 16.9’ (ACIS-I)
- angular resolution: **0.5”**
- energy resolution: 150~300 eV @6 keV

YU is a member of Chandra User Committee

XIS: X-ray CCD camera
- energy range: 0.2 – 10 keV
- field of view: 17.8’ x 17.8’
- angular resolution: 2’
- energy resolution: 130 eV @6 keV

HXD: Hard X-ray Detector
- energy range: 10 – 600 keV
- low background

1. ASTRO-H Mission (Launch in 2015)

PI: T. Takahashi (ISAS/JAXA)

ASTRO-H is an international X-ray observatory, which is the 6th in the series of the X-ray observatories from Japan. More than 160 scientists from Japan/US/Europe/Canada.

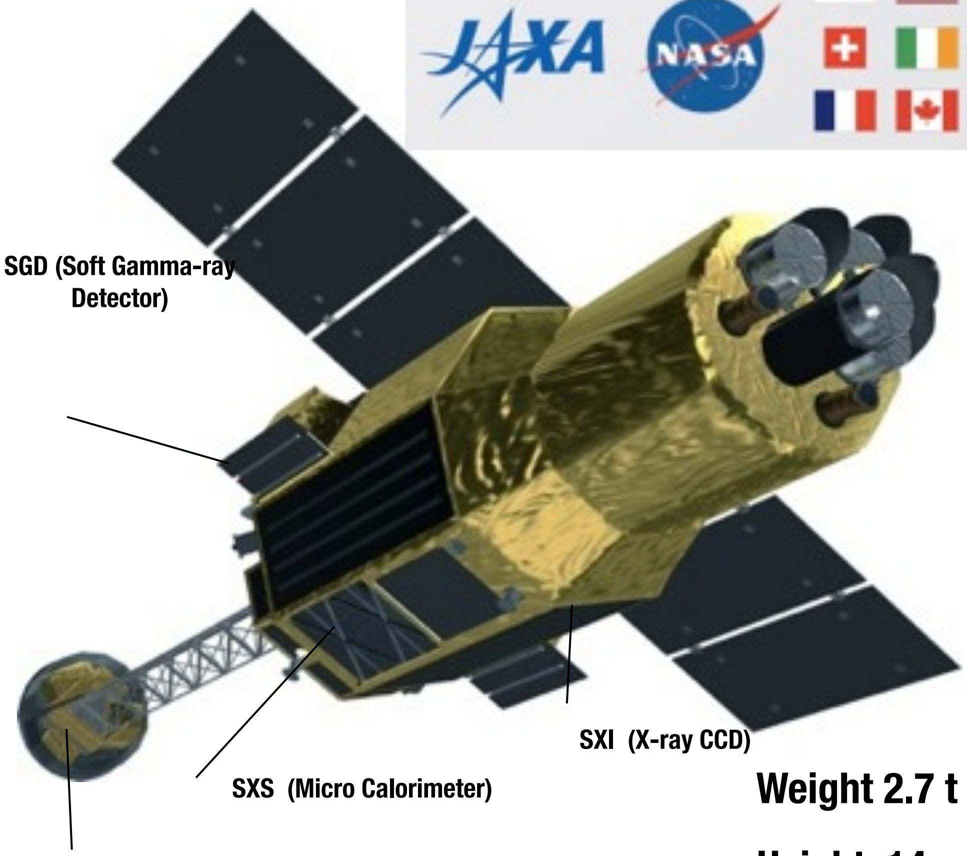

Weight 2.7 t

Height 14 m

- Launch site: Tanegashima Space Center, Japan
- Launch vehicle: JAXA H-IIA rocket
- Orbit Altitude: 550km
- Orbit Type: Approximate circular orbit
- Orbit Inclination: ~31 degrees
- Orbit Period: 96 minutes
- Launch : 2015

US Participation

NASA (US PI: Rich Kelley)
- Micro Calorimeter Array/ADR
- Two soft X-ray Telescopes
- Eight Science Advisors
- Pipeline Analysis

Science operations will be similar to those of Suzaku, with pointed observation of each target until the integrated observing time is accumulated, and then slewing to the next target.

Fermi Gamma-ray Space Telescope

Large Area Telescope (LAT)

energy range: **0.2 – 300 GeV**

field of view: **2.4 str**

angular resolution:

~ 1 deg @ 1 GeV

~ 0.1 deg >10 GeV

YU is a coordinator of the SNR/PWN working group

LAT sensitivity

for various exposures ➜

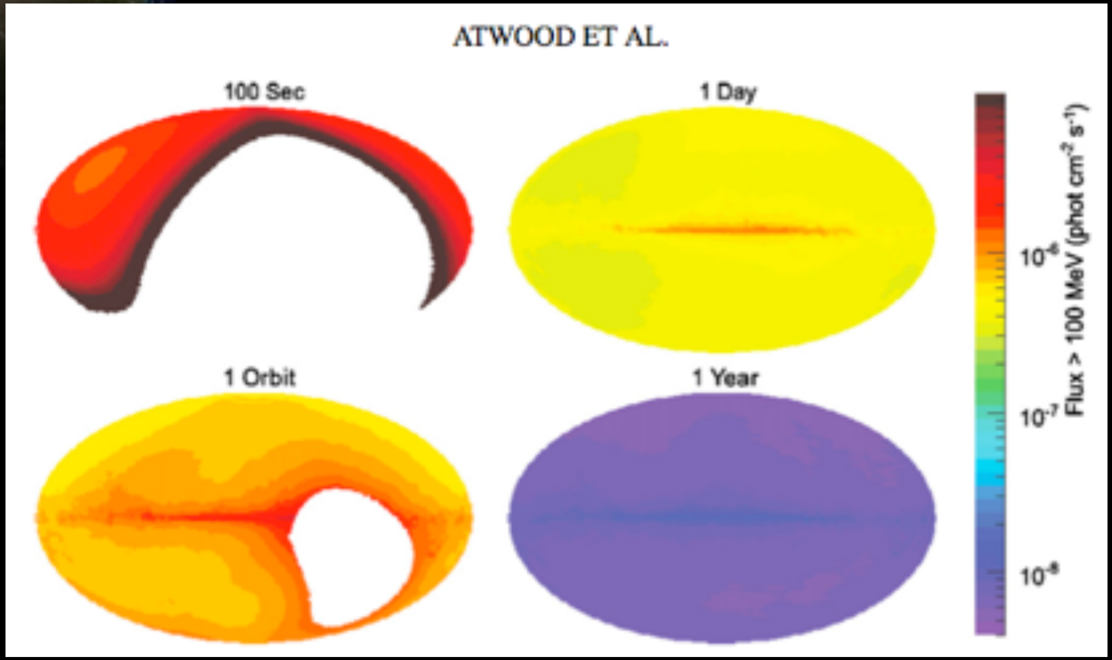

Milky Way in Gamma Rays

Galactic CRs (p/e) produce γ-rays:

- **π^0-decay γ-rays (CR p + H → π^0 → 2γ)**
- **bremsstrahlung/inverse Compton scattering by CR e**

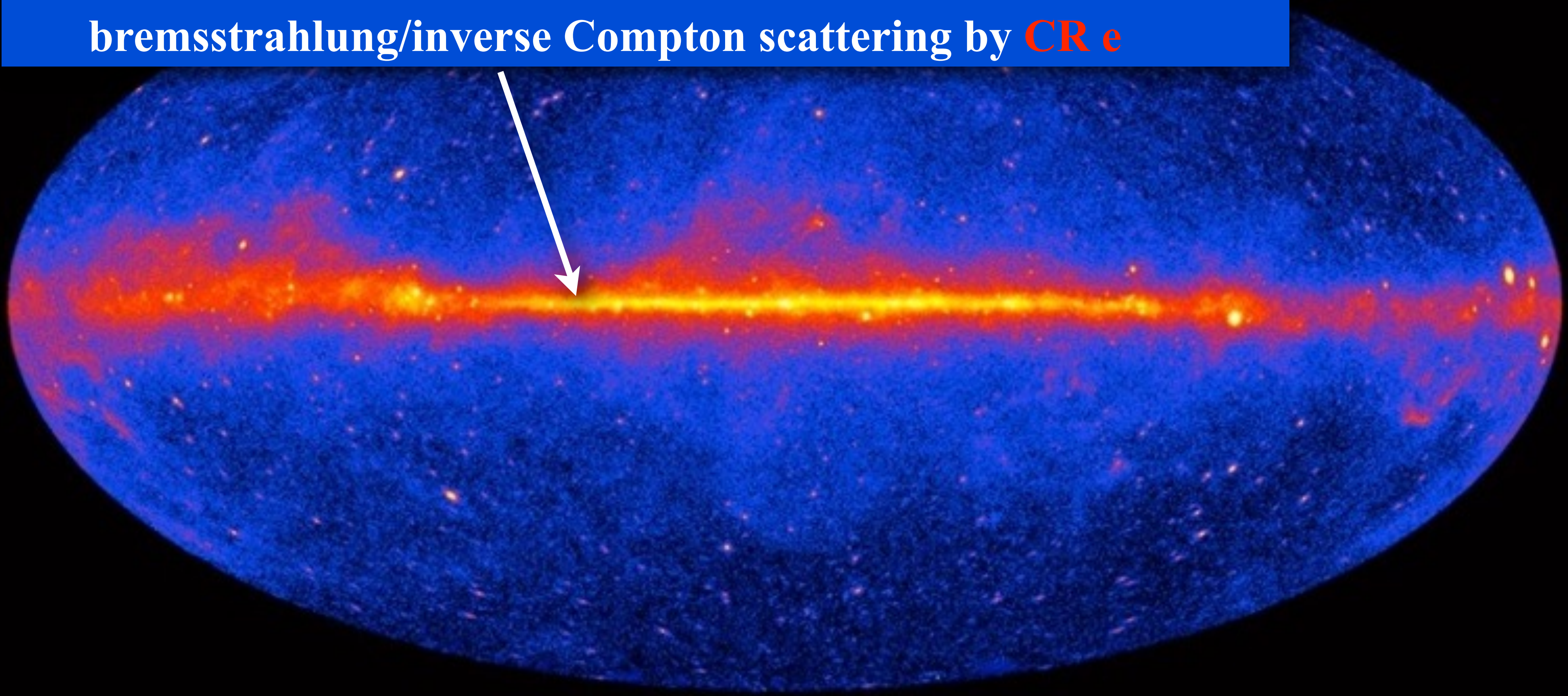

All sky γ-ray map made by Fermi Gamma-ray Space Telescope

Galactic Diffuse Emission

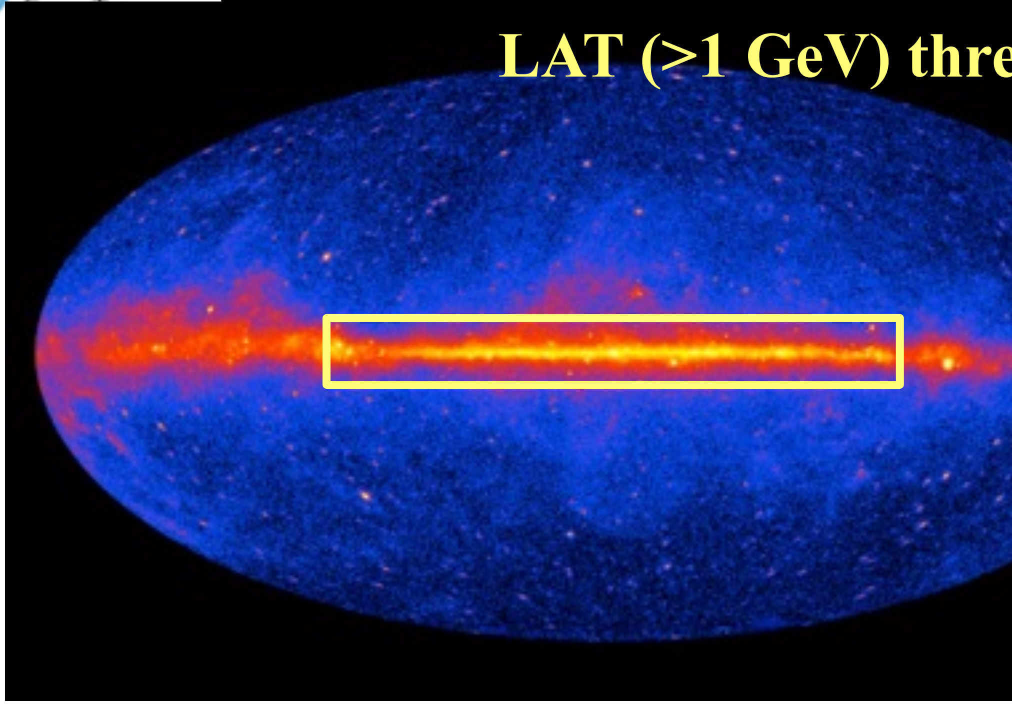

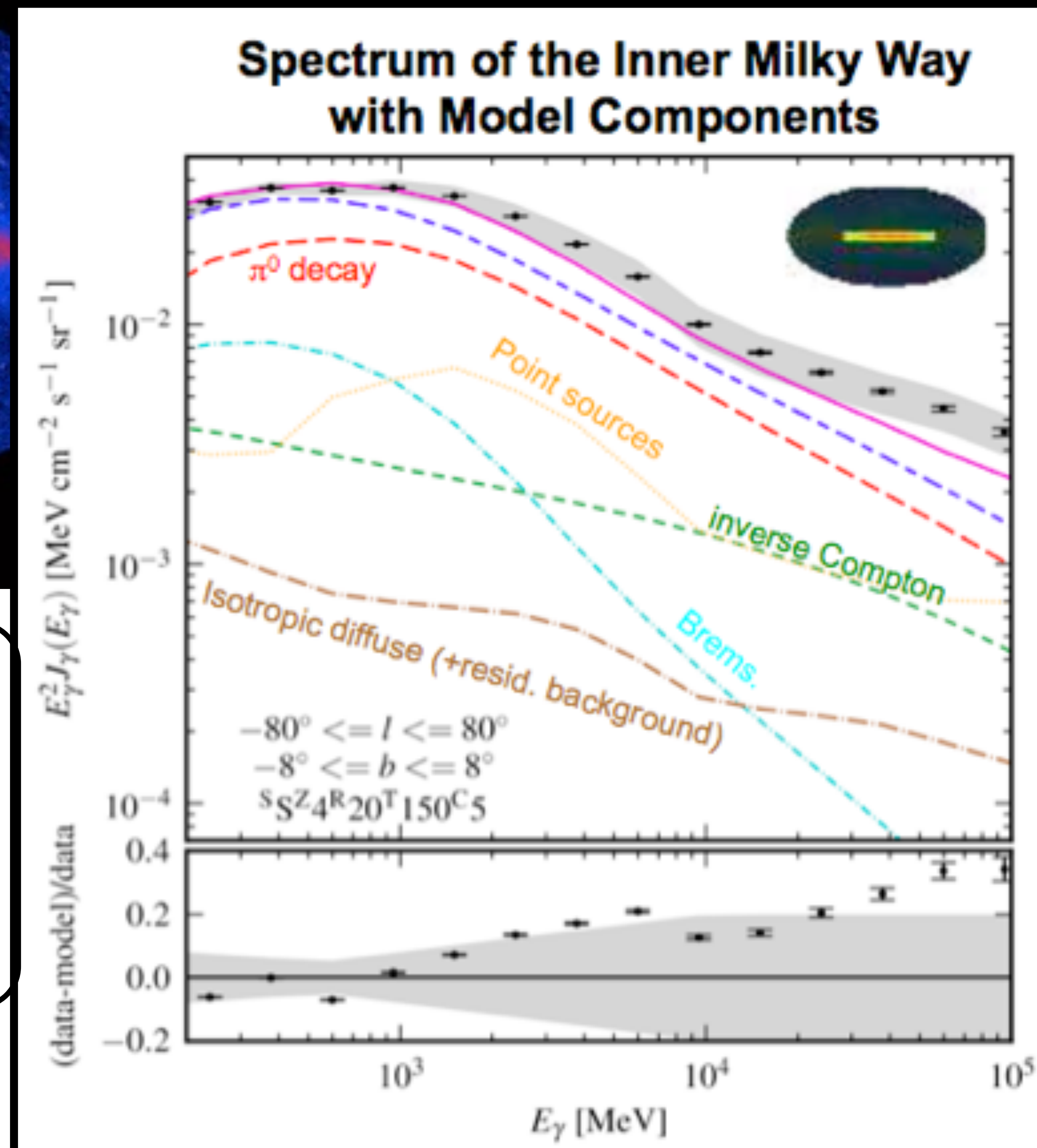

Ackermann et al. (2012)

Hadronic:

π^0-decay γ-rays   CR p + H → π^0 → 2γ

Leptonic:

bremsstrahlung   CR e + H → γ

Inverse Compton   CR e + γ → γ

Galactic diffuse emission

– the distribution of interstellar gas; and

– the distribution of Galactic cosmic rays

"Fermi Bubbles"

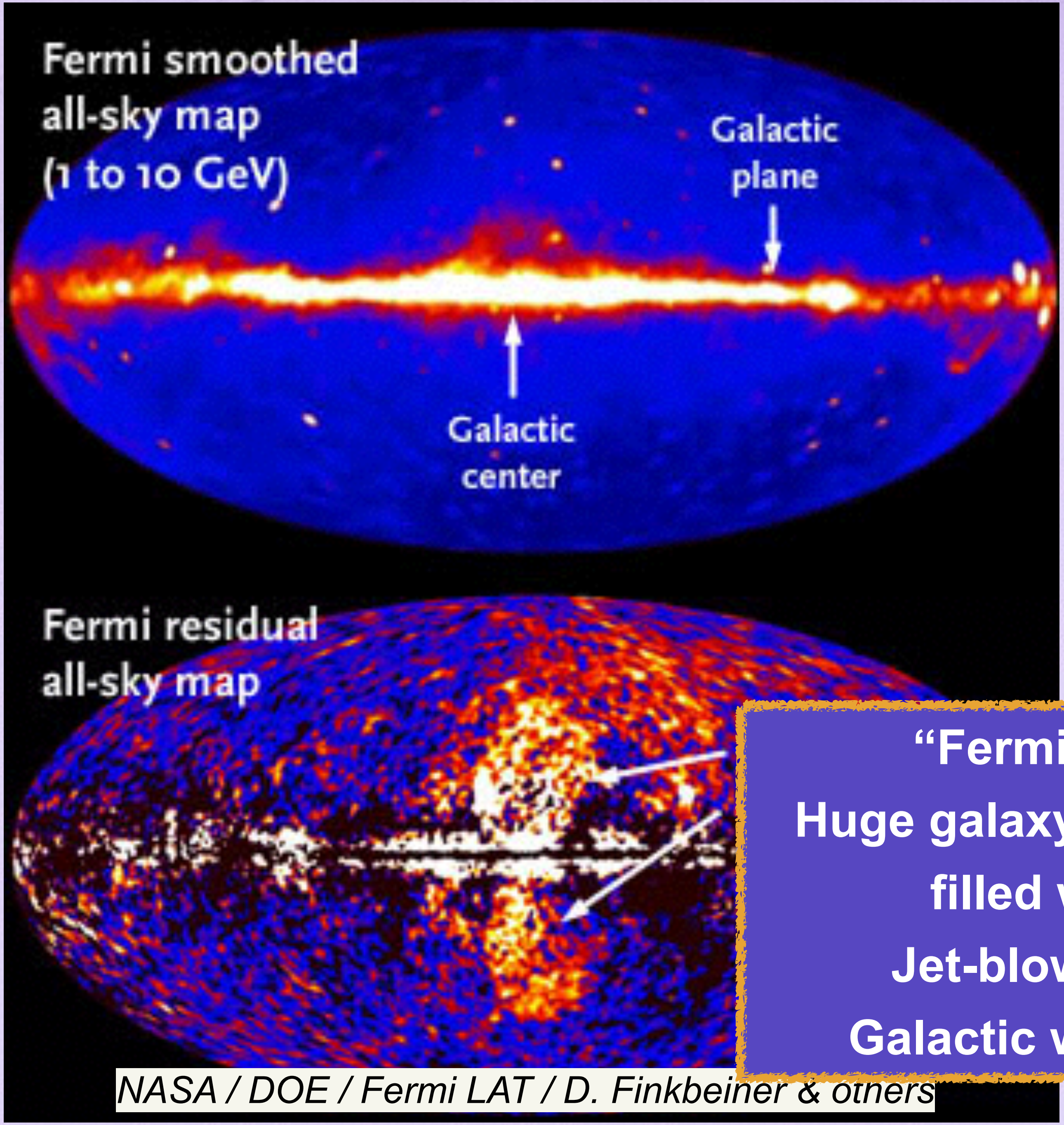

NASA / DOE / Fermi LAT / D. Finkbeiner & others

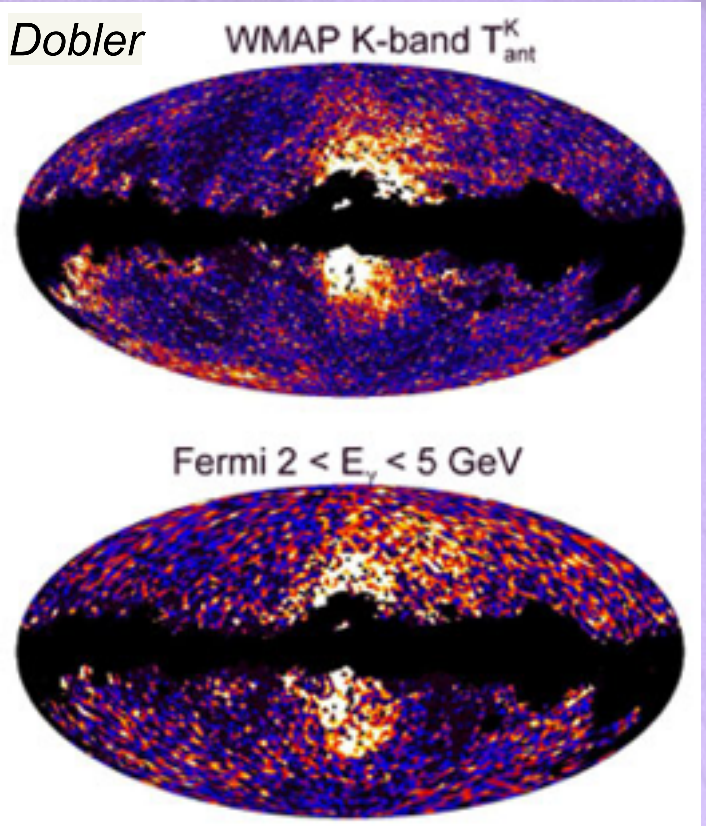

Dobler

"Fermi Bubbles"
Huge galaxy-scale bubbles filled with CRs:
Jet-blown bubble?
Galactic wind bubble?

“Fermi Bubbles”: of hadronic origin?

“Fermi Bubbles” luminosity

~ 4×10^{37} erg/s (1−100 GeV)

~ 10× WMAP haze

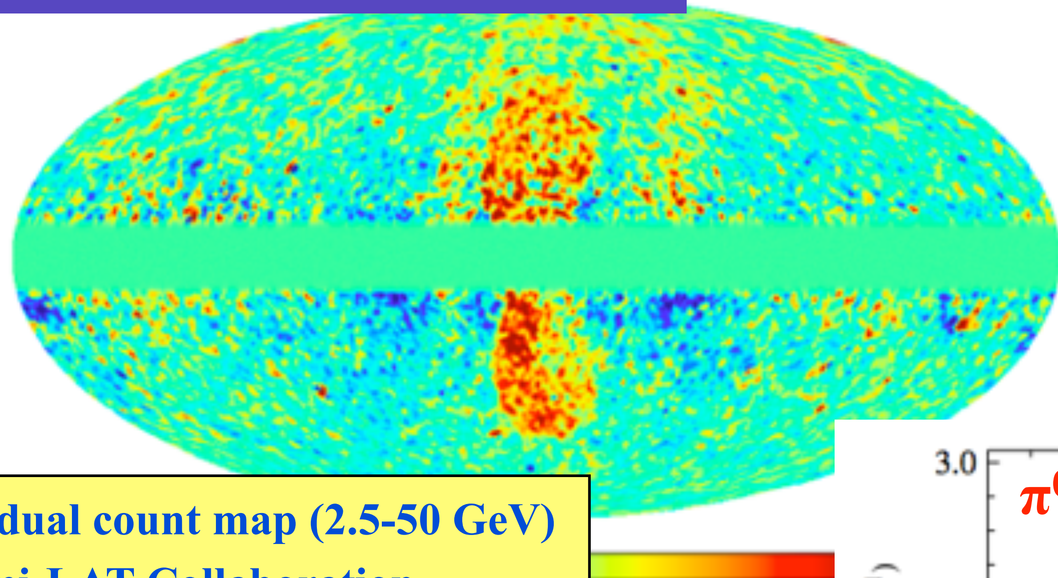

Residual count map (2.5-50 GeV)
Fermi-LAT Collaboration

FBs are giant reservoirs of Galactic Center CRs:

L_{SN} (GC) ∼ 1×10^{40} erg/s

➜ L_{CR} (GC) ∼ 1×10^{39} erg/s

If this CR injection occurs for a period of > t_{pp} ∼ 5 Gyr, the observed gamma-ray luminosity can be explained.

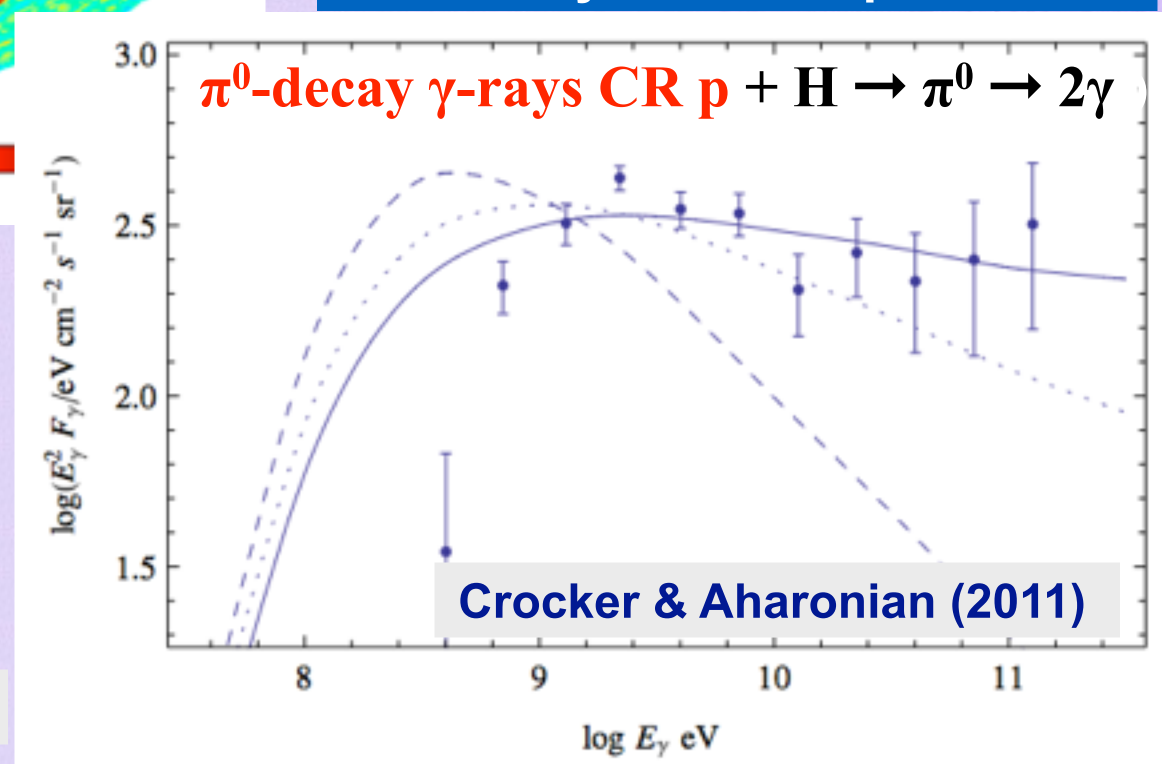

The hadronic model predicts **neutrinos**:

∼100 events (∼300 BGD events)

for the KM3NeT Detector (1yr)

The KM3NeT Collaboration (2012)

Supernova Remnants (SNRs)

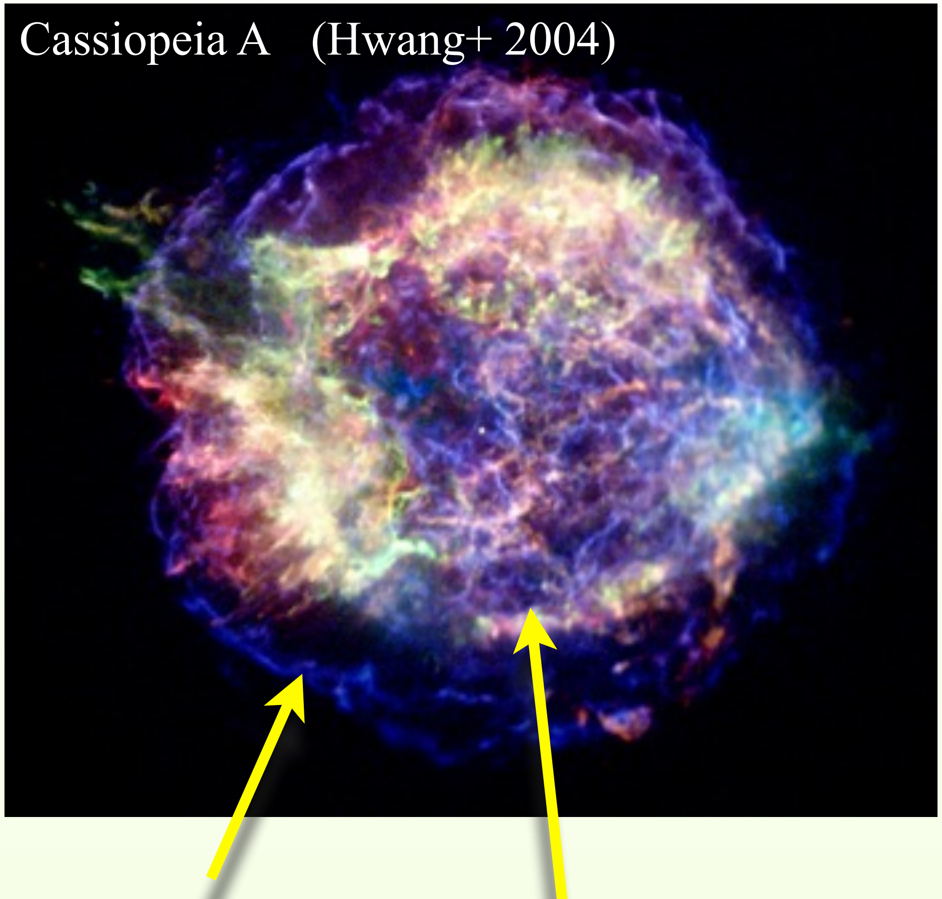

Nucleosynthesis

- X-ray lines (**ASTRO-H SXS**)
- SN types, progenitors
- Explosion mechanisms
- Origin of heavy elements

Cosmic-ray Acceleration

- Synchrotron x-rays (**ASTRO-H SXI-HXI**)
- Diffusive Shock Acceleration (DSA)
- Magnetic Field Amplification (MFA)
- Origin of gamma-rays
- Origin of Galactic cosmic rays

Well-known conditions:
Age, shock velocity, density, B-field, etc.

Detailed multi-wavelength observations:
morphology, variability, polarization, etc.

Physics of Collisionless Shock

Heating

Acceleration

Thermal ions kT*i*

Coulomb + Plasma waves

Thermal electrons kT*e*

Fermi Acceleration

CR back pressure

Cosmic Rays:
ions and electrons

Amplification

Cooling

Turbulent B-fields

kT*i* > kT*e*
in young SNRs

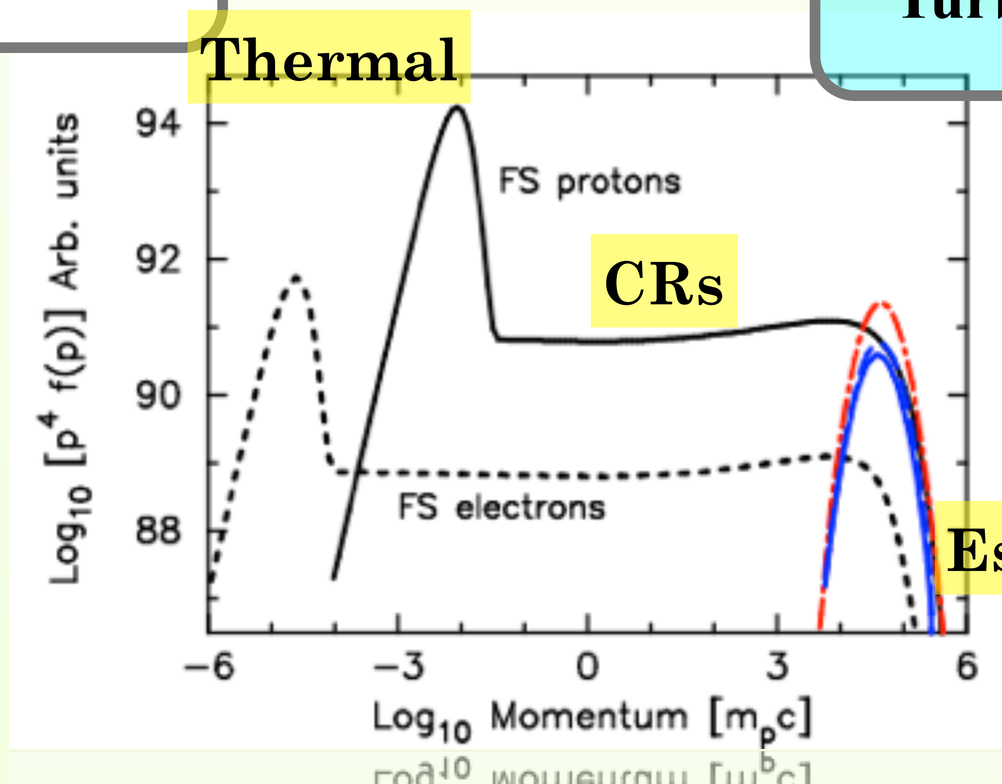

Evidence for Collisionless Electron Heating

Yamaguchi+13

Tycho's SNR

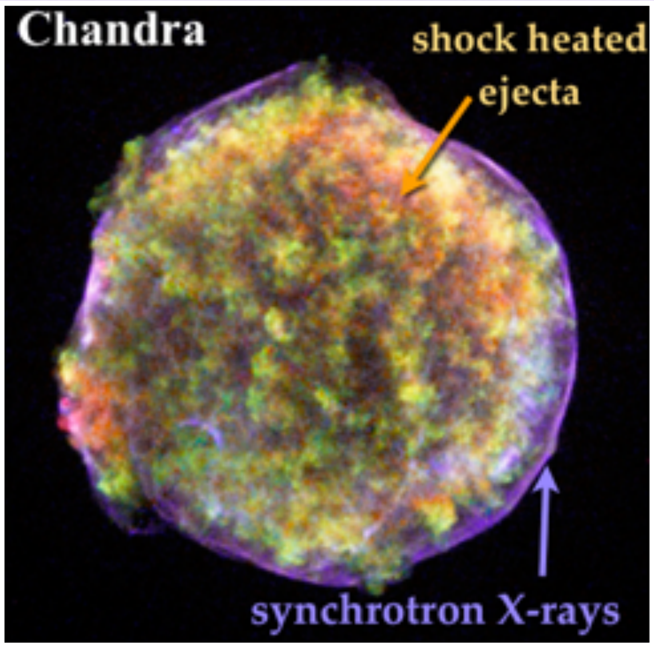

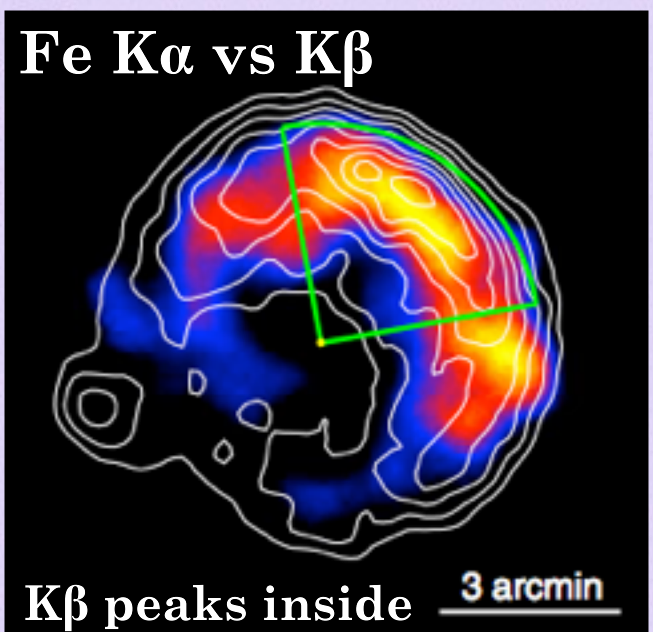

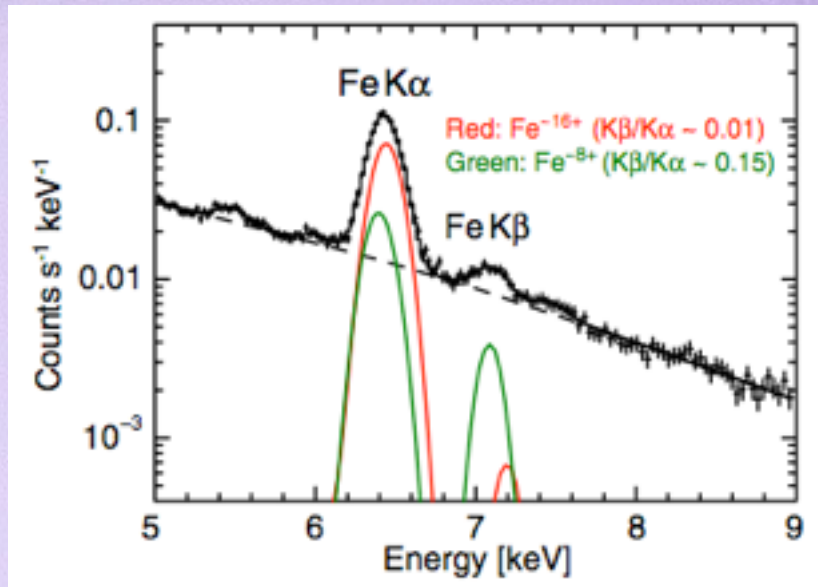

Kα: Fe 16+

Kβ: Fe 8+

(low ionization)

$\beta \equiv T_e/T_{Fe}$

$\beta = 10^{-5}$:

pure Coulomb heating

$\beta = 0.01$

(collisionless heating)

can reproduce the

Suzaku observations.

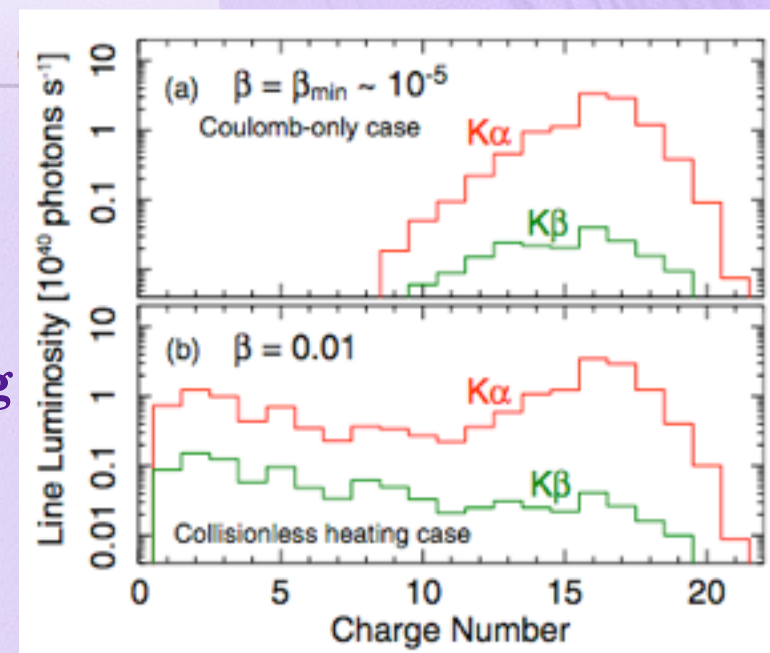

ASTRO-H Science

Physics of Collisionless Shock

Heating

Thermal ions kT_i

Coulomb + Plasma waves

Thermal electrons kT_e

$kT_i > kT_e$
in young SNRs

Fermi Acceleration

CR back pressure

Acceleration

Cosmic Rays:
ions and electrons

Amplification

Cooling

Turbulent B-fields

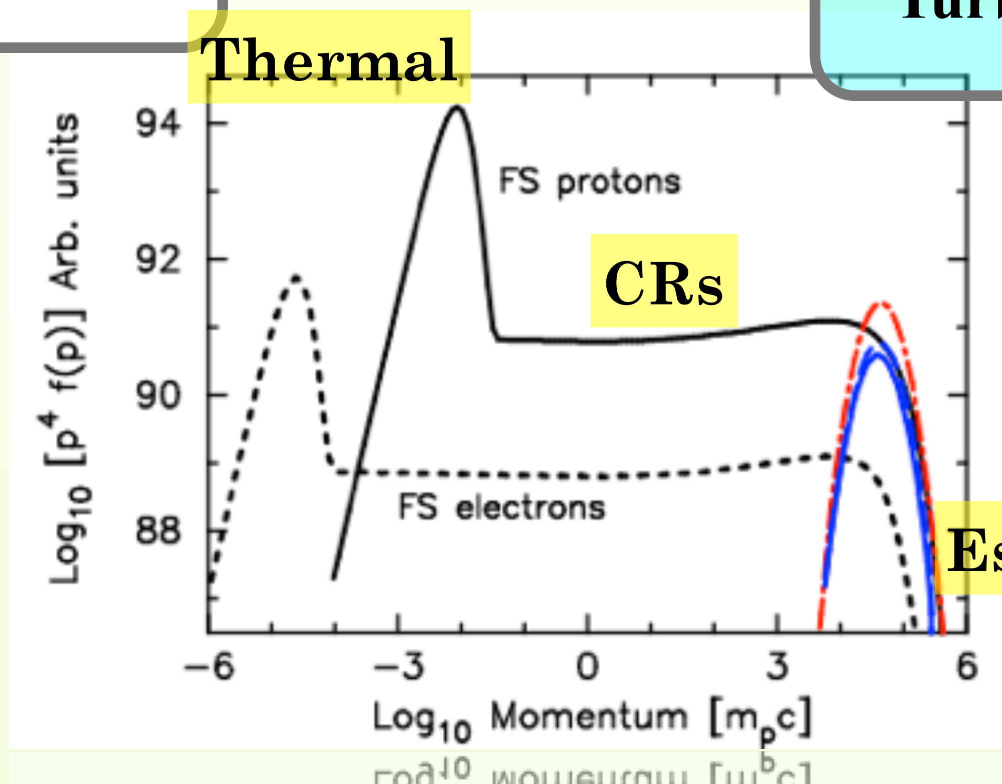

Diffusive Shock Acceleration (DSA)

Big Problem: **"injection"**
How thermal (Maxwellian) particles can be injected into Fermi acceleration?
➔ Energy transferred to CRs

Protons are expected to carry most CR energy, but they were difficult to observe.

Big Problem: **"escape"**
How highest energy particles escape from a shock?
➔ Maximum attainable energy
(key: "self-generated" MHD waves)

Protons : E_{max} limited by escape
Electrons : E_{max} limited by radiative loss

(1) "Injection" → Energy transferred to CRs

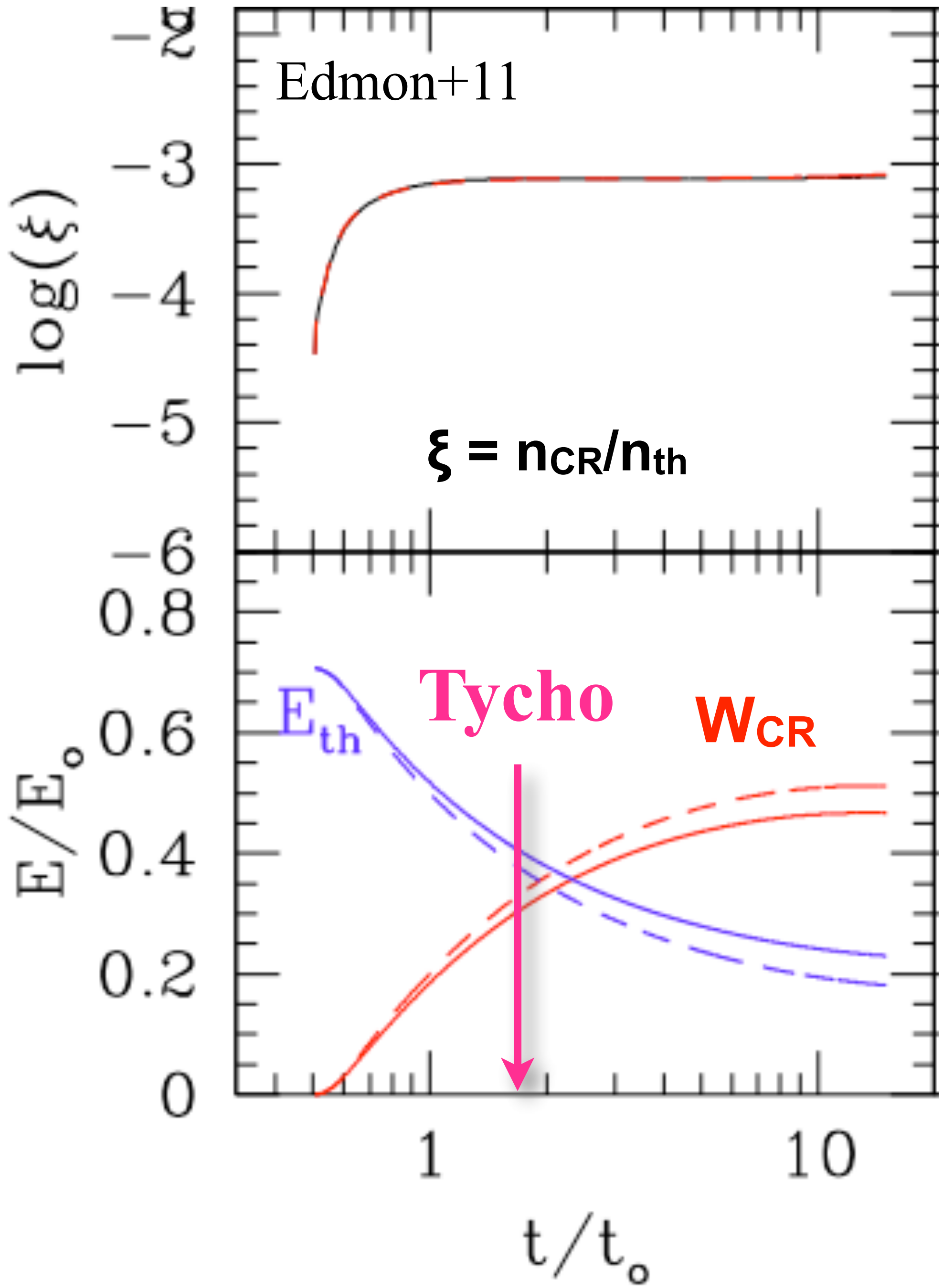

$\xi = n_{CR}/n_{th}$ = CR particles / thermal particles

"ad hoc" ξ is assumed to be constant

From the gamma-ray data, the amount of CRs in Tycho's SNR at its age of t = 439 yr is:

$W_{CR} \sim 7\%$ of E_{SN}

↓

W_{CR} will reach 14% of E_{SN}

Supporting SNR origin of Galactic CRs

(2) "Escape" → Maximum Energy

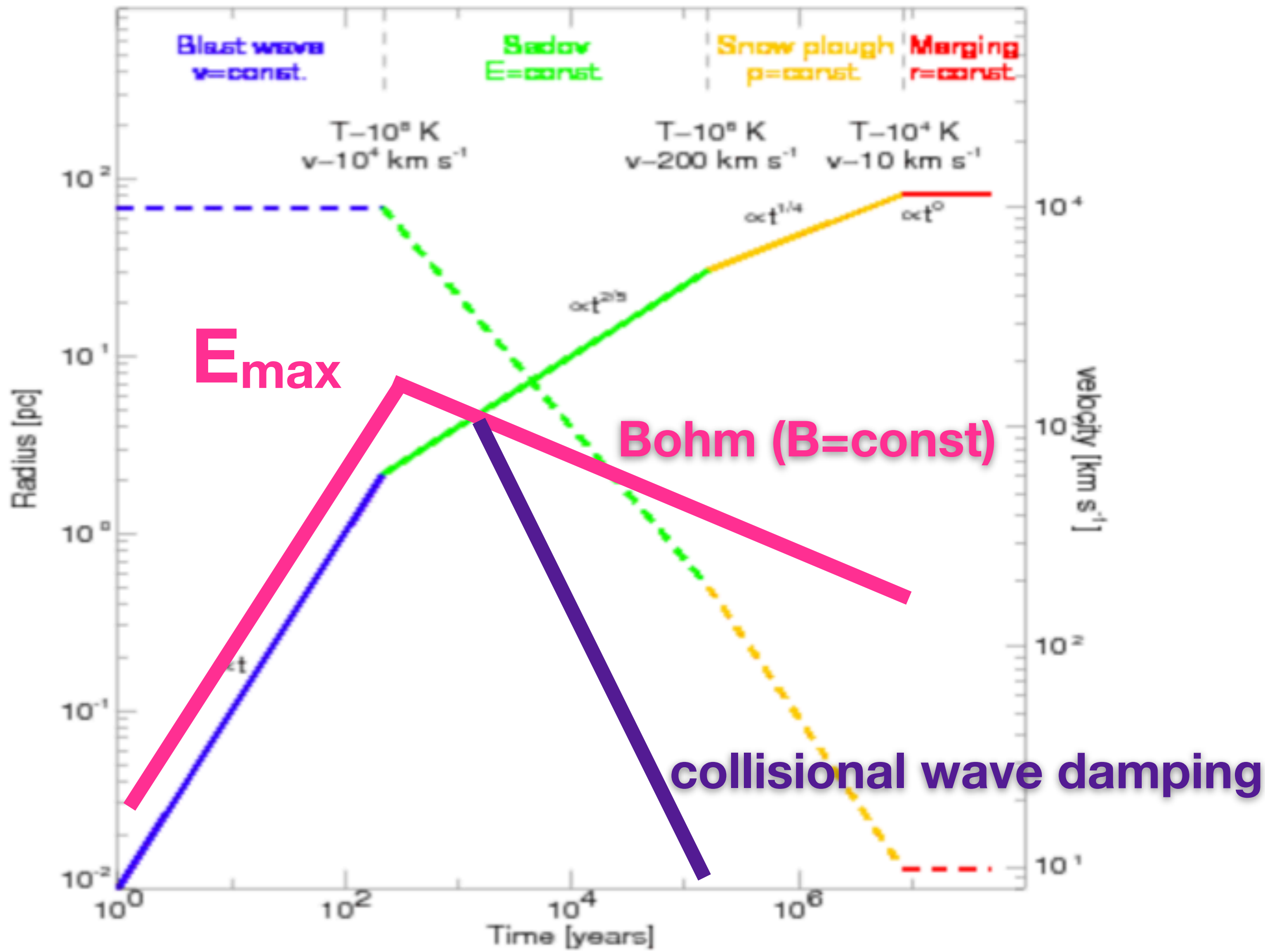

Cutoff from ion-neutral wave damping (e.g. Drury+ 1996)

$$E_{\max} \approx u_{0,7}^{3} T_{4}^{-0.4} n_{n}^{-1} n_{i}^{0.5} \xi_{\mathrm{CR},-1}\ \mathrm{GeV}$$

Origin: loss of CR trapping power
→ enhanced escape in partially ionized medium

π^0-decay γ-rays: Direct Probe of Accelerated Protons

$dN_\gamma/d\varepsilon$:
symmetric
about 68 MeV

→

$\varepsilon^2\, dN_\gamma/d\varepsilon$:
hard spectrum below 300 MeV

γ-ray spectrum: dN/dε

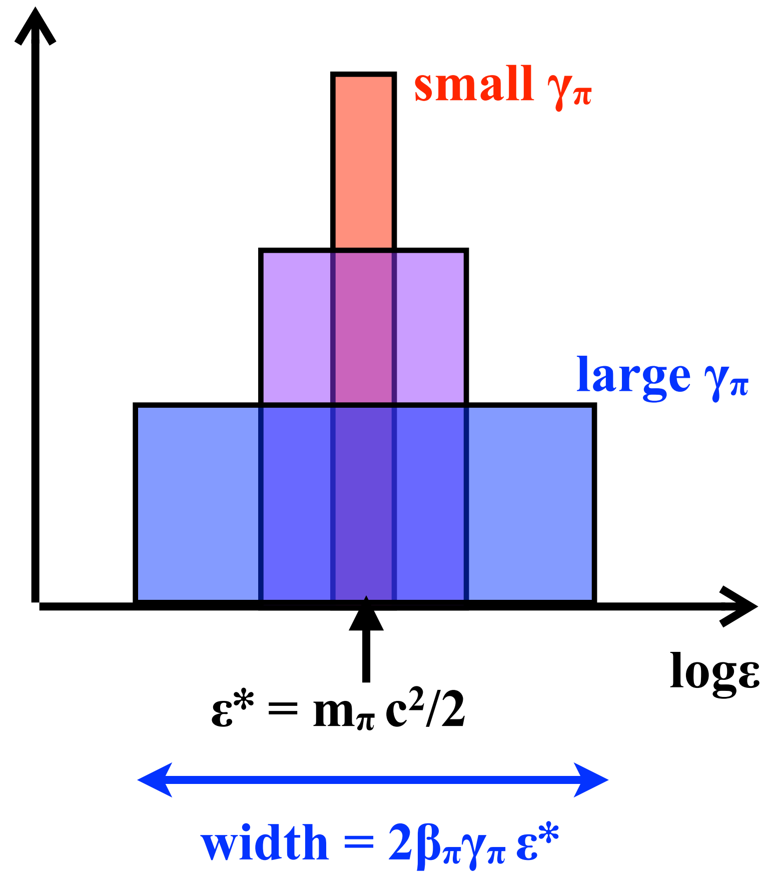

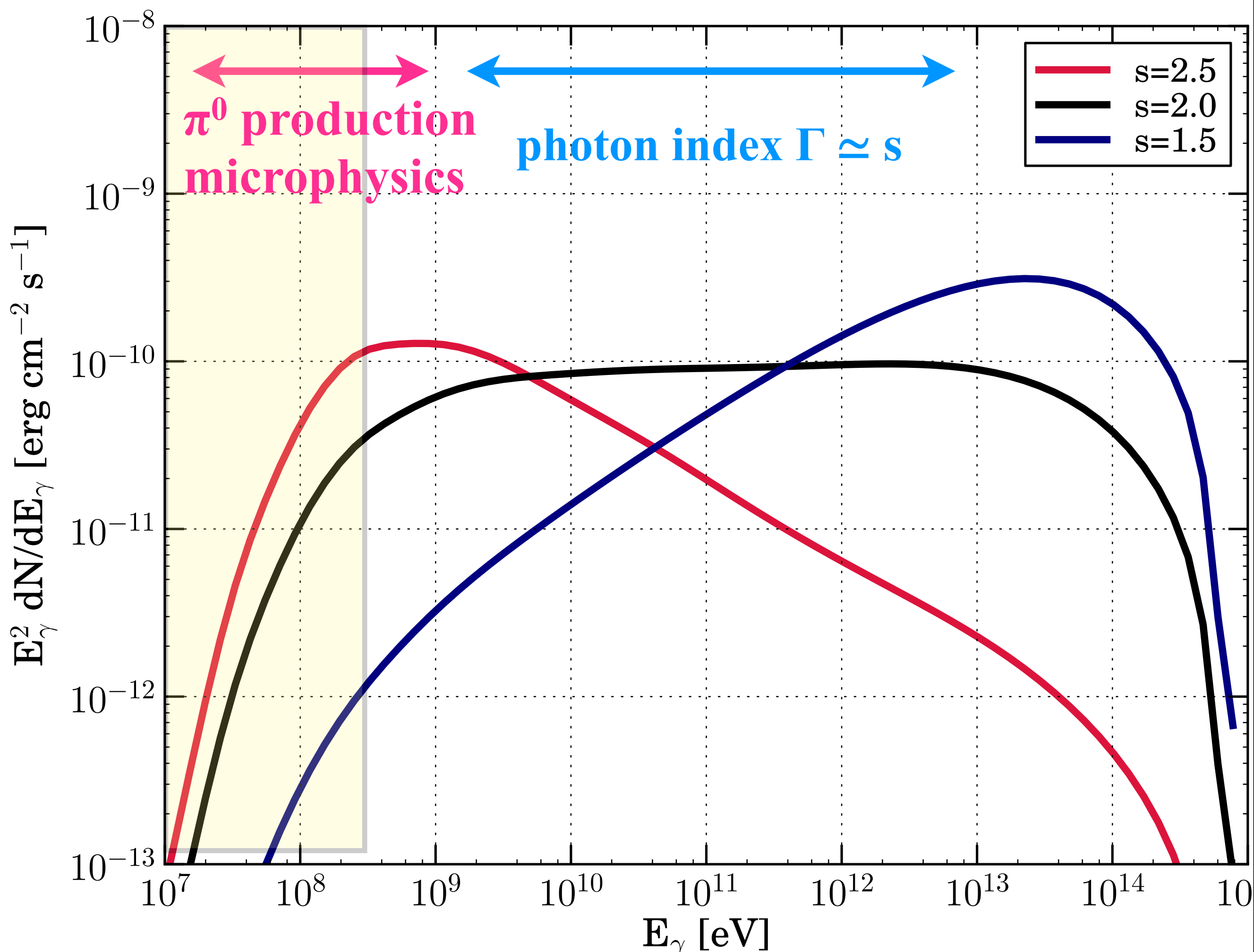

Very hard spectrum below 300 MeV for any reasonable proton index

Hard X-rays & Neutrinos as “Hadronic” Messengers

cf Aharonian (2004)

CR p + p → π + anything

- $\pi^0 \rightarrow 2\gamma$
- $\pi^{+/-} \rightarrow \mu^{+/-} + \nu_\mu$
  $\mu^{+/-} \rightarrow e^{+/-} + \nu_e + \nu_\mu$

Direct link between γ-ray and neutrino astronomy

Deep link between X-ray and γ-ray astronomy

Synchrotron radiation by secondary e-/e+ produced at interactions of PeV-EeV protons with ambient gas or photons.

$$p + p \rightarrow \pi^\pm \rightarrow \mu^\pm \rightarrow e^\pm \xrightarrow[B]{} \gamma \text{ (hard X-ray)}$$

Also, VHE protons can collide with photons:

$$p + \gamma \rightarrow \pi^\pm \rightarrow \mu^\pm \rightarrow e^\pm \xrightarrow[B]{} \gamma \text{ (hard X-ray)}$$

$$p + \gamma \rightarrow e\text{-}e\text{+} \xrightarrow[B]{} \gamma \text{ (hard X-ray)}$$

Sensitive hard X-ray observations with ASTRO-H HXI can probe the highest energy CR protons in SNRs and galaxy clusters.

Transparency of γ-rays (& protons) in the Universe

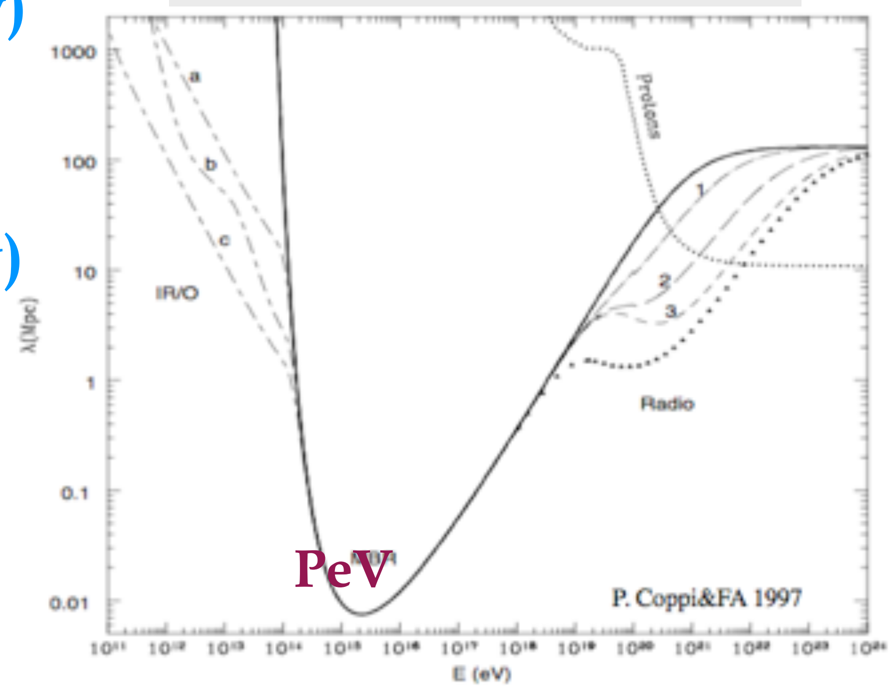

PeV protons in SNRs

EeV protons in Galaxy Clusters

Young SNRs with 3 PeV protons:

Radiation from secondaries

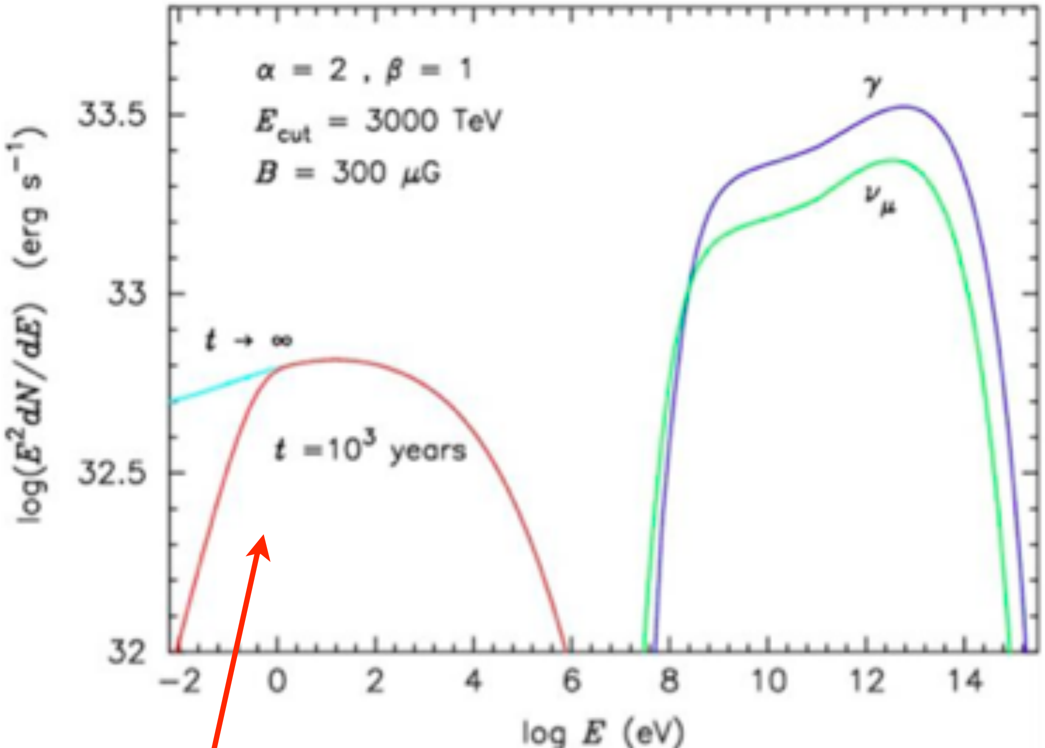

synchrotron by secondary $e^{\pm}$ **:**
(synchrotron by primary electrons with an unavoidable cutoff of $h\nu_0 \sim 1$ **keV is expected to be steep at hard X-rays.)**

Galaxy Clusters with strong accretion shocks

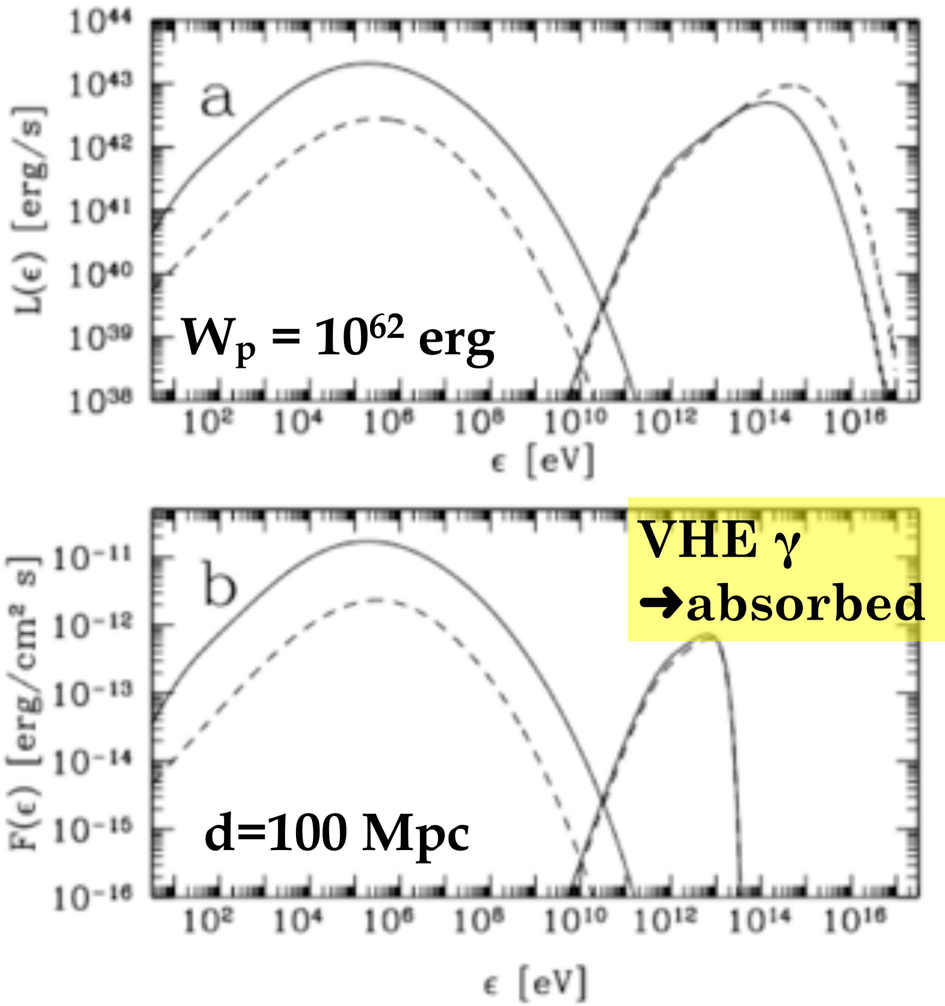

Vannoni+2011

Fermi Observations of SNRs

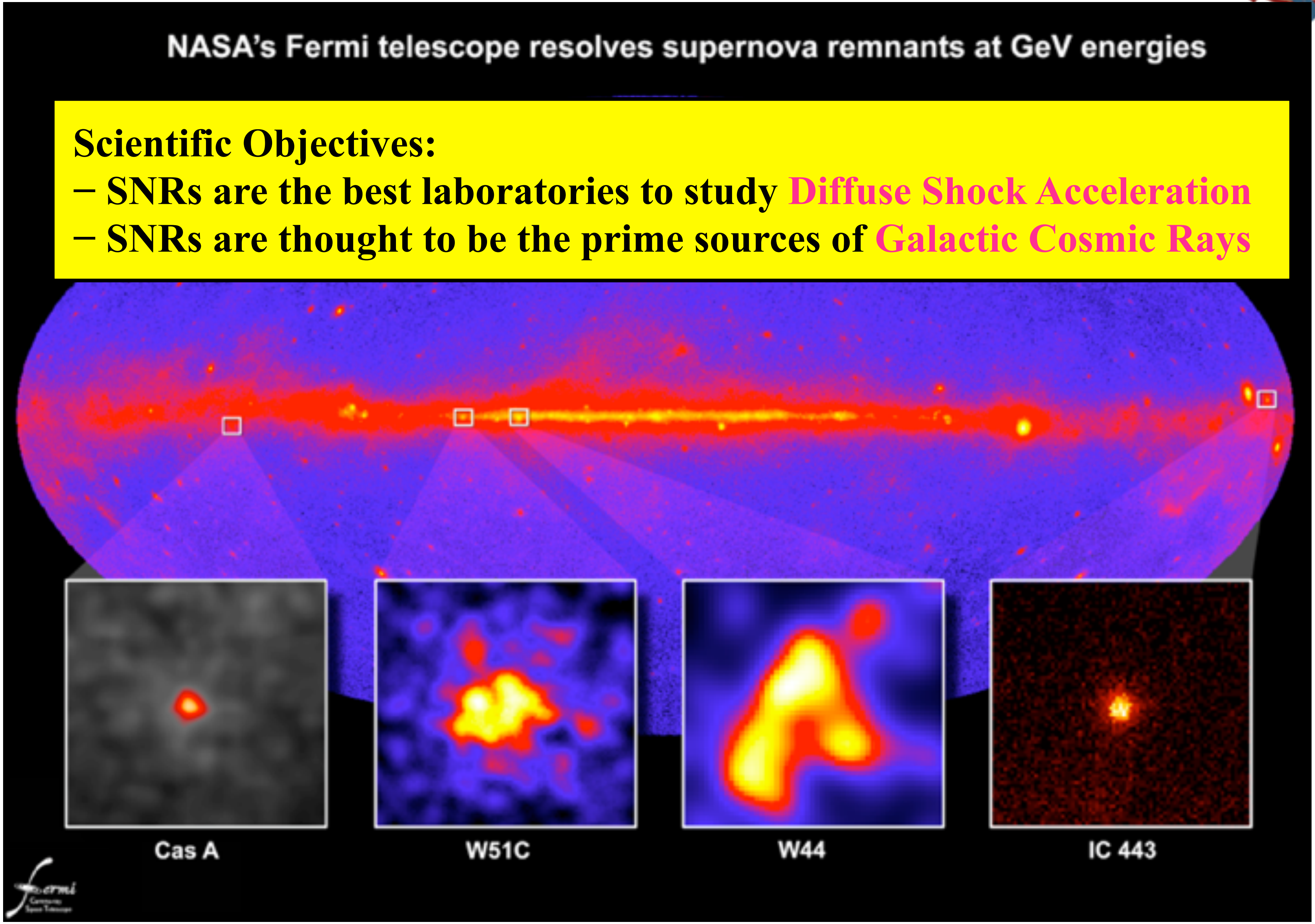

Detection of the Characteristic Pion-Decay Signature in Supernova Remnants

CA: Funk, Tanaka, Uchiyama

M. Ackermann,[1] M. Ajello,[2] A. Allafort,[3] L. Baldini,[4] J. Ballet,[5] G. Barbiellini,[6,7] M. G. Baring,[8] D. Bastieri,[9,10] K. Bechtol,[3] R. Bellazzini,[11] R. D. Blandford,[3] E. D. Bloom,[3] E. Bonamente,[12,13] A. W. Borgland,[3] E. Bottacini,[3] T. J. Brandt,[14] J. Bregeon,[11] M. Brigida,[15,16] P. Bruel,[17] R. Buehler,[3] G. Busetto,[9,10] S. Buson,[9,10] G. A. Caliandro,[18] R. A. Cameron,[3] P. A. Caraveo,[19] J. M. Casandjian,[5] C. Cecchi,[12,13] Ö. Çelik,[14,20,21] E. Charles,[3] S. Chaty,[5] R. C. G. Chaves,[5] A. Chekhtman,[22] C. C. Cheung,[23] J. Chiang,[3] G. Chiaro,[24] A. N. Cillis,[14,25] S. Ciprini,[13,26] R. Claus,[3] J. Cohen-Tanugi,[27] L. R. Cominsky,[28] J. Conrad,[29,30,31] S. Corbel,[5,32] S. Cutini,[33] F. D'Ammando,[12,34,35] A. de Angelis,[36] F. de Palma,[15,16] C. D. Dermer,[37] E. do Couto e Silva,[3] P. S. Drell,[3] A. Drlica-Wagner,[3] L. Falletti,[27] C. Favuzzi,[15,16] E. C. Ferrara,[14] A. Franckowiak,[3] Y. Fukazawa,[38] S. Funk,[3*] P. Fusco,[15,16] F. Gargano,[16] S. Germani,[12,13] N. Giglietto,[15,16] P. Giommi,[33] F. Giordano,[15,16] M. Giroletti,[39] T. Glanzman,[3] G. Godfrey,[3] I. A. Grenier,[5] M.-H. Grondin,[40,41] J. E. Grove,[37] S. Guiriec,[14] D. Hadasch,[18] Y. Hanabata,[38] A. K. Harding,[14] M. Hayashida,[3,42] K. Hayashi,[38] E. Hays,[14] J. W. Hewitt,[14] A. B. Hill,[3,43] R. E. Hughes,[44] M. S. Jackson,[30,45] T. Jogler,[3] G. Jóhannesson,[46] A. S. Johnson,[3] T. Kamae,[3] J. Kataoka,[47] J. Katsuta,[3] J. Knödlseder,[48,49] M. Kuss,[11] J. Lande,[3] S. Larsson,[29,30,50] L. Latronico,[51] M. Lemoine-Goumard,[52,53] F. Longo,[6,7] F. Loparco,[15,16] M. N. Lovellette,[37] P. Lubrano,[12,13] G. M. Madejski,[3] F. Massaro,[3] M. Mayer,[1] M. N. Mazziotta,[16] J. E. McEnery,[14,54] J. Mehault,[27] P. F. Michelson,[3] R. P. Mignani,[55] W. Mitthumsiri,[3] T. Mizuno,[56] A. A. Moiseev,[20,54] M. E. Monzani,[3] A. Morselli,[57] I. V. Moskalenko,[3] S. Murgia,[3] T. Nakamori,[47] R. Nemmen,[14] E. Nuss,[27] M. Ohno,[58] T. Ohsugi,[56] N. Omodei,[3] M. Orienti,[39] E. Orlando,[3] J. F. Ormes,[59] D. Paneque,[3,60] J. S. Perkins,[14,21,20,61] M. Pesce-Rollins,[11] F. Piron,[27] G. Pivato,[10] S. Rainò,[15,16] R. Rando,[9,10] M. Razzano,[11,62] S. Razzaque,[22] A. Reimer,[3,63] O. Reimer,[3,63] S. Ritz,[62] C. Romoli,[10] M. Sánchez-Conde,[3] A. Schulz,[1] C. Sgrò,[11] P. E. Simeon,[3] E. J. Siskind,[64] D. A. Smith,[52] G. Spandre,[11] P. Spinelli,[15,16] F. W. Stecker,[14,65] A. W. Strong,[66] D. J. Suson,[67] H. Tajima,[3,68] H. Takahashi,[38] T. Takahashi,[58] T. Tanaka,[3,69*] J. G. Thayer,[3] J. B. Thayer,[3] D. J. Thompson,[14] S. E. Thorsett,[70] L. Tibaldo,[9,10] O. Tibolla,[71] M. Tinivella,[11] E. Troja,[14,72] Y. Uchiyama,[3*] T. L. Usher,[3] J. Vandenbroucke,[3] V. Vasileiou,[27] G. Vianello,[3,73] V. Vitale,[57,74] A. P. Waite,[3] M. Werner,[63] B. L. Winer,[44] K. S. Wood,[37] M. Wood,[3] R. Yamazaki,[75] Z. Yang,[29,30] S. Zimmer[29,30]

Cosmic rays are particles (mostly protons) accelerated to relativistic speeds. Despite wide agreement that supernova remnants (SNRs) are the sources of galactic cosmic rays, unequivocal evidence for the acceleration of protons in these objects is still lacking. When accelerated protons encounter interstellar material, they produce neutral pions, which in turn decay into gamma rays. This offers a compelling way to detect the acceleration sites of protons. The identification of pion-decay gamma rays has been difficult because high-energy electrons also produce gamma rays via bremsstrahlung and inverse Compton scattering. We detected the characteristic pion-decay feature in the gamma-ray spectra of two SNRs, IC 443 and W44, with the Fermi Large Area Telescope. This detection provides direct evidence that cosmic-ray

ejecta and is then transferred to kinetic and thermal energies of shocked interstellar gas and relativistic particles. The shocked gas and relativistic ...hermal ...). The ... (DSA) can explain the production of relativistic particles in SNRs (*1*). DSA generally predicts that a substantial fraction of the shock energy is transferred to relativistic protons. Indeed, if SNRs are the main sites of acceleration of the galactic cosmic rays, then 3 to 30% of the supernova kinetic energy must end up transferred to relativistic protons. However, the presence of relativistic protons in SNRs has been mostly inferred from indirect arguments (*2*–*5*).

A direct signature of high-energy protons is provided by gamma rays generated in the decay of neutral pions (π^0); proton-proton (more generally nuclear-nuclear) collisions create π^0 mesons, which usually quickly decay into two gamma rays (*6*–*8*) (schematically written as $p + p \rightarrow \pi^0$ + other products, followed by $\pi^0 \rightarrow 2\gamma$), each having an energy of $m_{\pi^0}c^2/2 = 67.5$ MeV in the rest frame of the neutral pion (where m_{π^0} is the rest mass of the neutral pion and c is the speed of light). The gamma-ray number spectrum, $F(\varepsilon)$, is thus symmetric about 67.5 MeV in a log-log representation (*9*). The π^0-decay spectrum in the usual $\varepsilon^2F(\varepsilon)$ representation rises steeply below ~200 MeV and approximately traces the energy distribution of parent protons at energies greater than a few GeV. This characteristic spectral feature (often referred to as the "pion-decay bump") uniquely identifies π^0-decay gamma rays and thereby high-energy protons, allowing a measurement of the source spectrum of cosmic rays.

Massive stars are short-lived and end their lives with core-collapse supernova explosions. These explosions typically occur in the vicinity of molecular clouds with which they in-

Fermi Telescope Revealed Cosmic-ray Protons

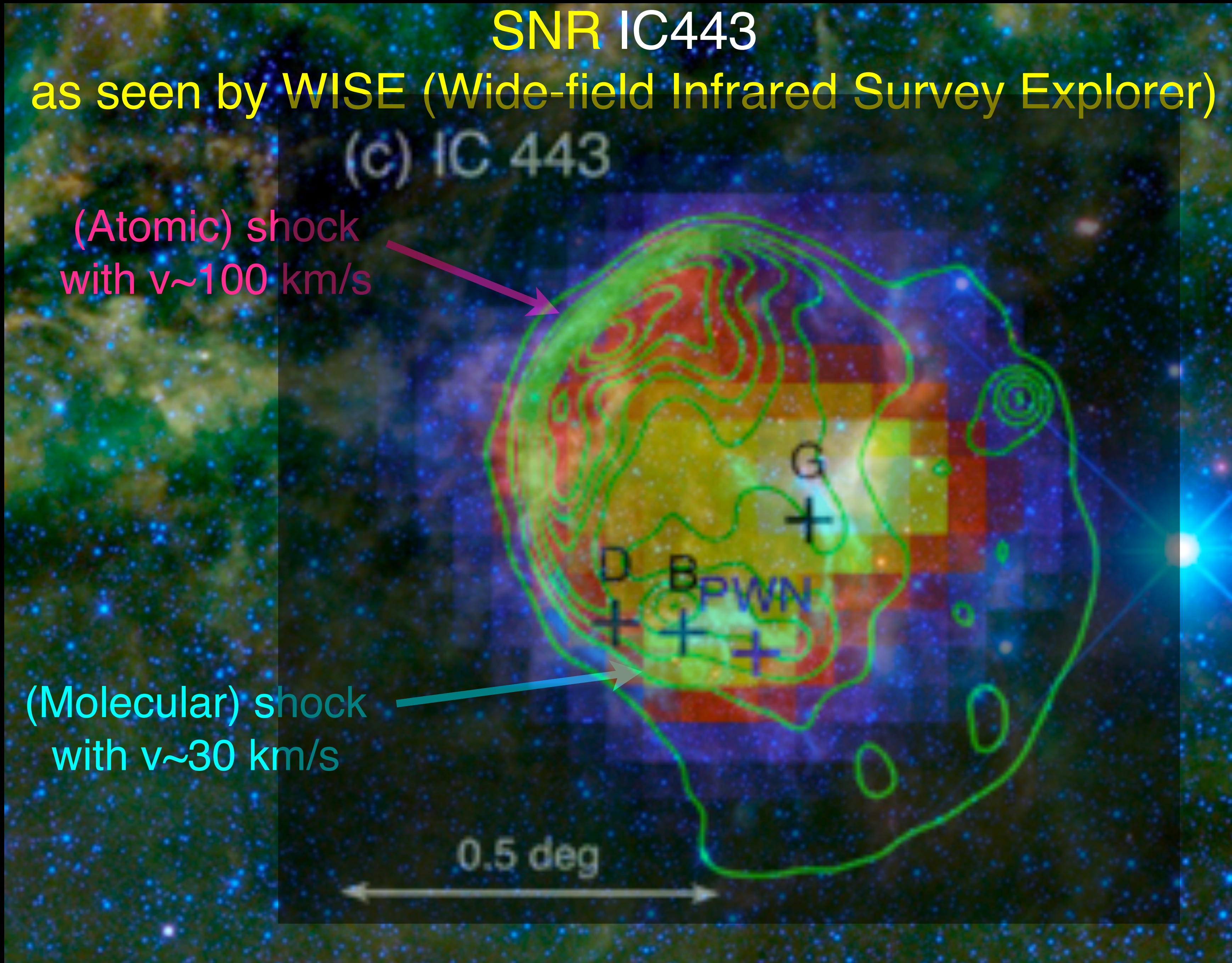

Signature of π^0-decay Gamma-rays

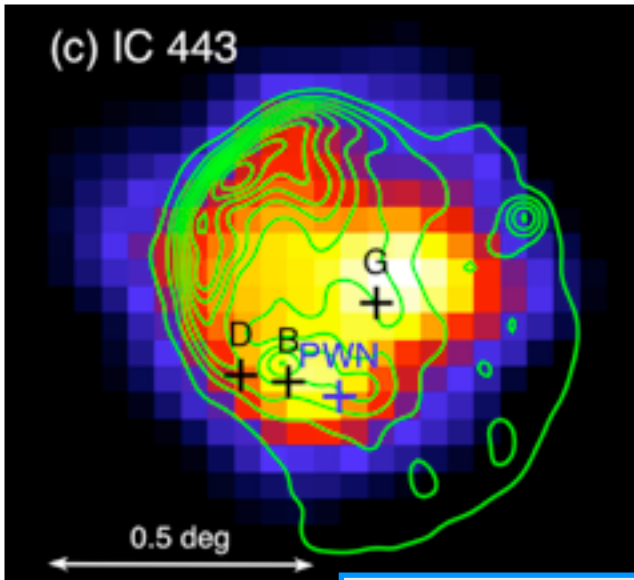

Uchiyama+11

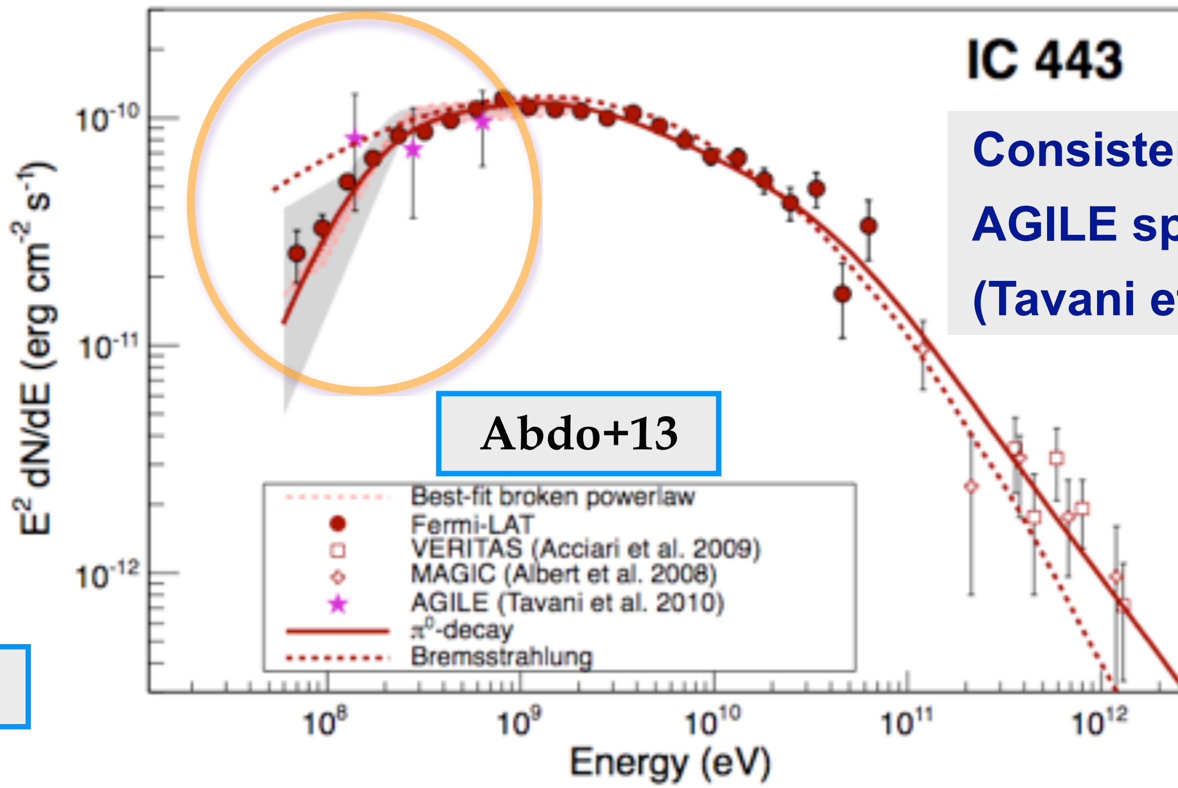

Abdo+13

Consistent with AGILE spectrum (Tavani et al. 10)

- ☑ Our previous papers reported spectra only >200 MeV.
- ☑ Here we report spectra down to 60 MeV thanks to:
  - ✱ Recent update ("Pass-7") of event reconstruction, which largely improved effective area at low energies.
  - ✱ Increased exposure time: 1 yr ➜ 4 yr

Sub-GeV spectra of IC443/W44 agree well with π^0-decay spectra.

SNRs Detections with Fermi

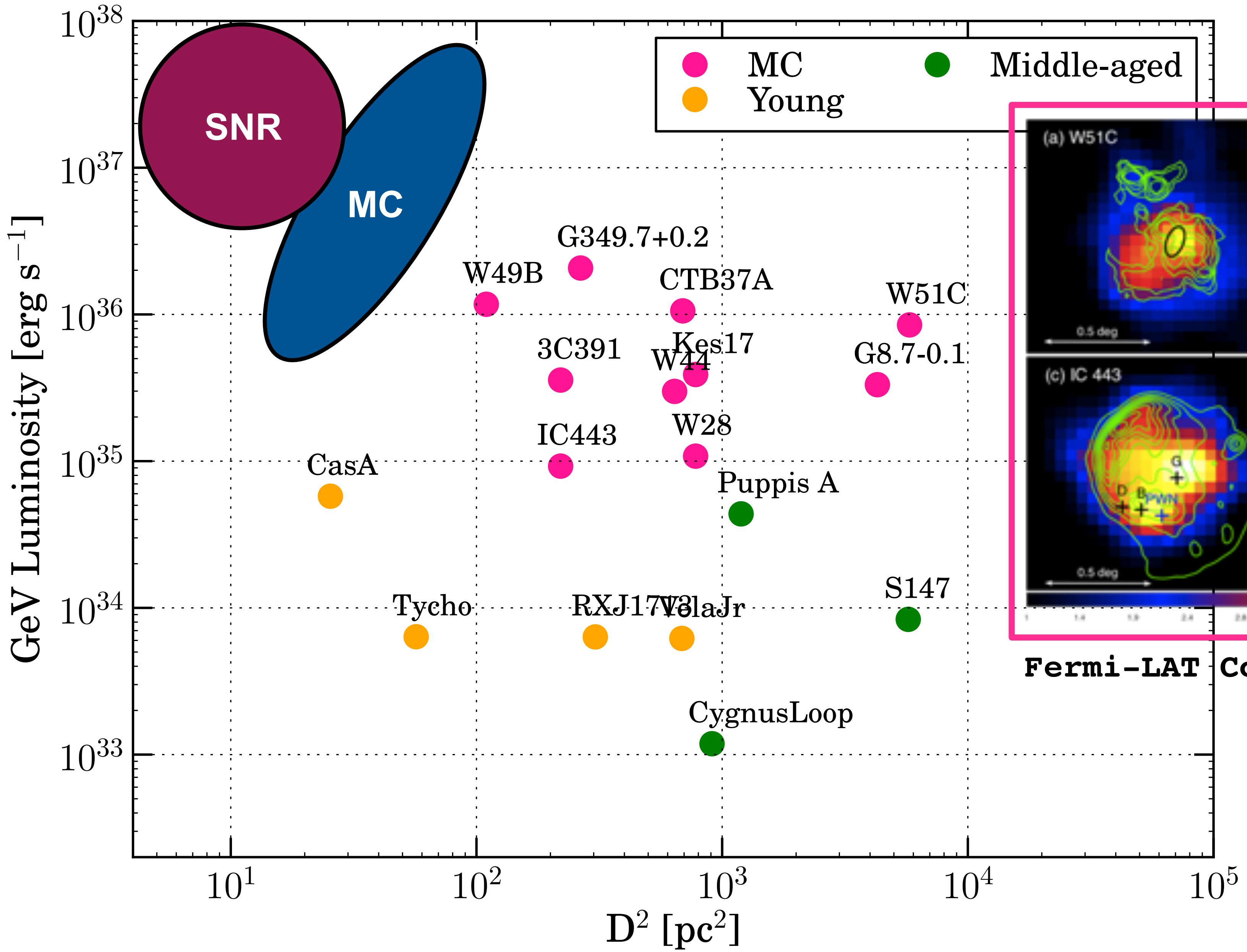

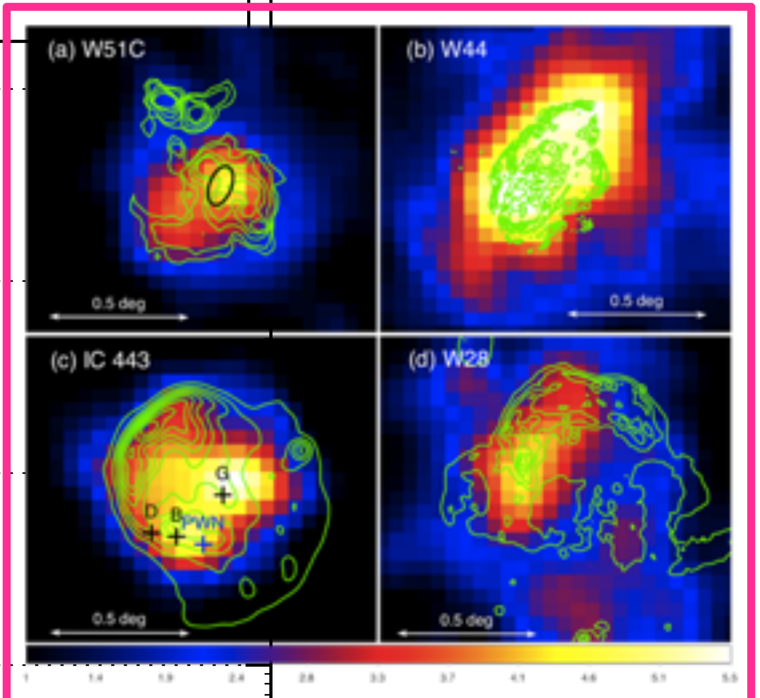

Fermi-LAT Coll(Uchiyama+)2011

Updated from Thompson, Baldini, Uchiyama (2012)

Gamma-ray Spectra of Fermi-Detected SNRs

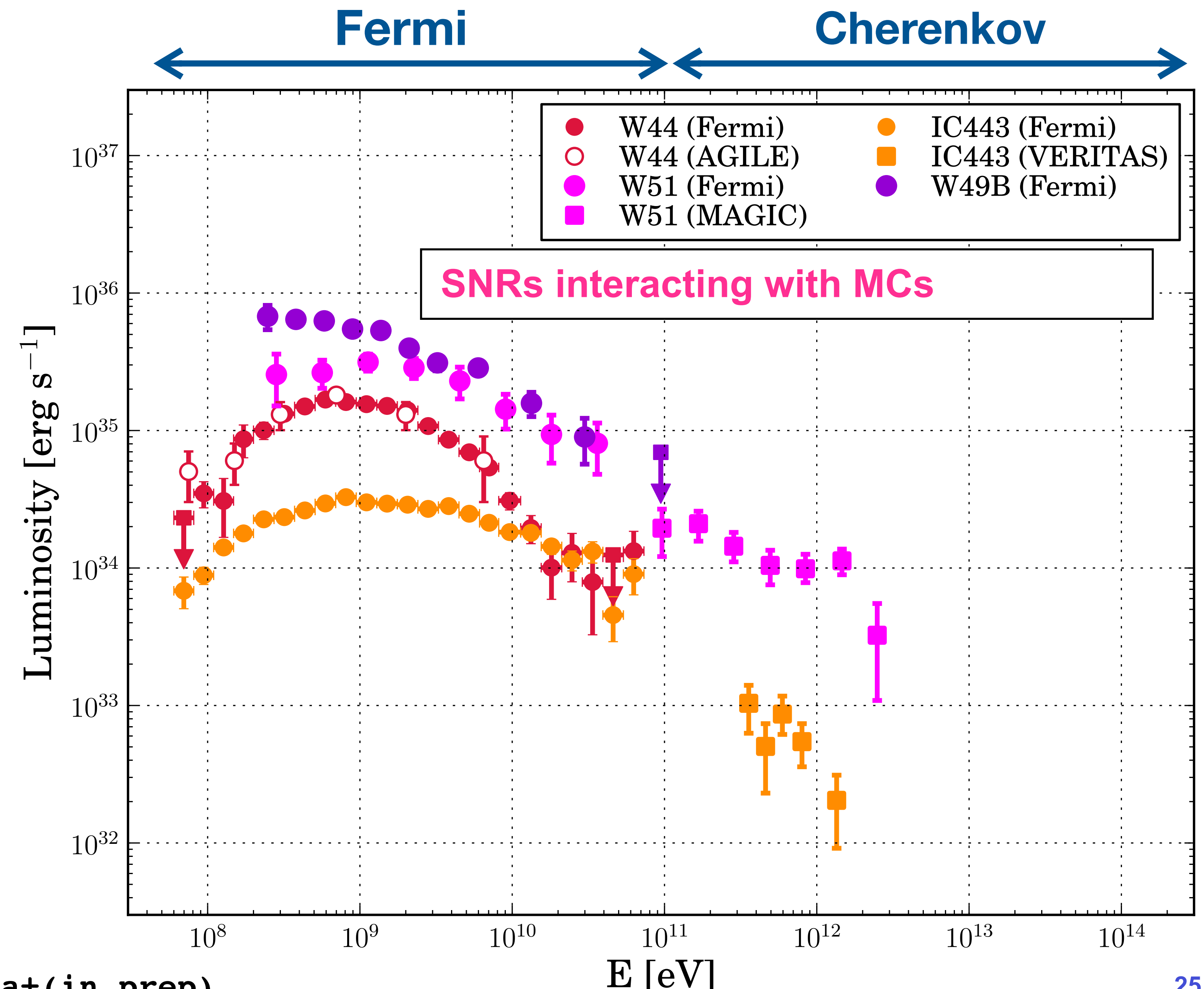

Uchiyama+(in prep)

Gamma-ray Spectra of Fermi-Detected SNRs

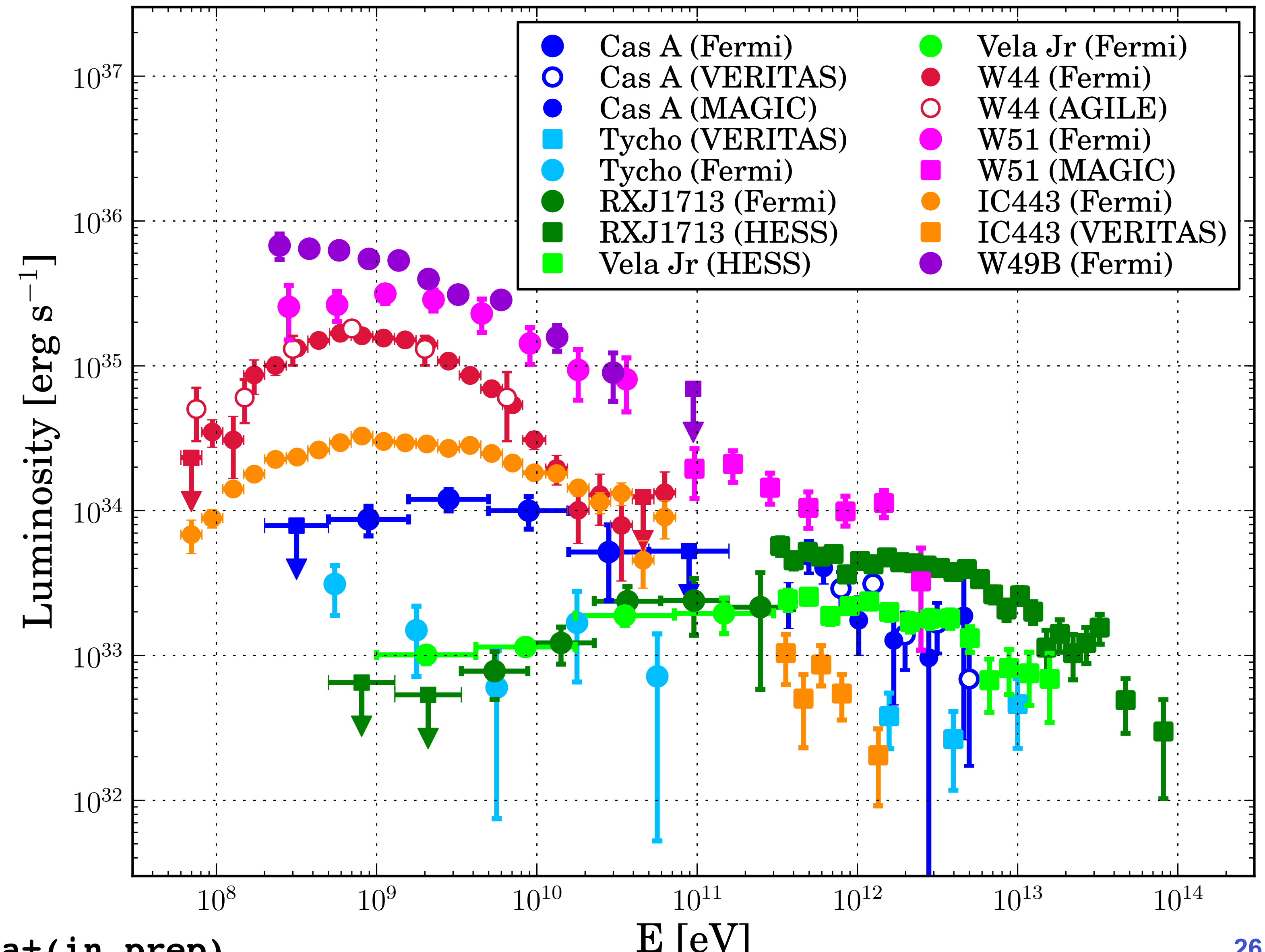

Uchiyama+(in prep)

★ Tycho's SNR

- SN 1572
- SN type: Ia
- distance: ~3 kpc
- radius: ~3.7 pc

★ Cassiopeia A

- SN ~1680
- SN type: IIb
- distance: ~3.4 kpc
- radius: ~2.5 pc

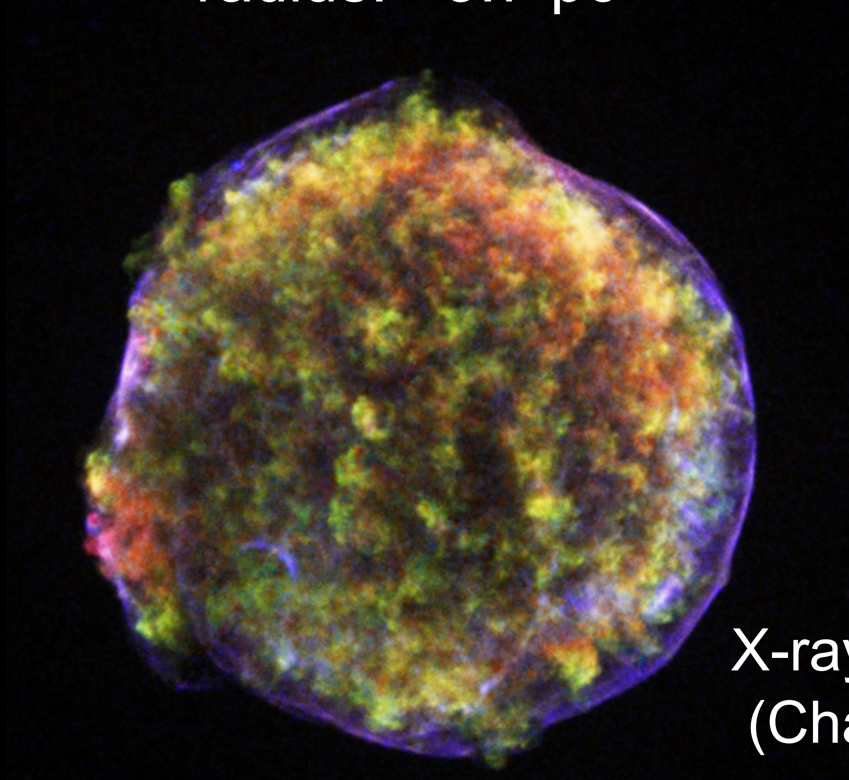

X-ray Images (Chandra)

Most parameters are reasonably well known.
➔ largely help us interpret gamma-ray results.

Young SNR: Tycho's SNR

Fermi-LAT Detection (5σ)

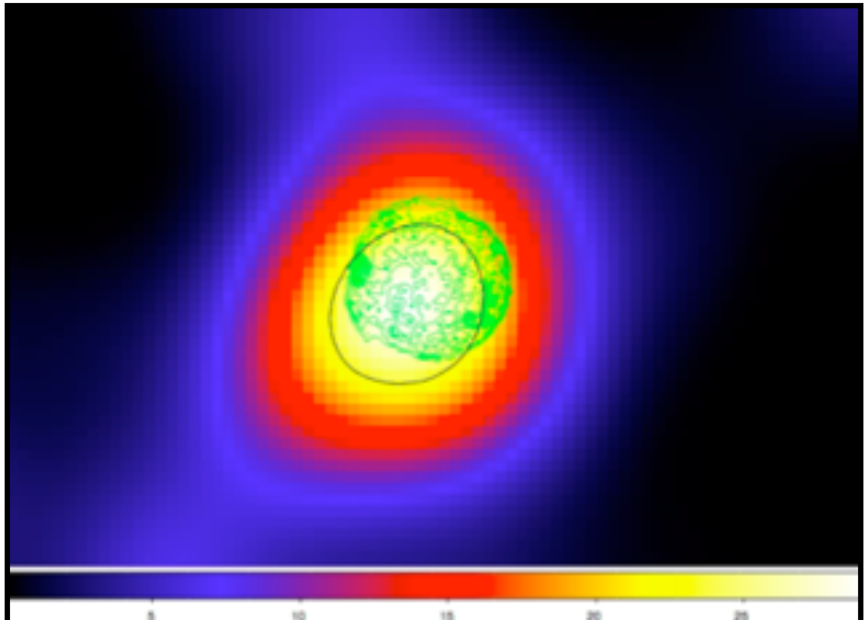

Figure 2: *Fermi TS map of Tycho in the 1 GeV – 100 GeV energy range. The green contours are from XMM-Newton and the black line denotes the 95% confidence area for the FERMI position.*

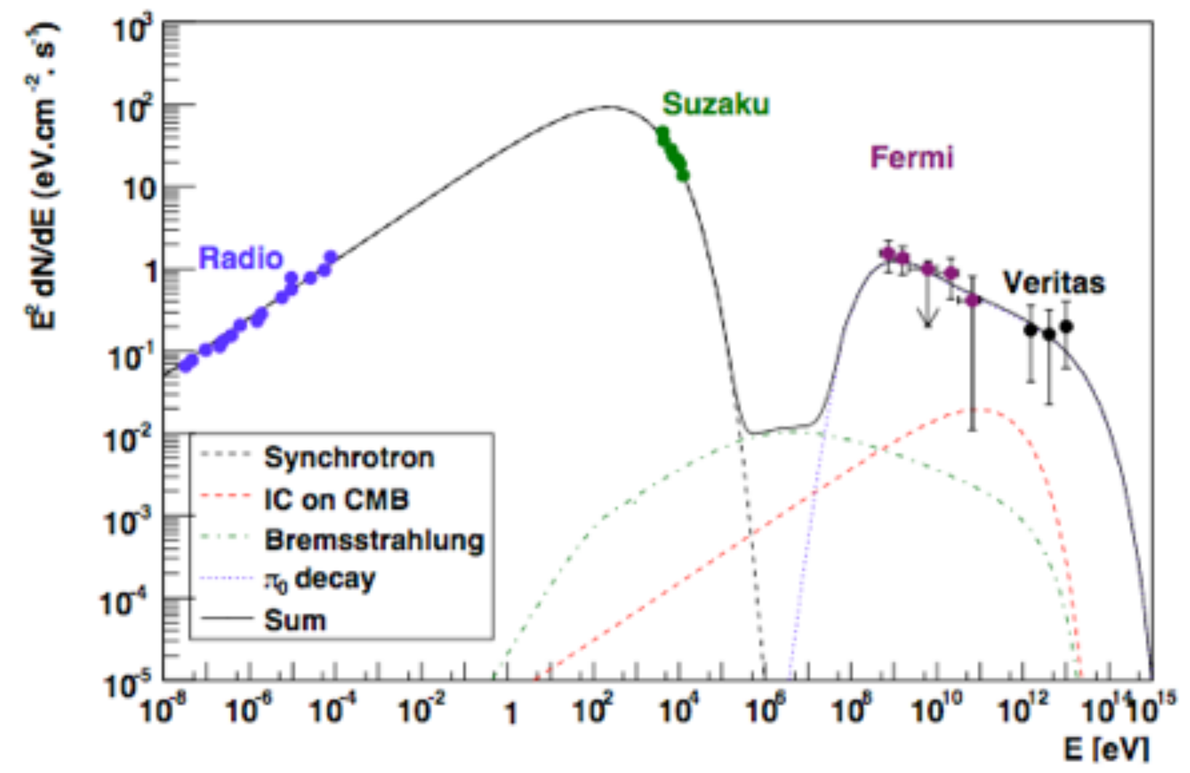

Case	D_{kpc}	n_H [cm^{-3}]	E_{SN} [10^{51}erg]	$E_{p,tot}$ [10^{51}erg]	K_{ep}
Far	3.50	0.24	2.0	0.150	4.5×10^{-4}
Nearby	2.78	0.30	1.0	0.061	7.0×10^{-4}

Photon index = 2.3 ± 0.1 (favors hadronic origin)

6-8% of E_{SN} transferred to CRs.

Young SNR: Cas A

CR proton:

- $W_p = 4\times10^{49}$ erg (n=10 cm^{-3}) (4% of 10^{51} erg)
- $E_{p,max}$ = 10 TeV **escaped?**
- B > 0.1 mG (consistent with X-ray)

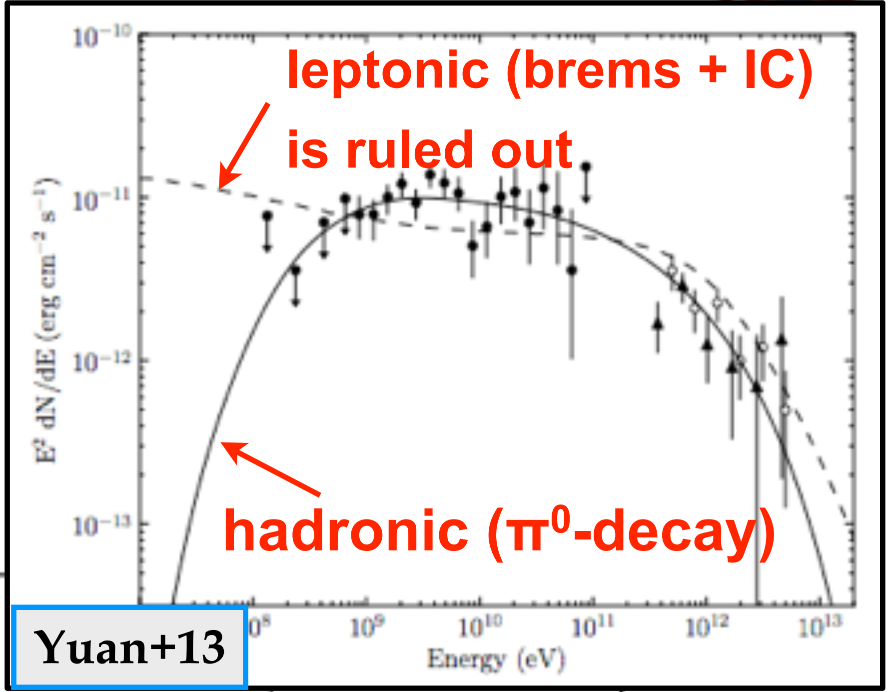

Zirakashvili et al. (2013): $W_{cr} = 3\times10^{50}$ erg

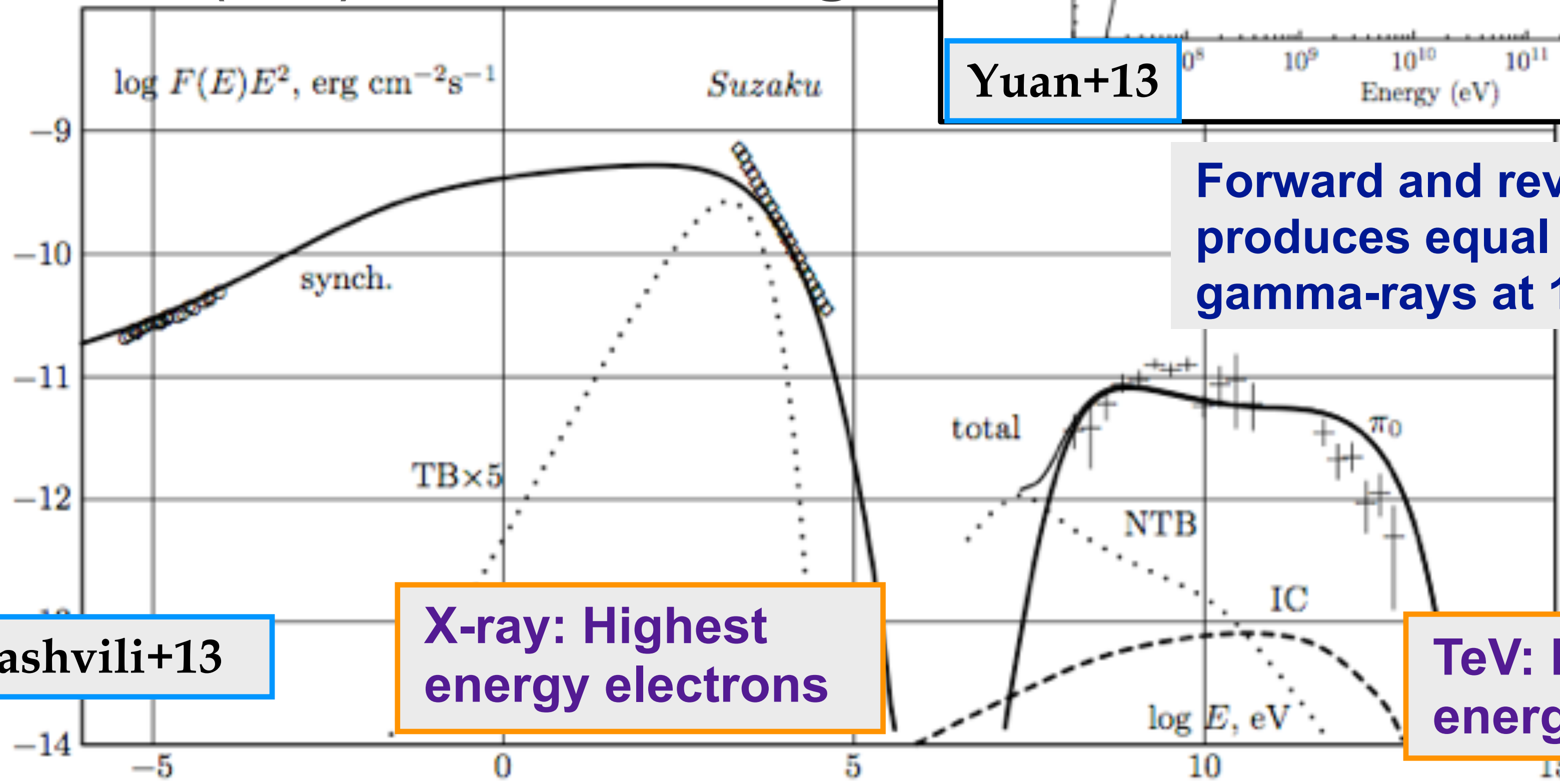

Forward and reverse shock produces equal amount of gamma-rays at 1 TeV

Synchrotron-dominated SNR: Vela Jr.

Suzaku X-ray
(Y. Uchiyama)

TeV (H.E.S.S.)

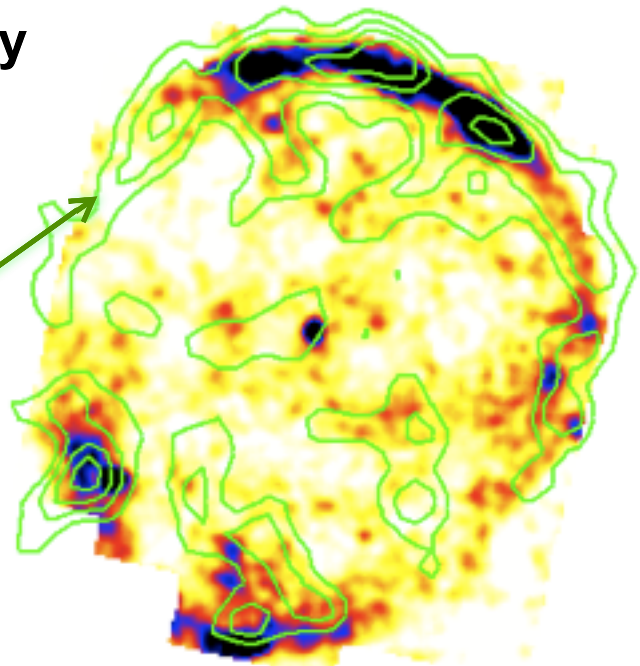

Tanaka+2011

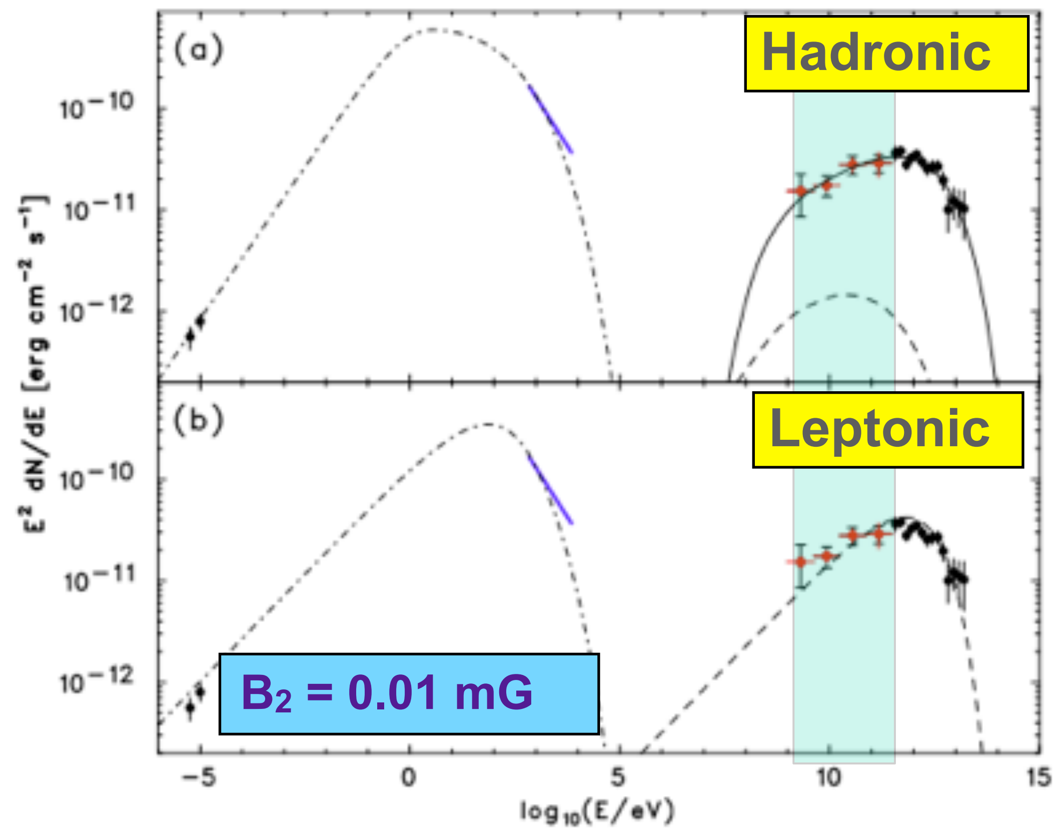

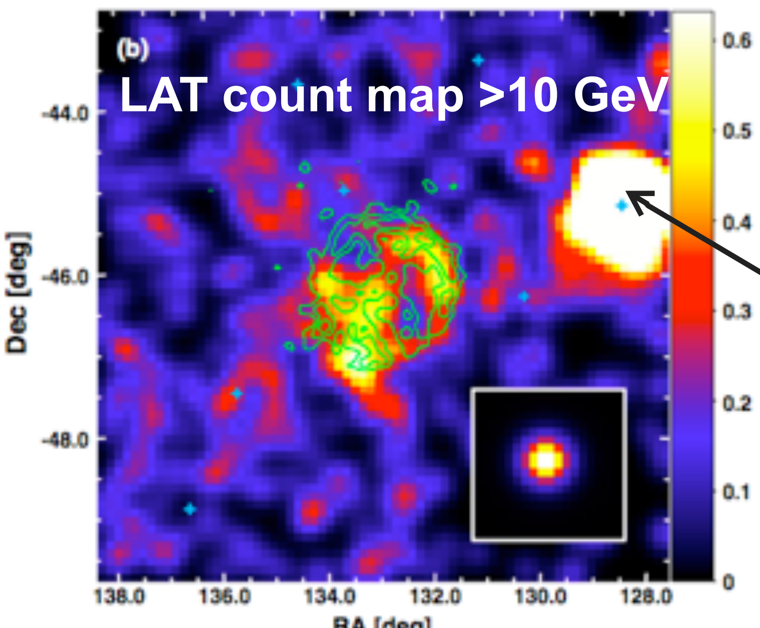

Vela pulsar

LAT Detection at ~15σ level
Γ_{LAT} = 1.87 ± 0.08(sta) ± 0.17(sys)

B_2 = 0.01 mG in leptonic model would be difficult to be reconciled with X-ray measurements.
Hadronic model would require a large CR content (5×10^{50} erg for n=0.1 cm^{-3})

Middle-Aged SNR: Puppis A

Hewitt+2012

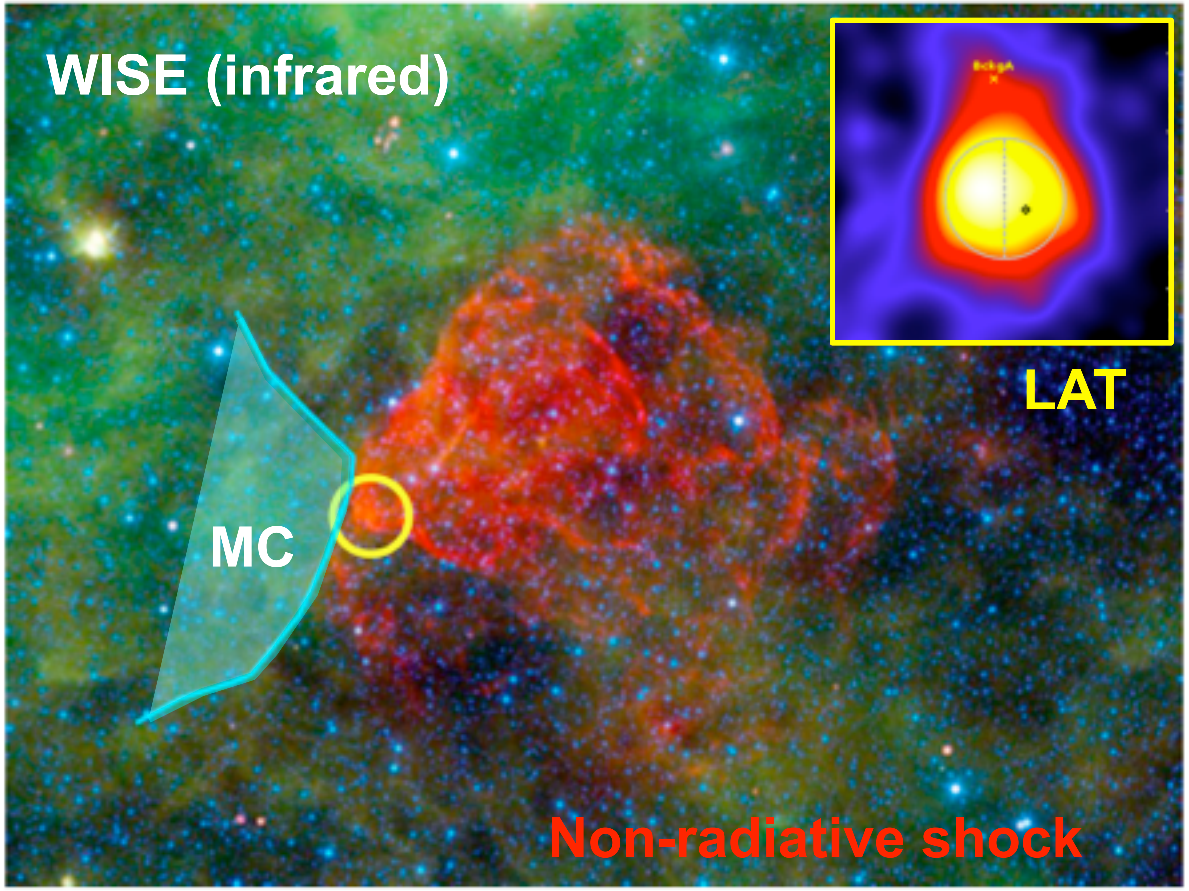

Figure 1: *Infrared emission from dust heated by the expanding shock-wave of Puppis A (courtesy WISE). Yellow circle indicates where the shock has encountered a small cloud. Cyan contours highlight the adjacent molecular cloud, just beyond the SNR.*

Diameter: 30 pc
Age: ~40,000 yr (Sedov phase)
ISM Density: 1 cm^{-3}

LAT Detection at ~13σ level
$\Gamma_{LAT} = 2.10 \pm 0.07(sta) \pm 0.10(sys)$

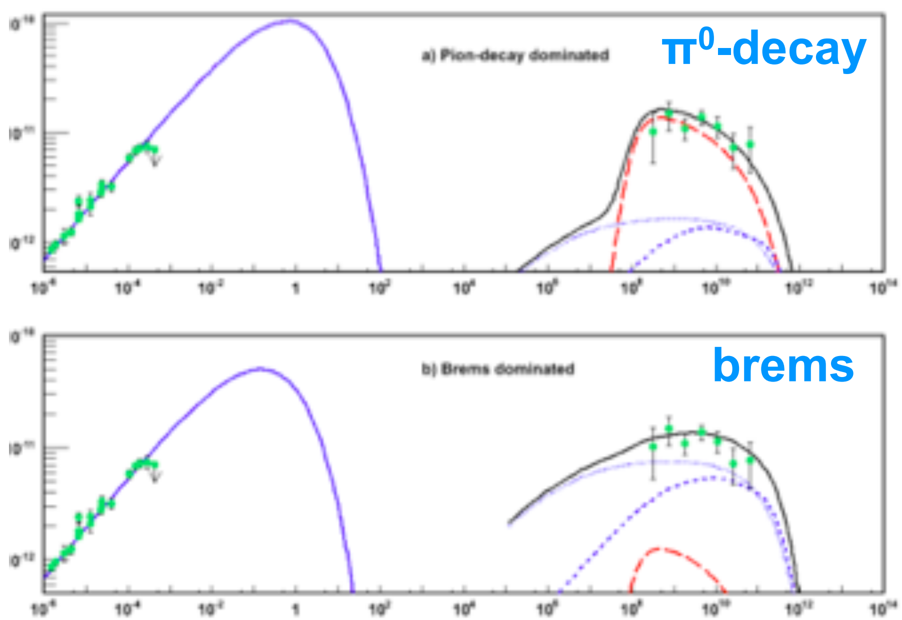

The gamma-ray emission can be modeled either by bremsstrahlung with $W_e = 1\times10^{49}$ erg or by hadronic (π^0-decay) with $W_p = 4\times10^{49}$ erg

Fermi-LAT Detection of W44 Surroundings

The presence of large-scale GeV emission was found in the vicinity of SNR W44

Uchiyama et al. (2012)

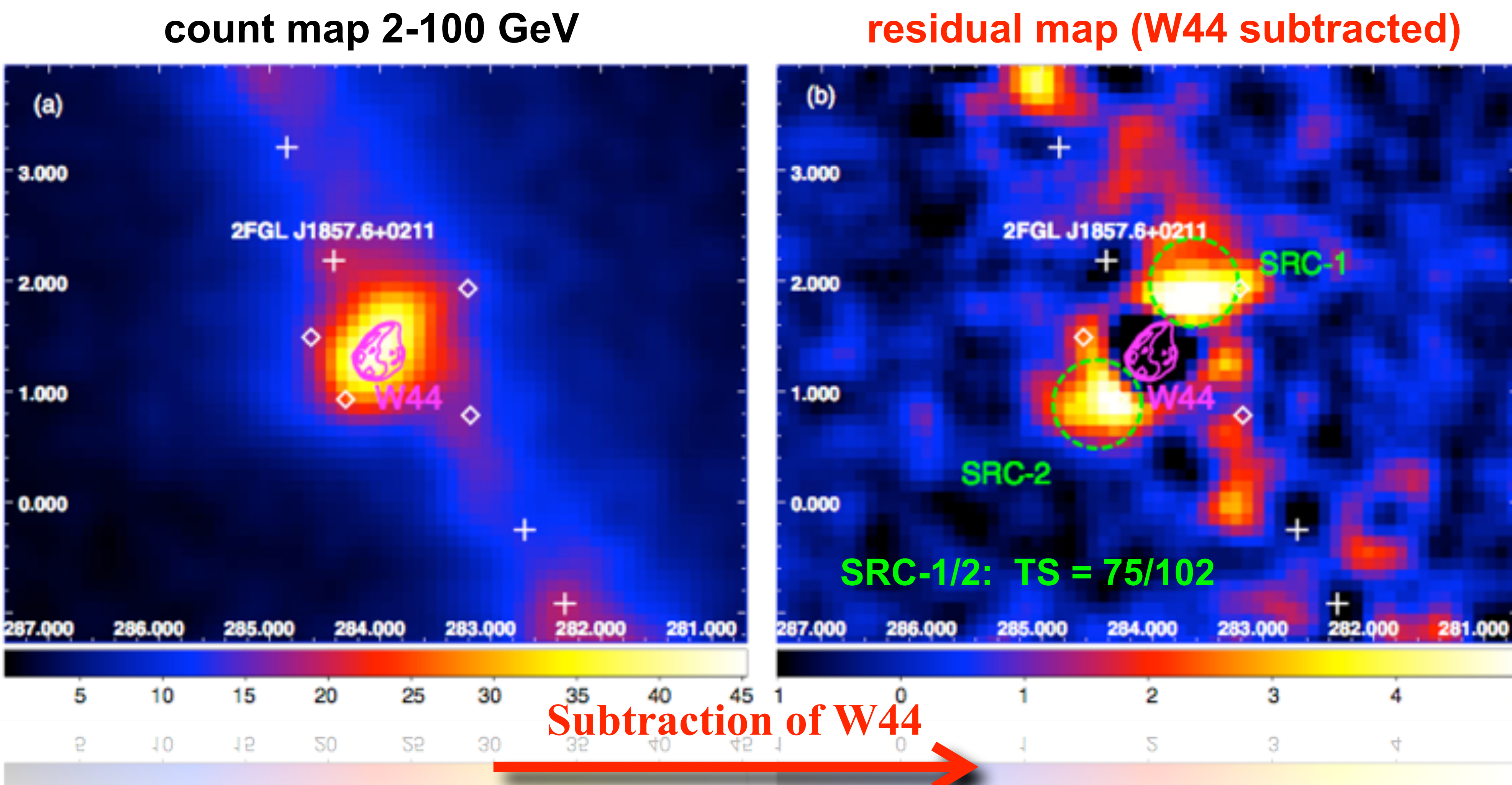

Gamma-rays from W44 itself are subtracted, assuming "radio map = gamma-ray map"

Large-scale GeV γ-rays vs CO map

W44 is known to be surrounded by a complex of MCs.
Size ~100 pc, Mass ~10^6 M_{sun} (Dame+1986)

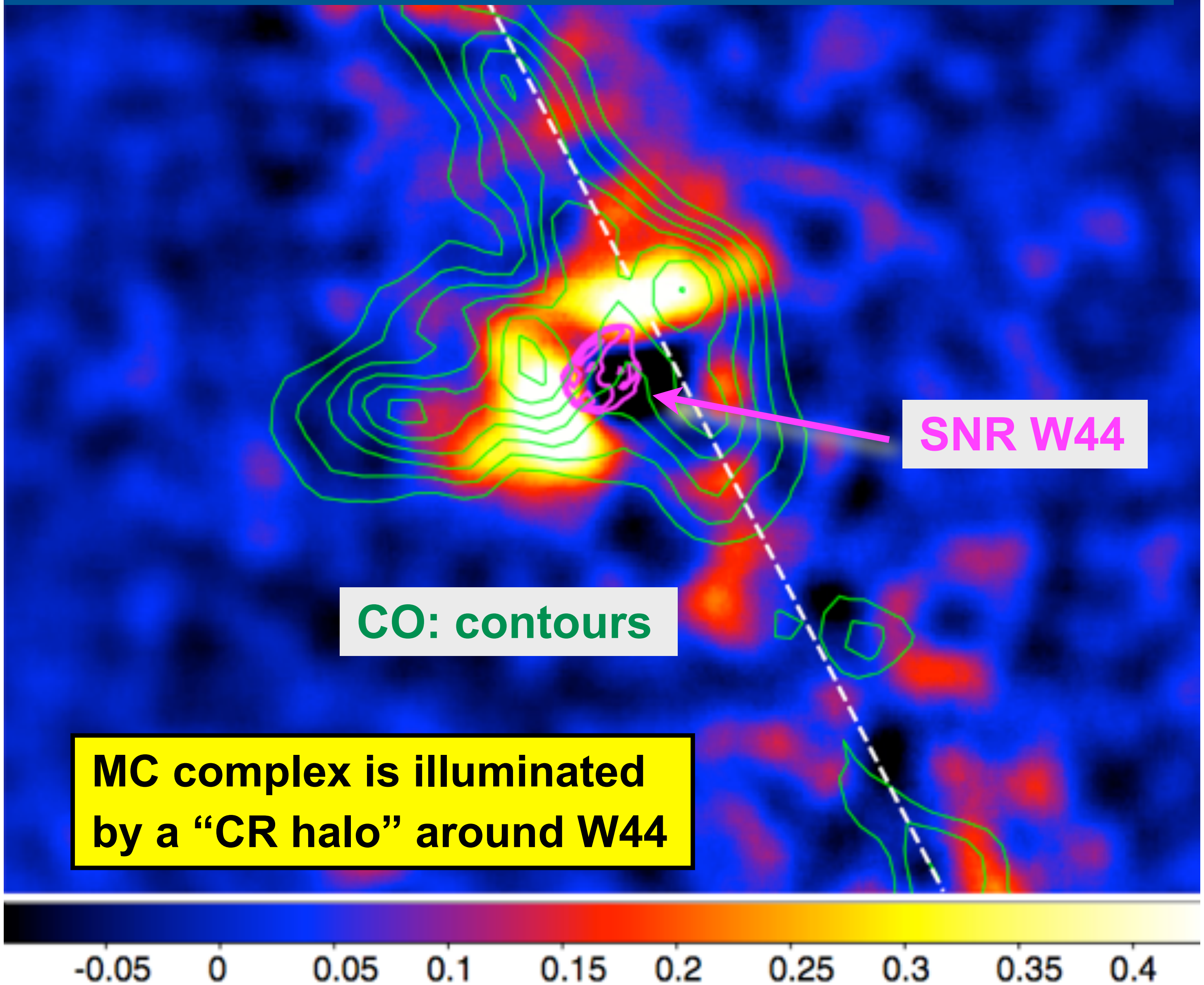

Gamma-ray Evidence for Leaking CRs

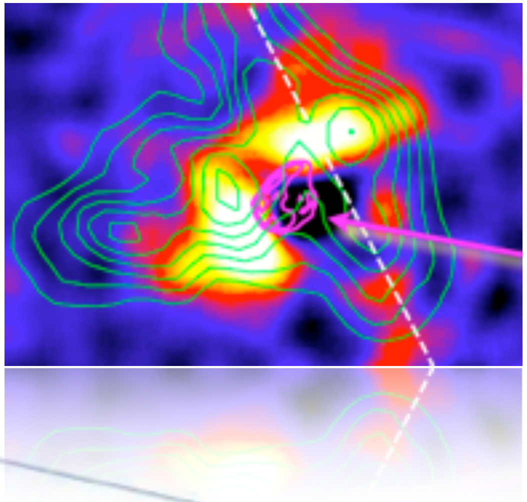

(c) M. Malkov (2012)

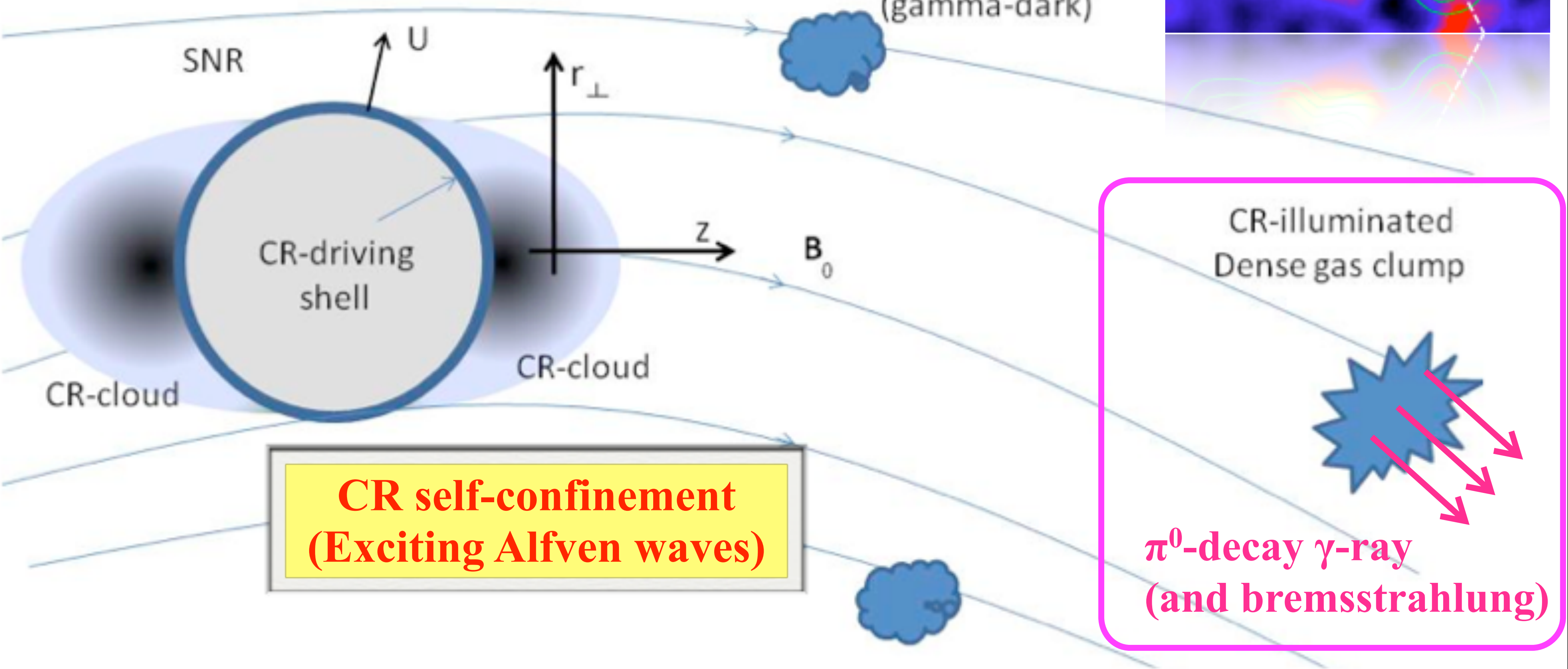

After leaving SNR W44, CRs diffuse along the external B-field direction ➜ bipolar morphology

Amount of CRs Escaped from W44

- Molecular clouds illuminated by escaping CRs (assumed to be uniform within r<L)
  - ✱ L ~100 pc, Mass = $0.5\times10^5\ M_\odot$
- Diffusion coefficient of the ISM (isotropic)
  - ✱ $D(p) = D_{28}\ (cp/10\ \mathrm{GeV})^{0.6}\ 10^{28}\ \mathrm{cm^2/s}$

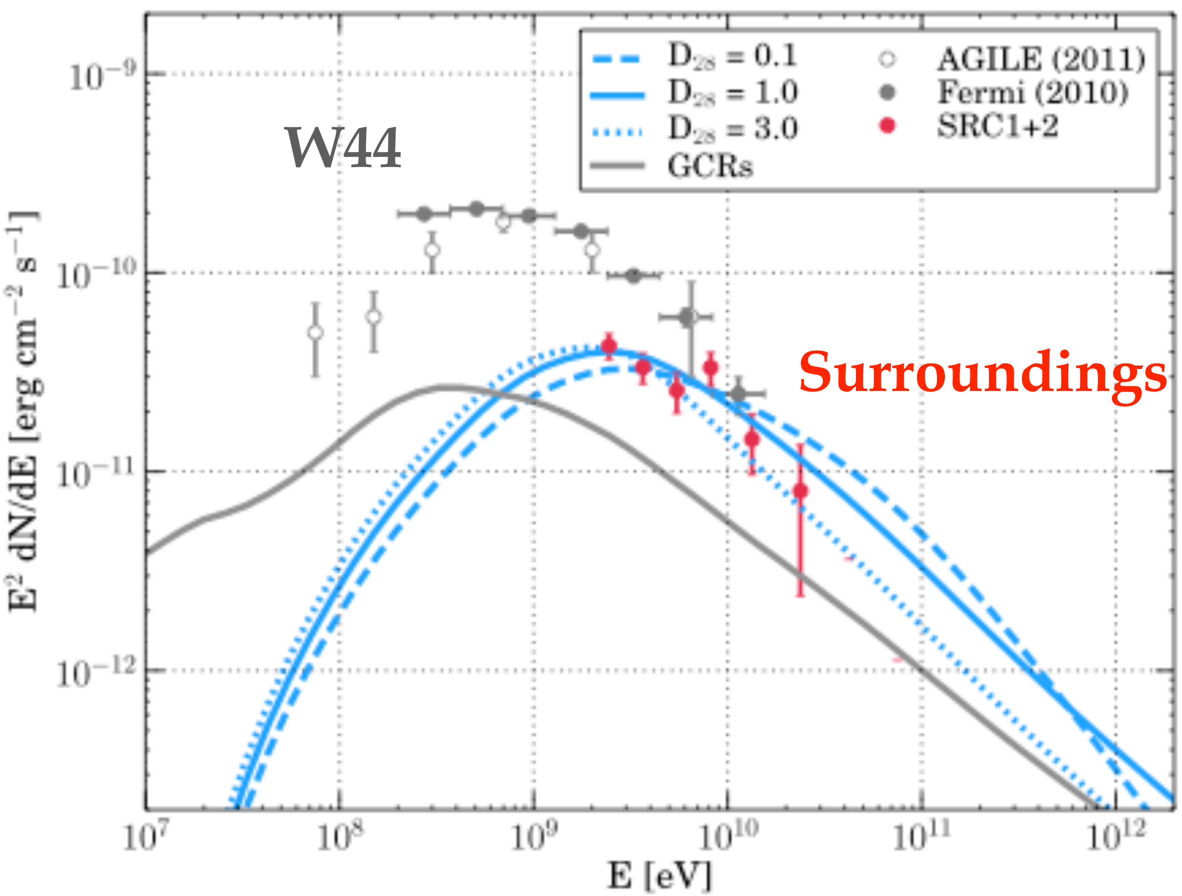

Solving the diffusion equation in the vicinity of W44, we can estimate **the energy spectrum of escaping CRs**.

✱ **Case 1:**

Slow diffusion ($D_{28} = 0.1$)

$N_{esc}(E) = k\ E^{-2.6}$

$W_{esc} = 0.3\times10^{50}$ erg

✱ **Case 2:**

$D_{28} = 1$

$N_{esc}(E) = k\ E^{-2.0}$

$W_{esc} = 1.1\times10^{50}$ erg

✱ **Case 3:**

Fast diffusion ($D_{28} = 3$)

$N_{esc}(E) = k\ E^{-2.0}$

$W_{esc} = 2.7\times10^{50}$ erg

Acceleration Efficiency (Simulation)

Caprioli & Spitokovsky 14

B-field Amplification

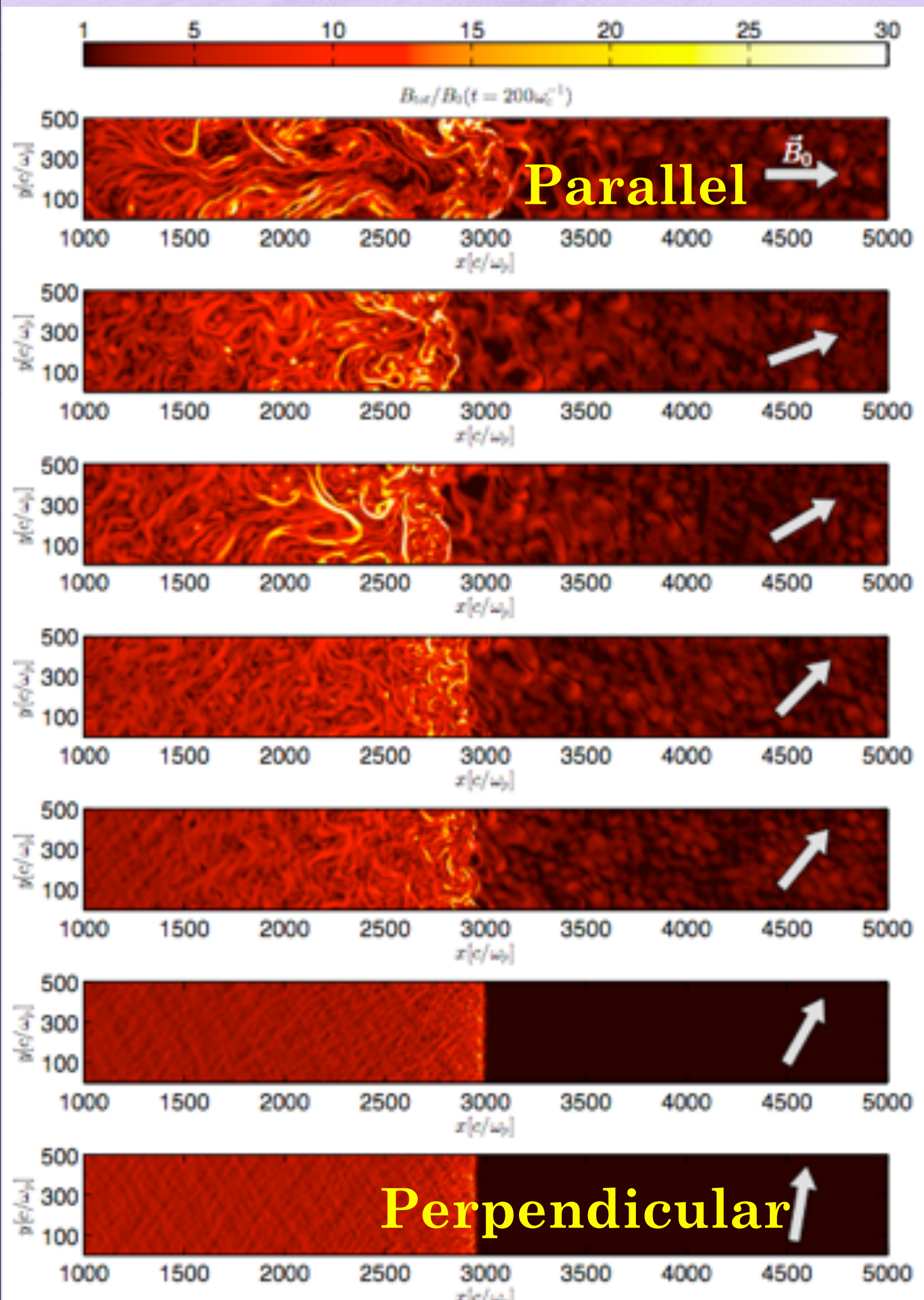

3D hybrid simulation (kinetic-ion & fluid electron)

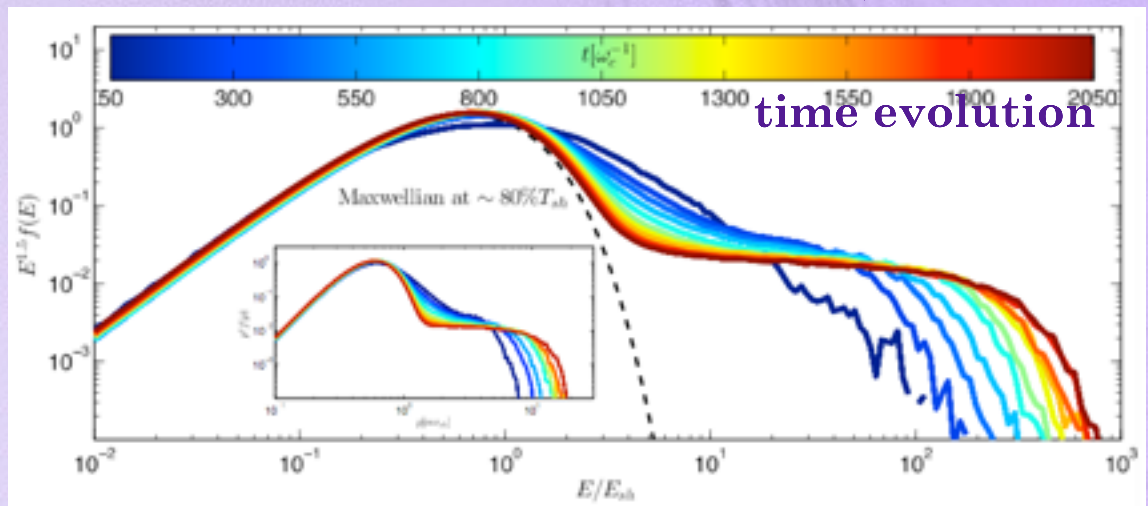

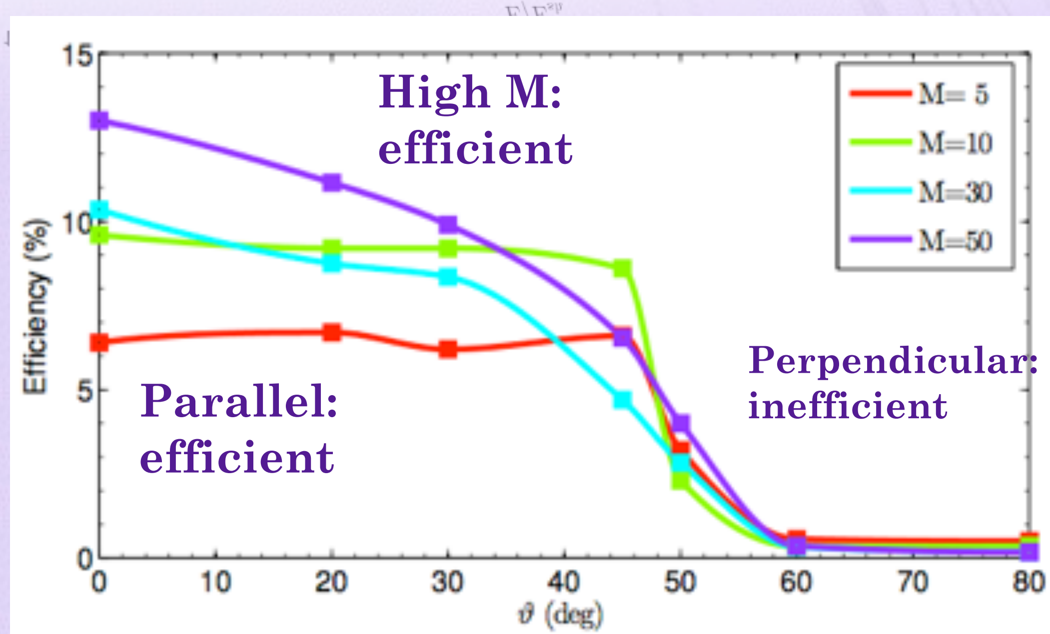

SN 1006: “Bilateral”

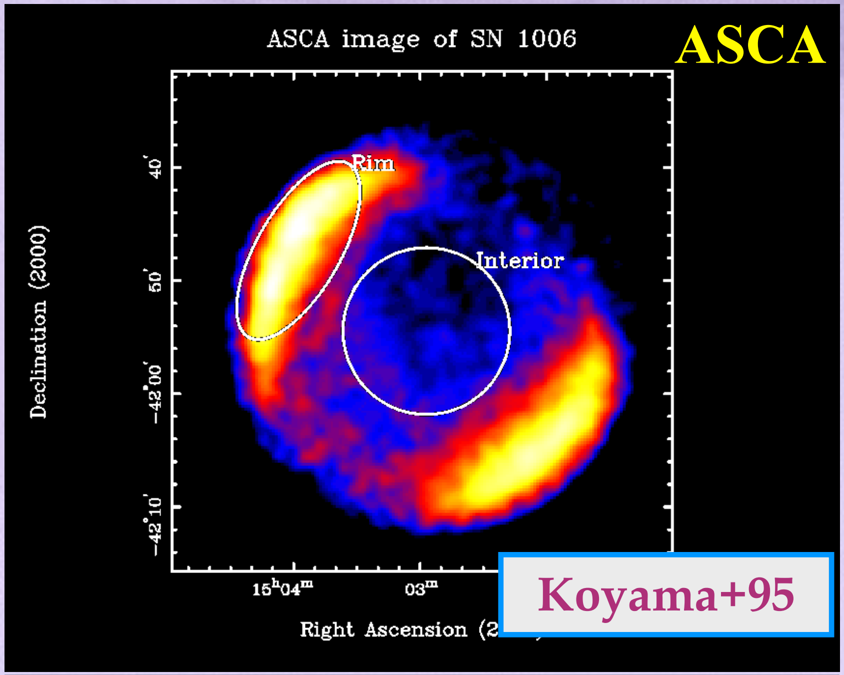

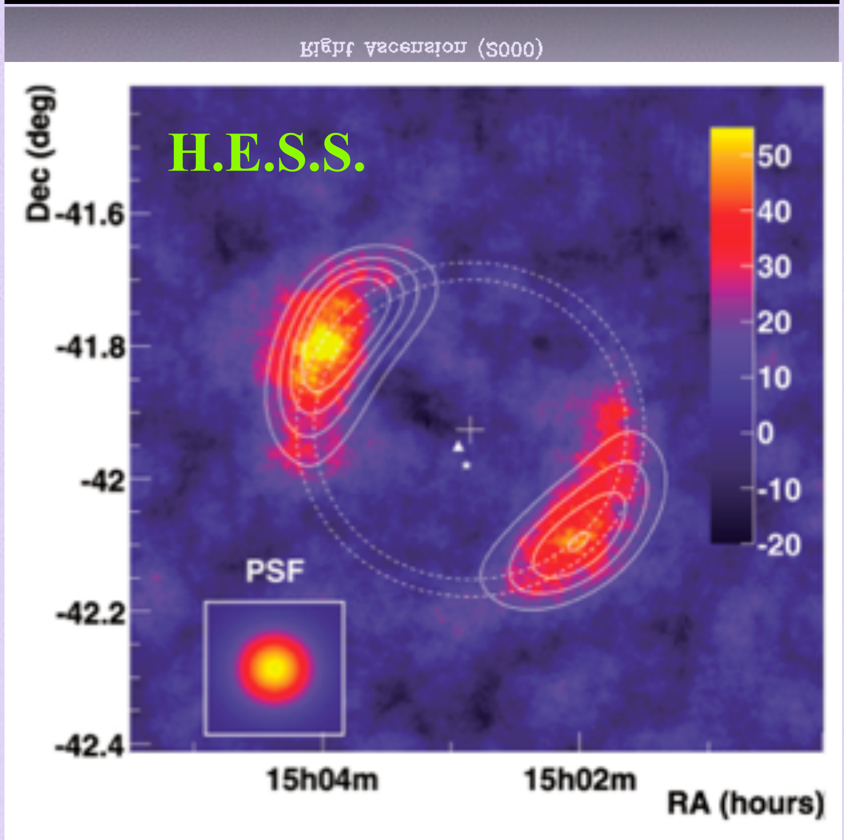

Radio polarization

Fractional polarization (p) at 1.4 GHz

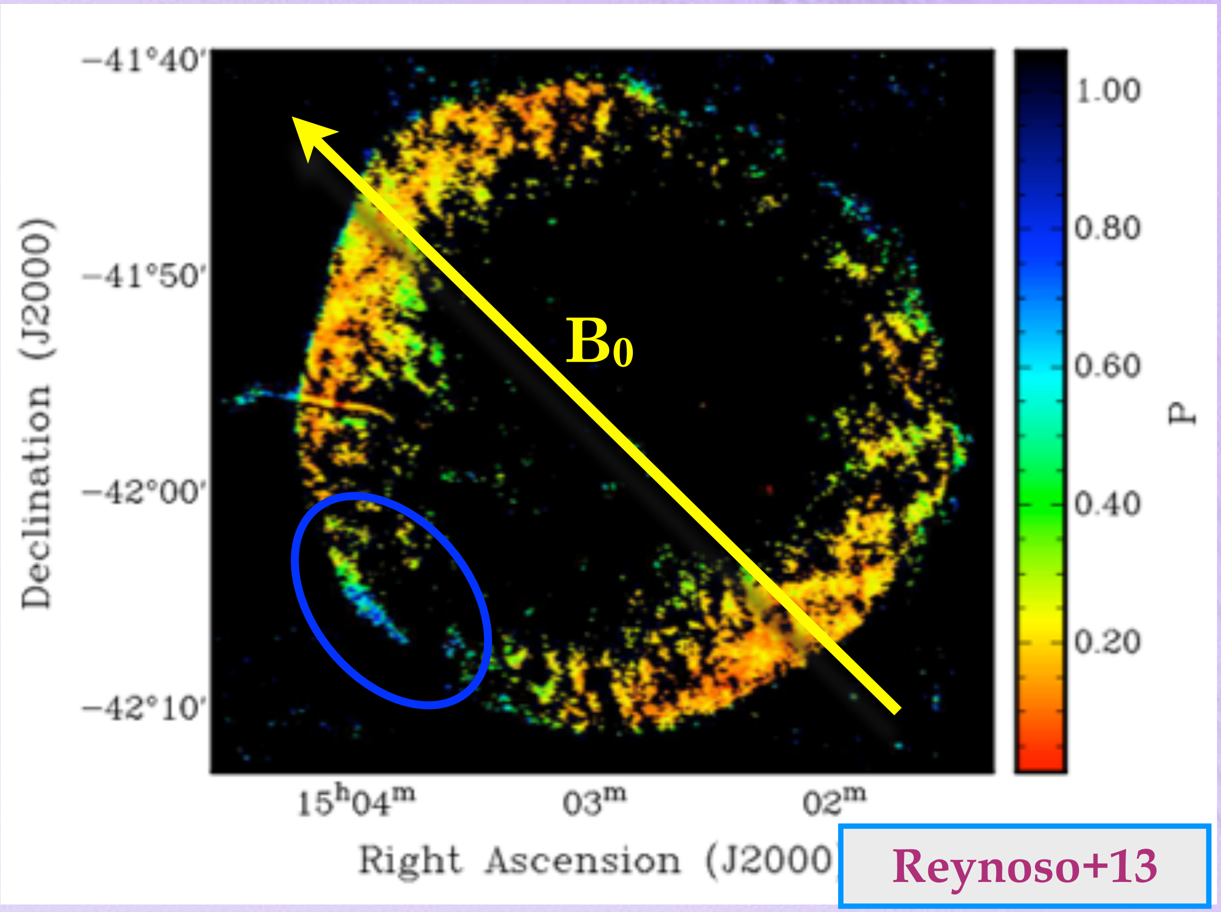

Very high polarization
close to maximally possible degree (< 70%)

B-field amplification & acceleration dependence on B-field direction

Bilateral Synchrotron-dominated SNRs

Vela Jr.

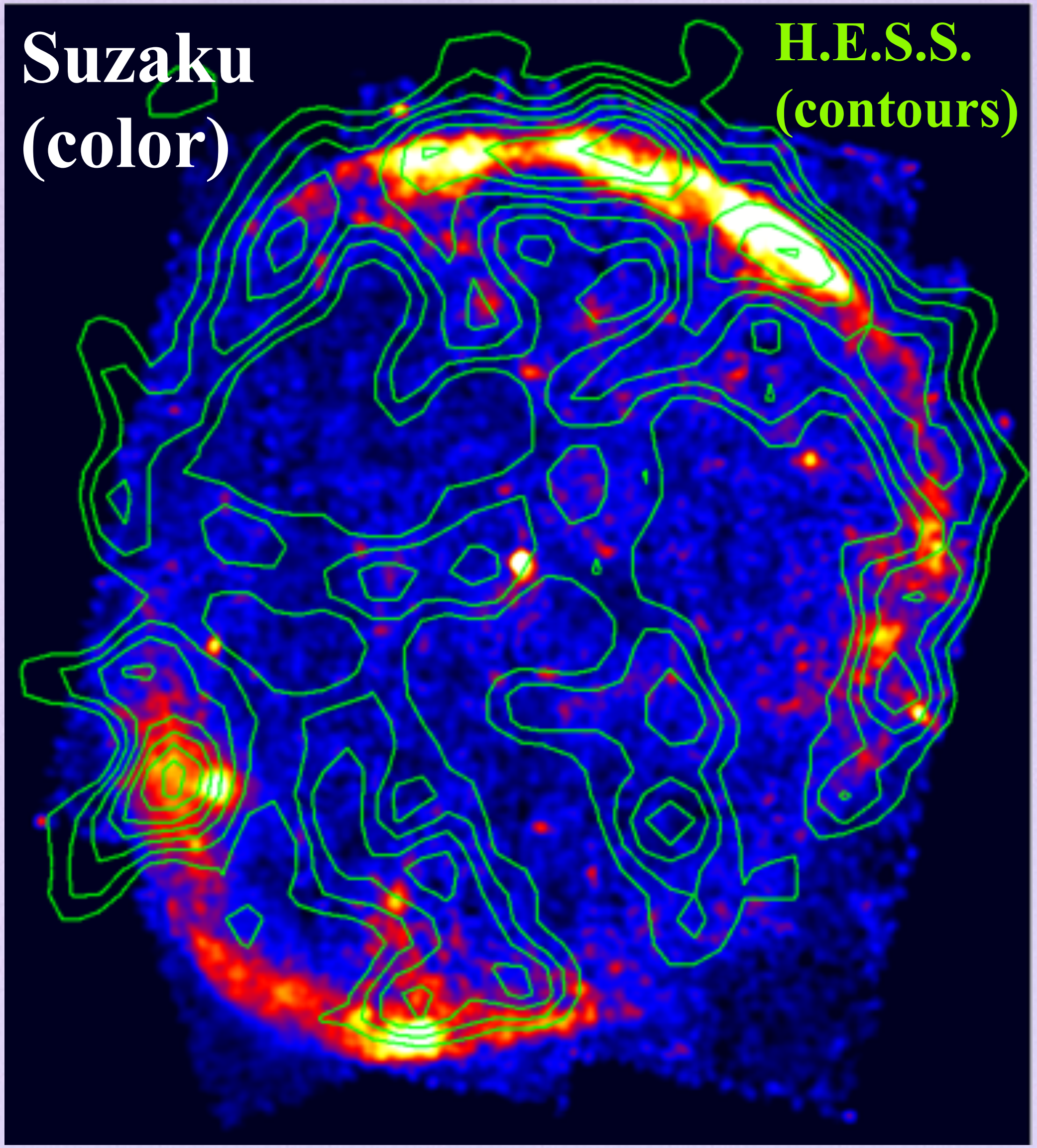

Fukuyama, YU+ in prep.

G1.9+0.3

"PeVatron" Search

ASTRO-H HXI will search for synchrotron by secondary $e^{\pm}$ above 10 keV:
(synchrotron by primary electrons with an unavoidable cutoff of $h\nu_0 \sim 1$ keV is expected to be steep at hard X-rays.)

Synchrotron X-ray Variability in Cas A

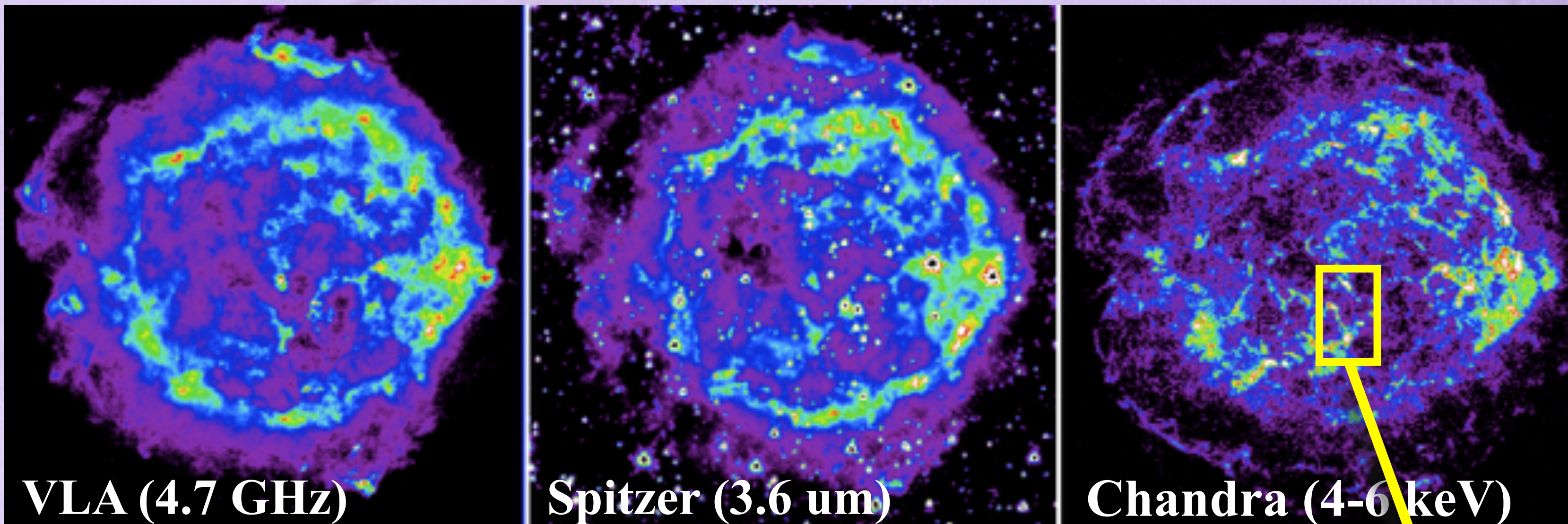

B ~ 0.5 mG

Local

Global variability

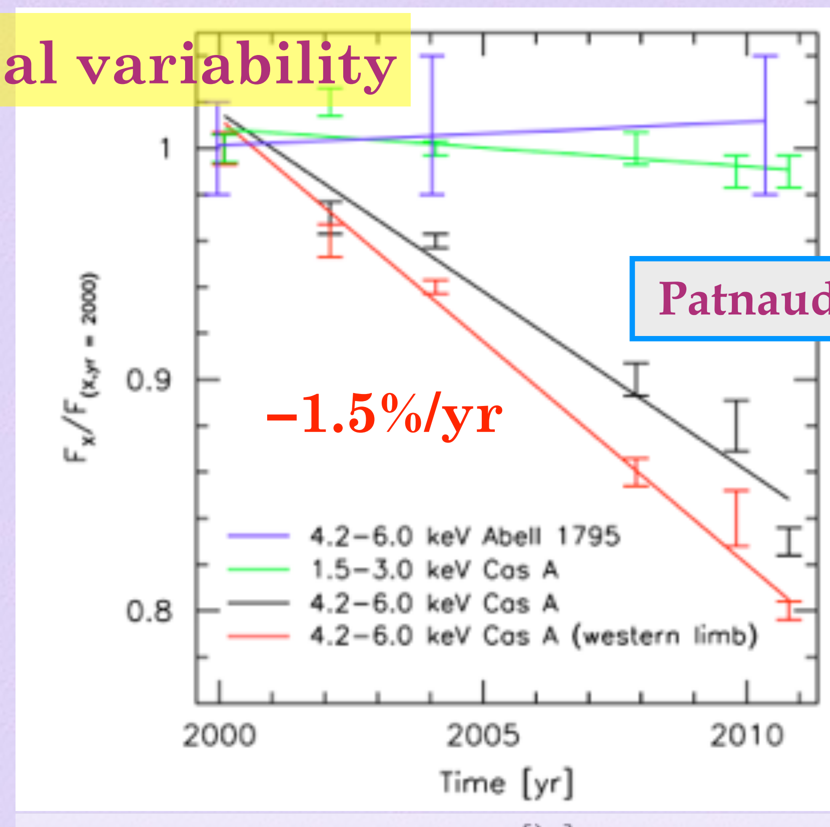

−1.5%/yr

Patnaude+11

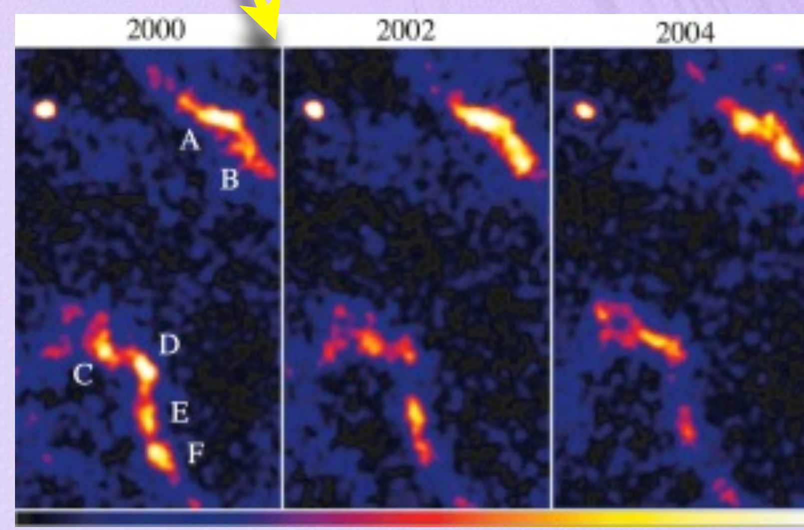

Synchrotron knots/filaments: brightening and decaying ~10%/yr

Uchiyama & Aharonian 08

Synchrotron X-ray Brightening in G1.9+0.3

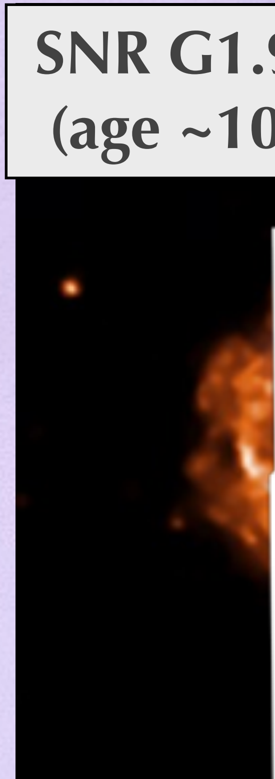

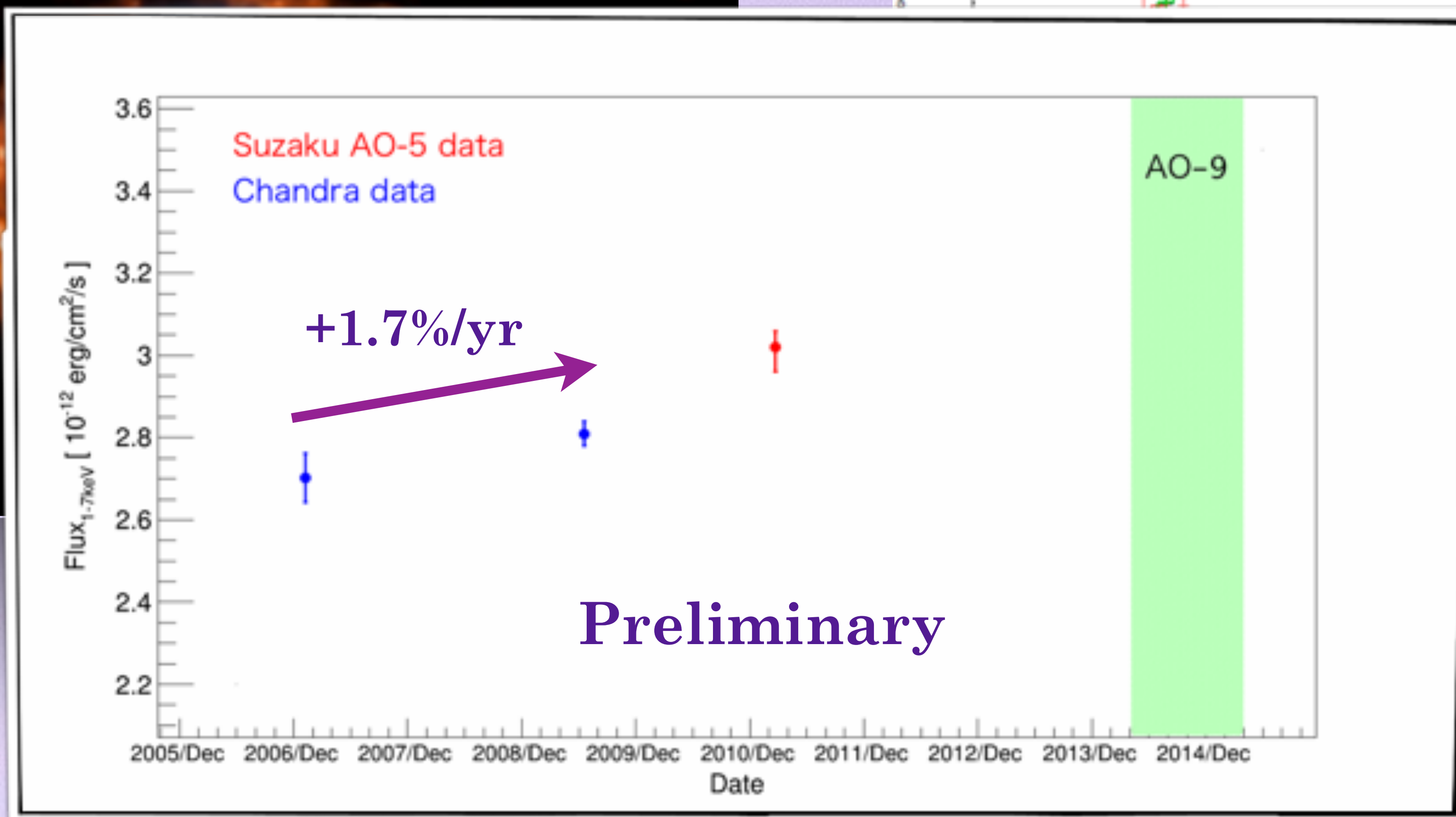

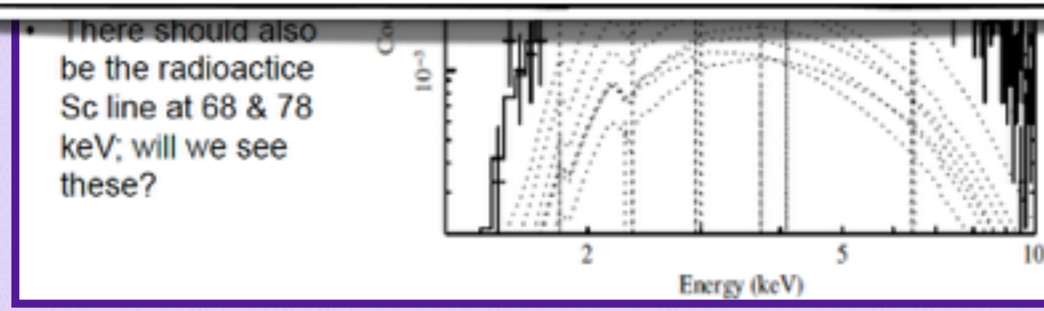

ASTRO-H Measurement of Synchrotron X-ray Spectra

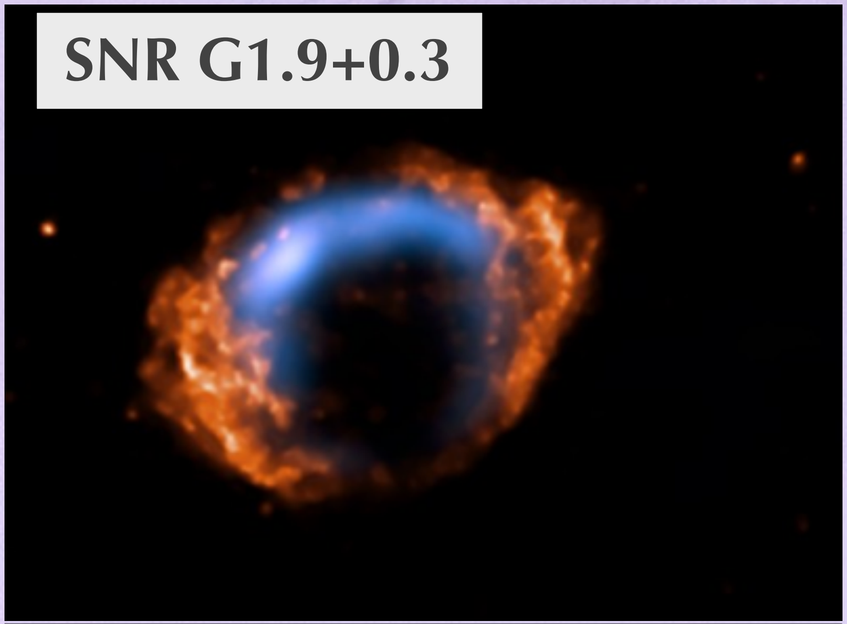

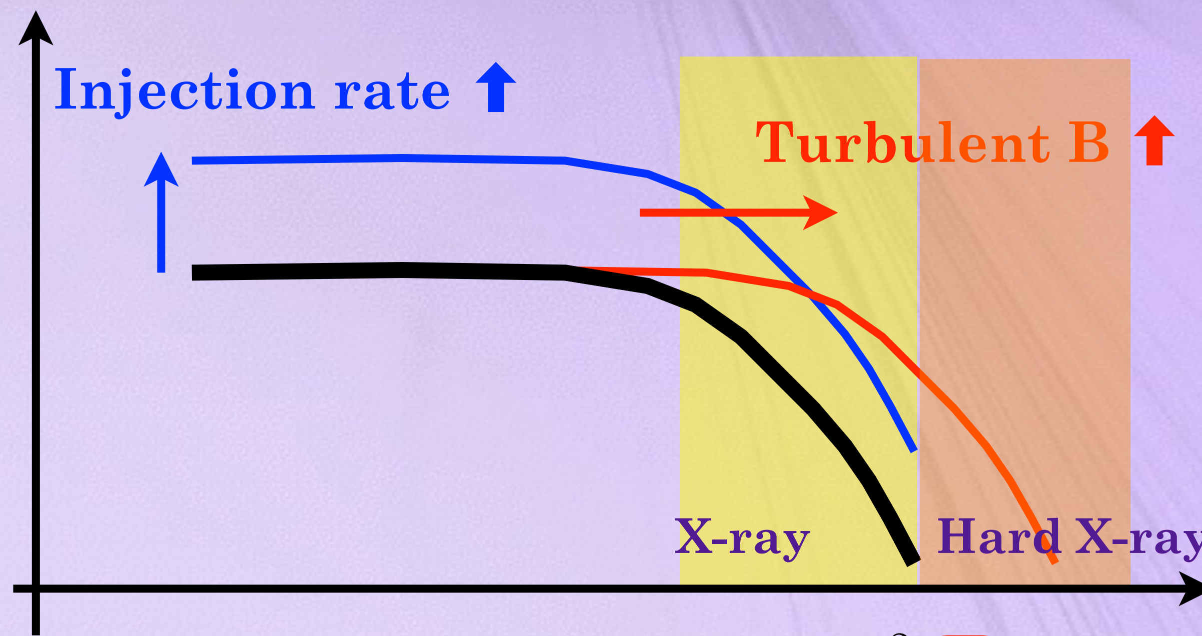

$$\varepsilon_{\rm cutoff} \sim 2 \left(\frac{V}{2000 \ {\rm km \ s^{-1}}} \right)^2 \eta^{-1} \ {\rm keV}$$

Turbulent B-field

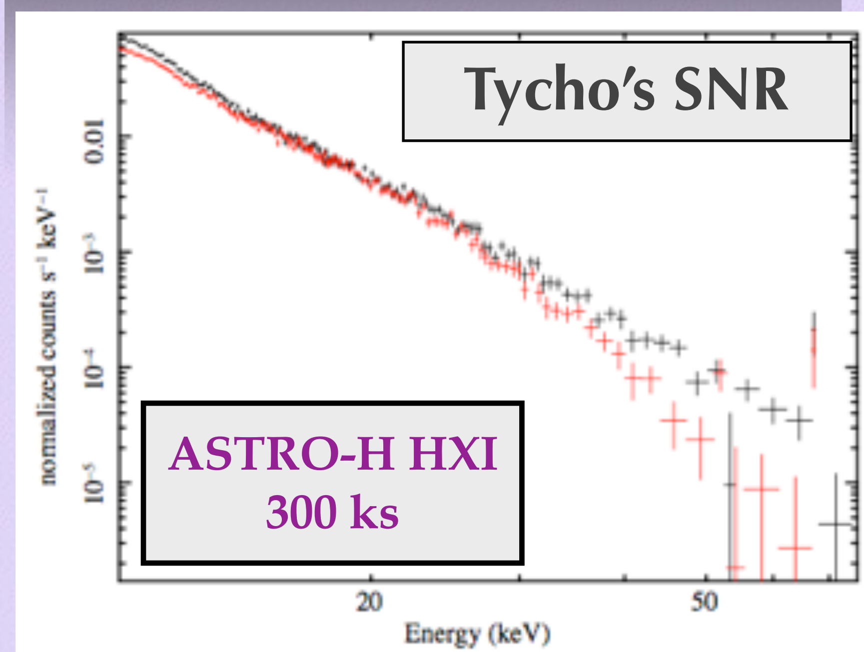

Cutoff of synchrotron X-ray spectrum can test DSA theory

G1.9+0.3: V ~ 14,000 km/s

Cutoff energy > 100 keV can be expected.
ASTRO-H HXI will test this expectation

The Crab Nebula: the only known "PeVatron" (e±)

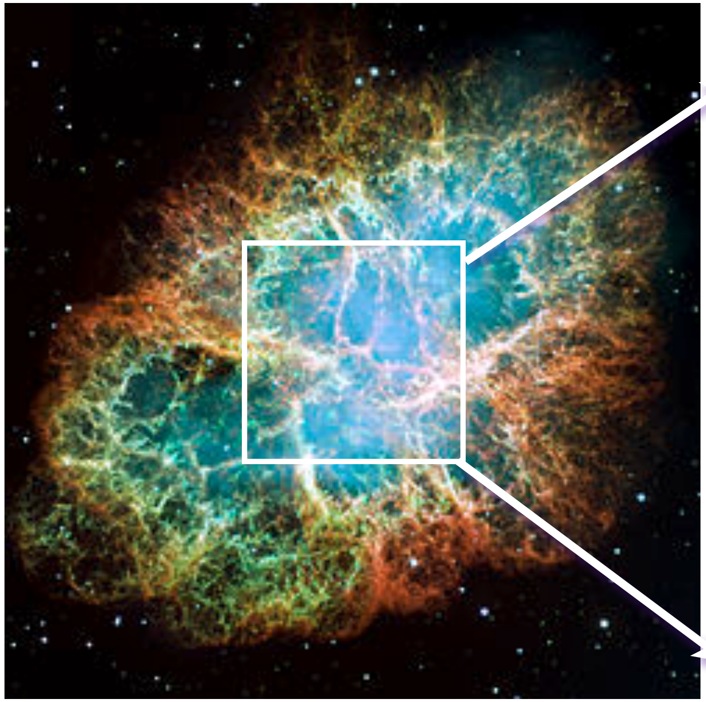

Crab pulsar:
✔ a neutron star
✔ spin period of 33 ms
✔ produced by SN 1054

The Crab Nebula:
a relativistic wind from the Crab pulsar is thermalized at the termination shock, and also power-law particles are generated.

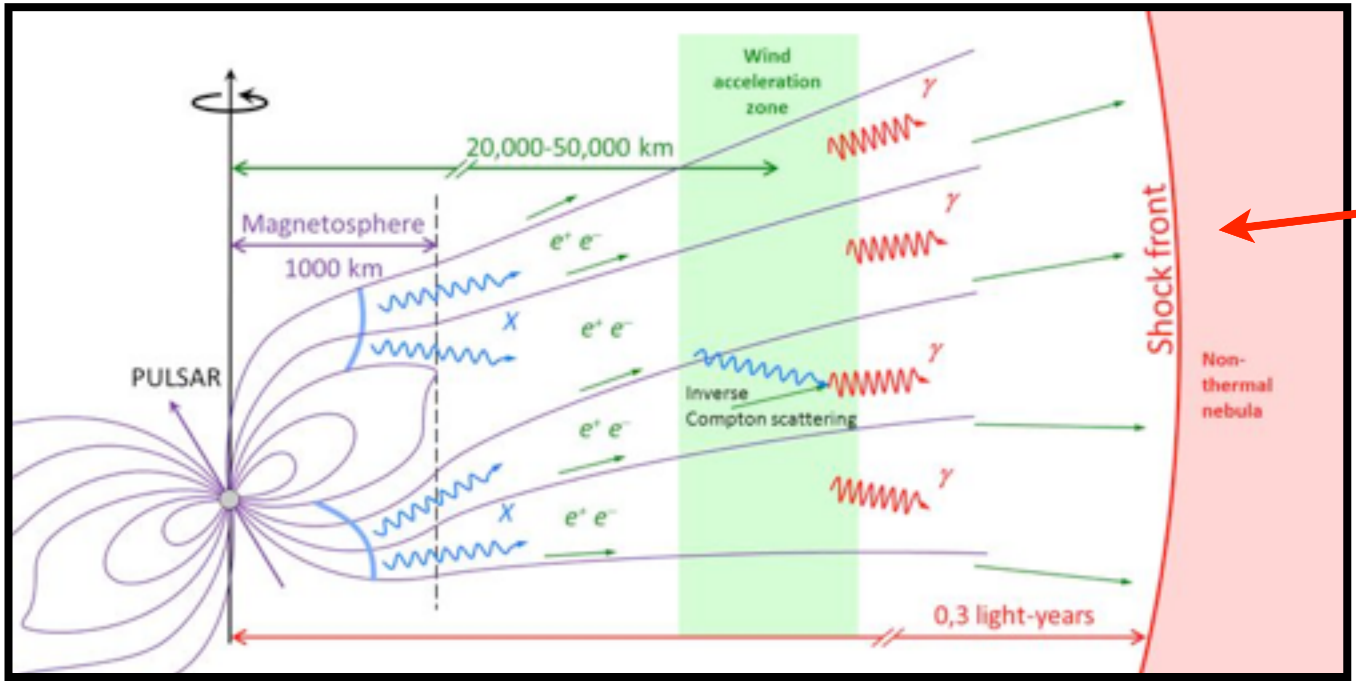

Sites of nebular emission (shocked pulsar wind)

PeV e+/e- in the Crab Nebula

➔ the highest energy particles seen in astronomical objects

The Crab: Full of Surprises

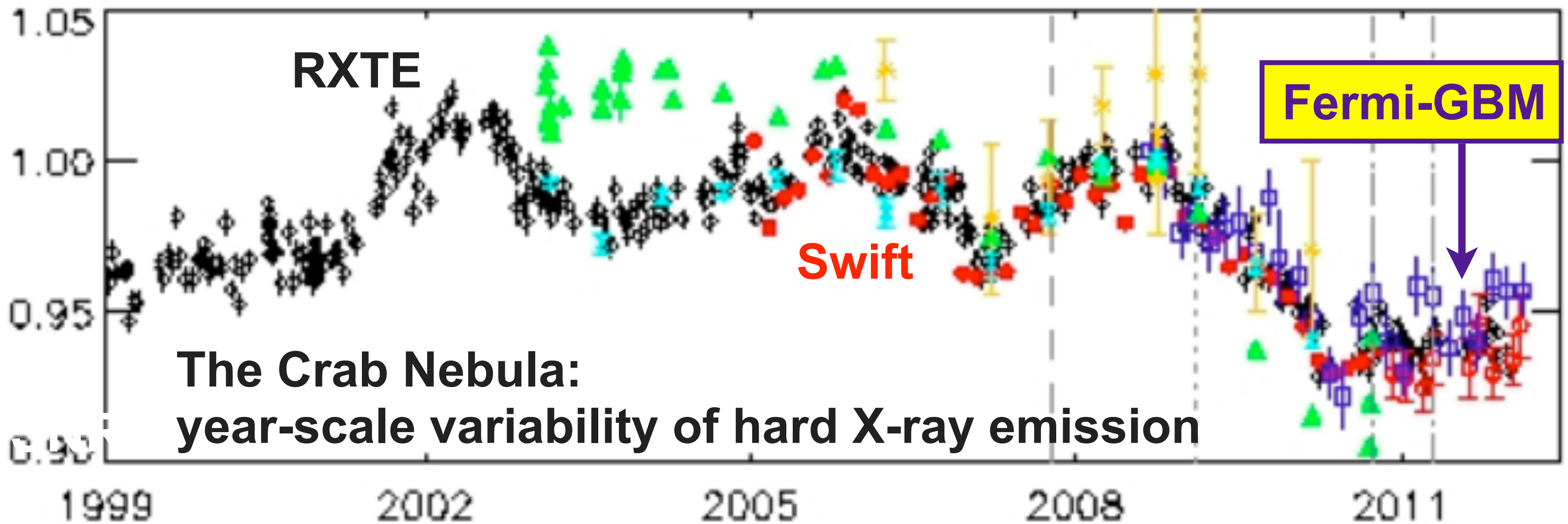

The Crab pulsar: extra TeV emission

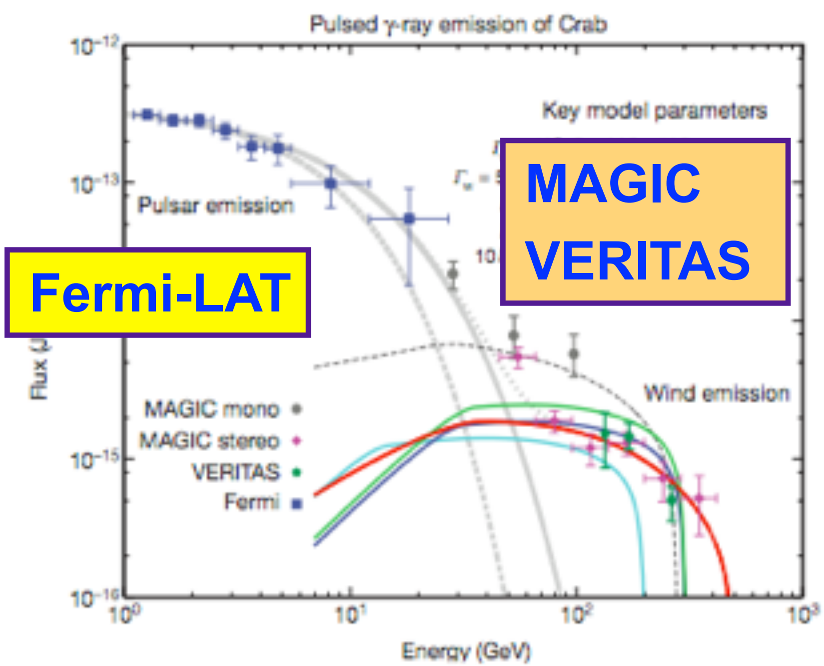

The Crab Nebula: GeV flares

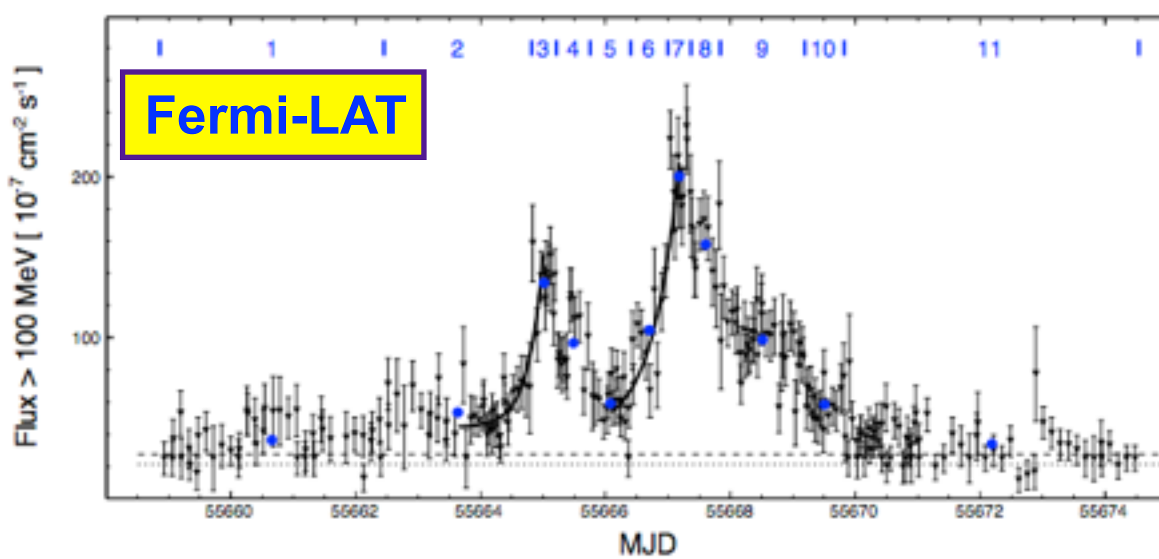

“Crab Flare”

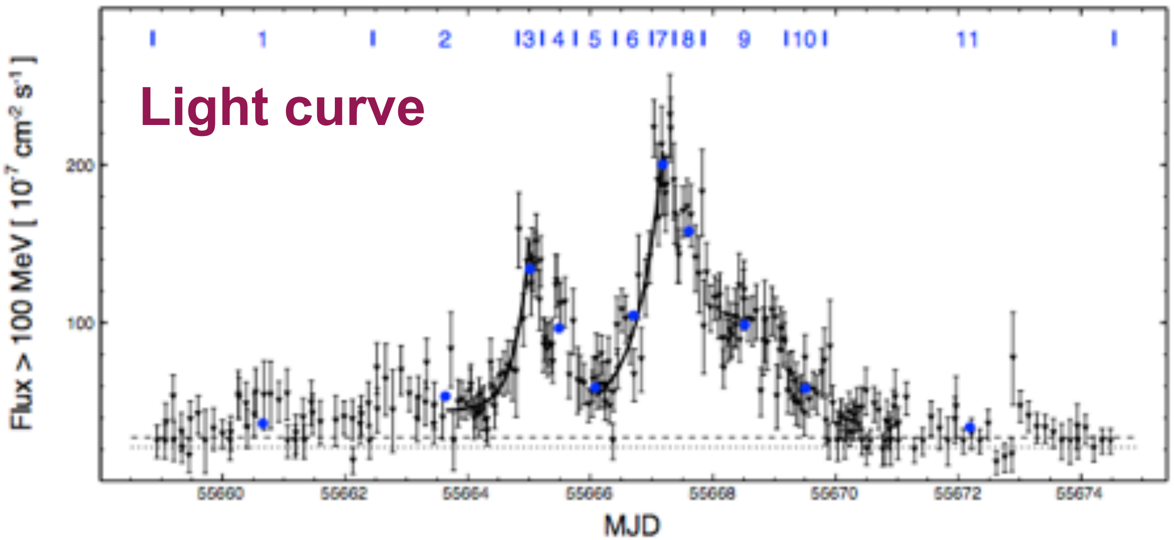
Light curve
1
2
3
4
5
6
7
8
9
10
11
Flux > 100 MeV [10^{-7} cm^{-2} s^{-1}]
200
100
55660
55662
55664
55666
55668
55670
55672
55674
MJD

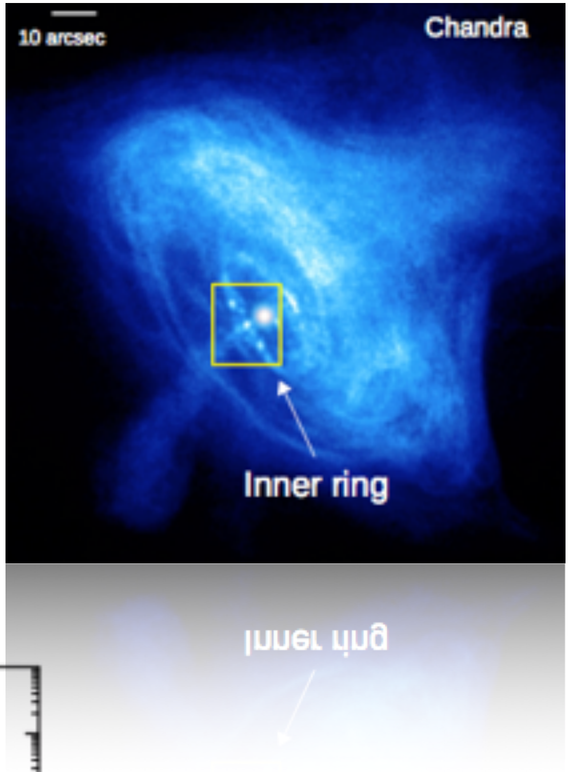
10 arcsec
Chandra
Inner ring

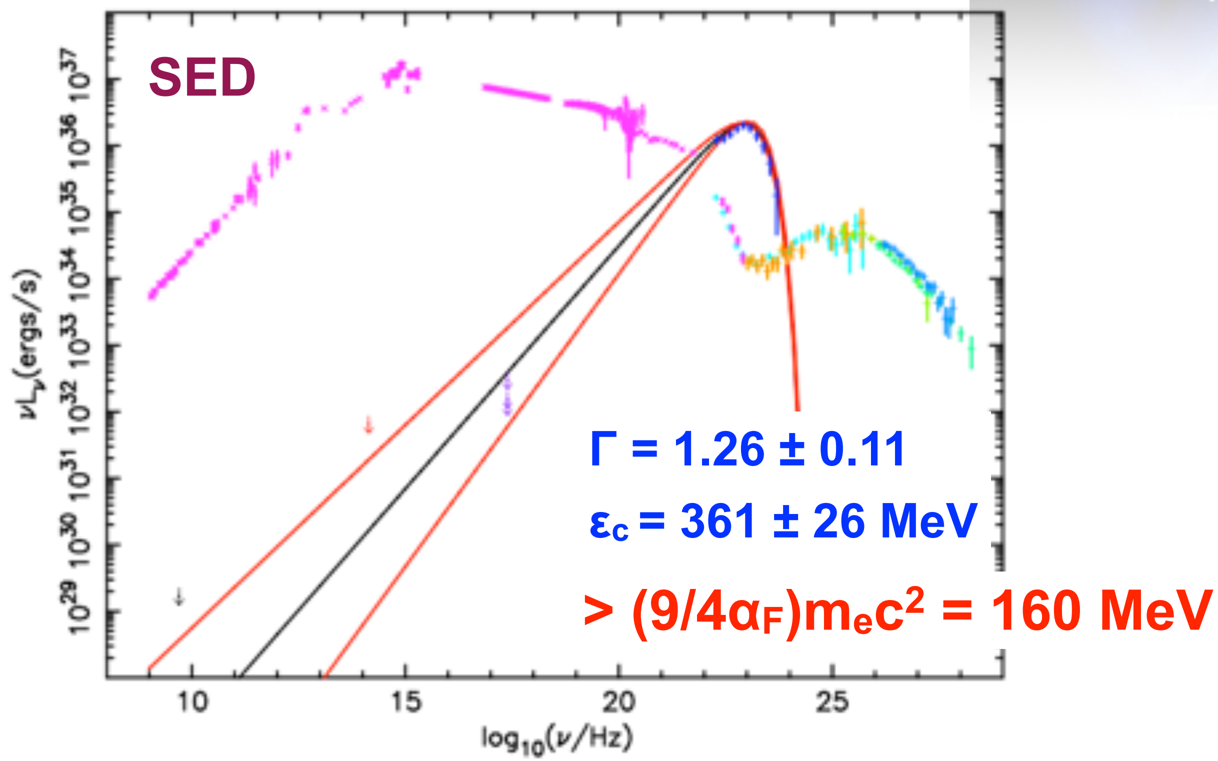
SED
νL_ν(ergs/s)
10^{29} 10^{30} 10^{31} 10^{32} 10^{33} 10^{34} 10^{35} 10^{36} 10^{37}
10
15
20
25
$\log_{10}(\nu/\text{Hz})$
$\Gamma = 1.26 \pm 0.11$
$\varepsilon_c = 361 \pm 26$ MeV
$> (9/4\alpha_F)m_ec^2 = 160$ MeV

The Crab Seen by Fermi-LAT

Average gamma-ray spectra

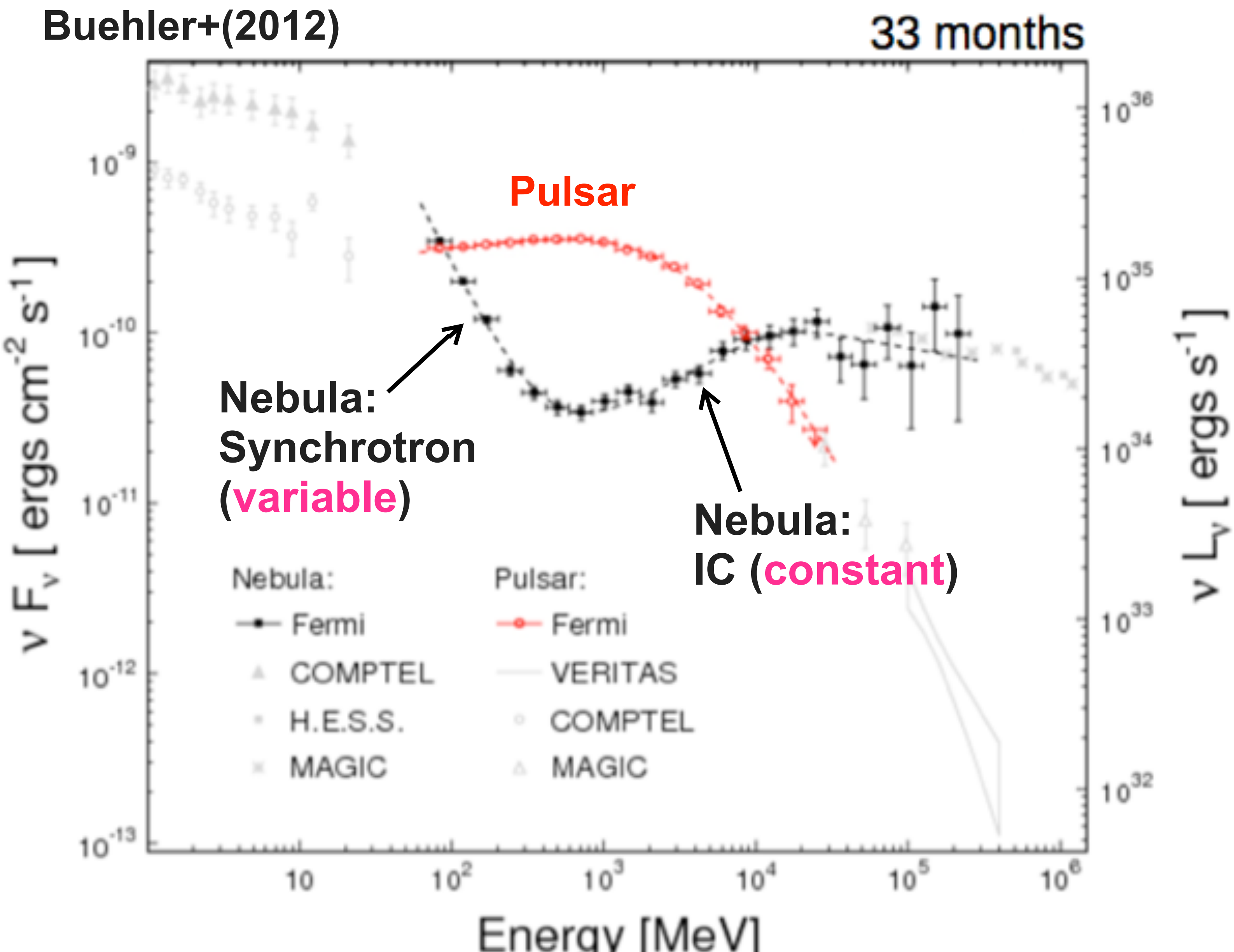

Long Term Lightcurve

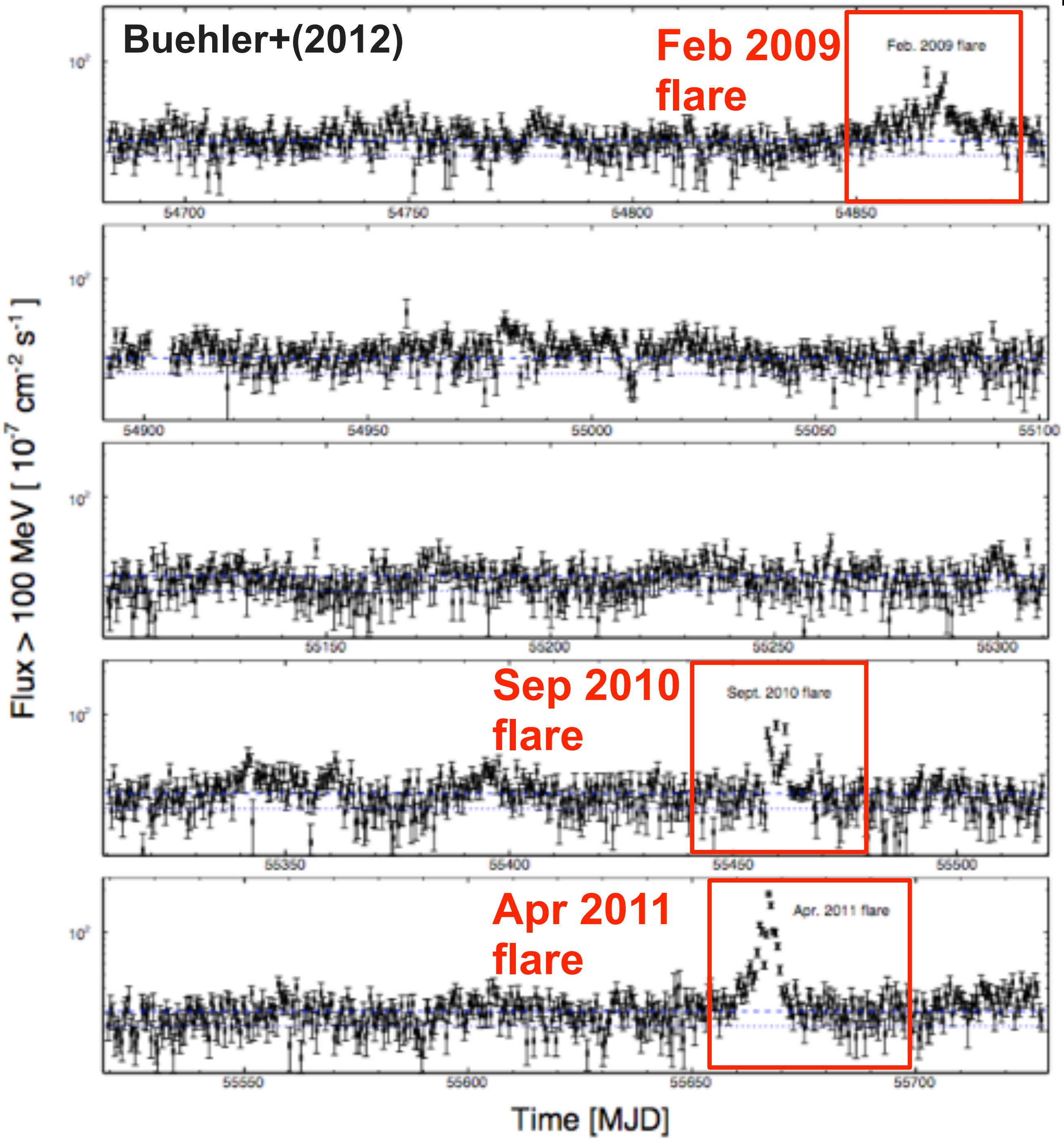

The April 2011 Flare

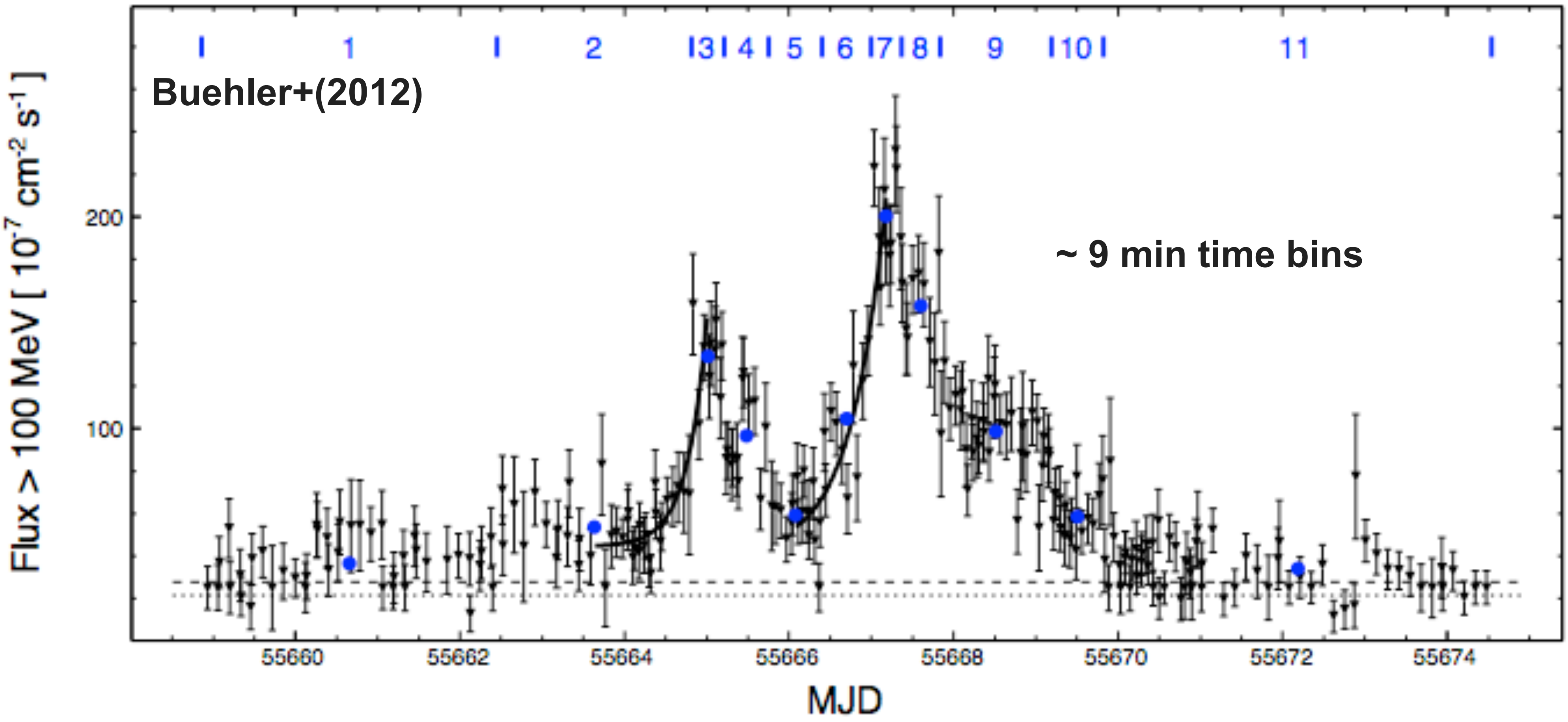

- Synchrotron nebula brightened by a factor of ~30
- Flux doubling time : 4-8 hours
- No change in pulsar flux and phase

The April 2011 Flare: Spectral Evolution

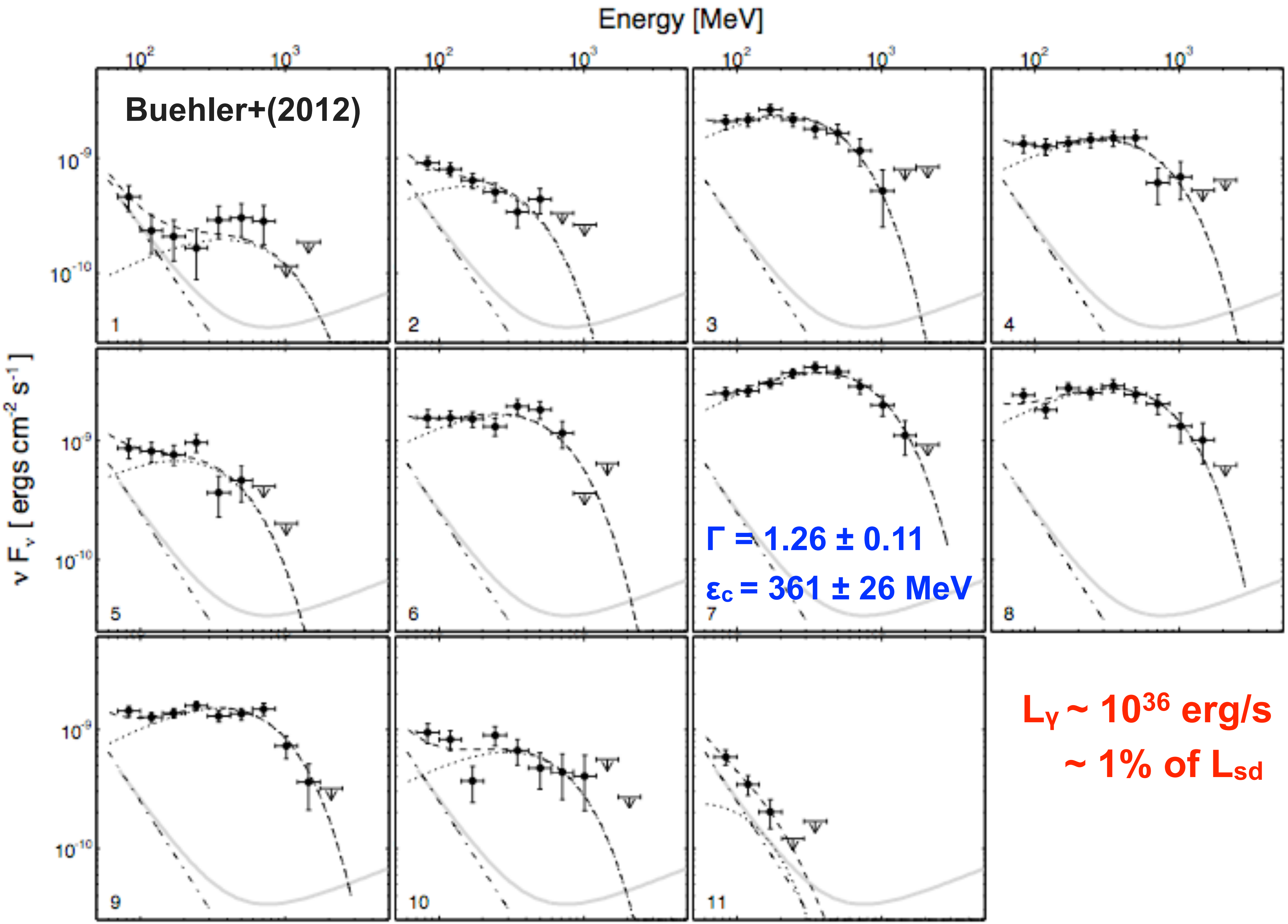

$L_\gamma \sim 10^{36}$ erg/s

$\sim$ 1% of L_{sd}

A New Flare in March 2013

The second strongest flare so far.

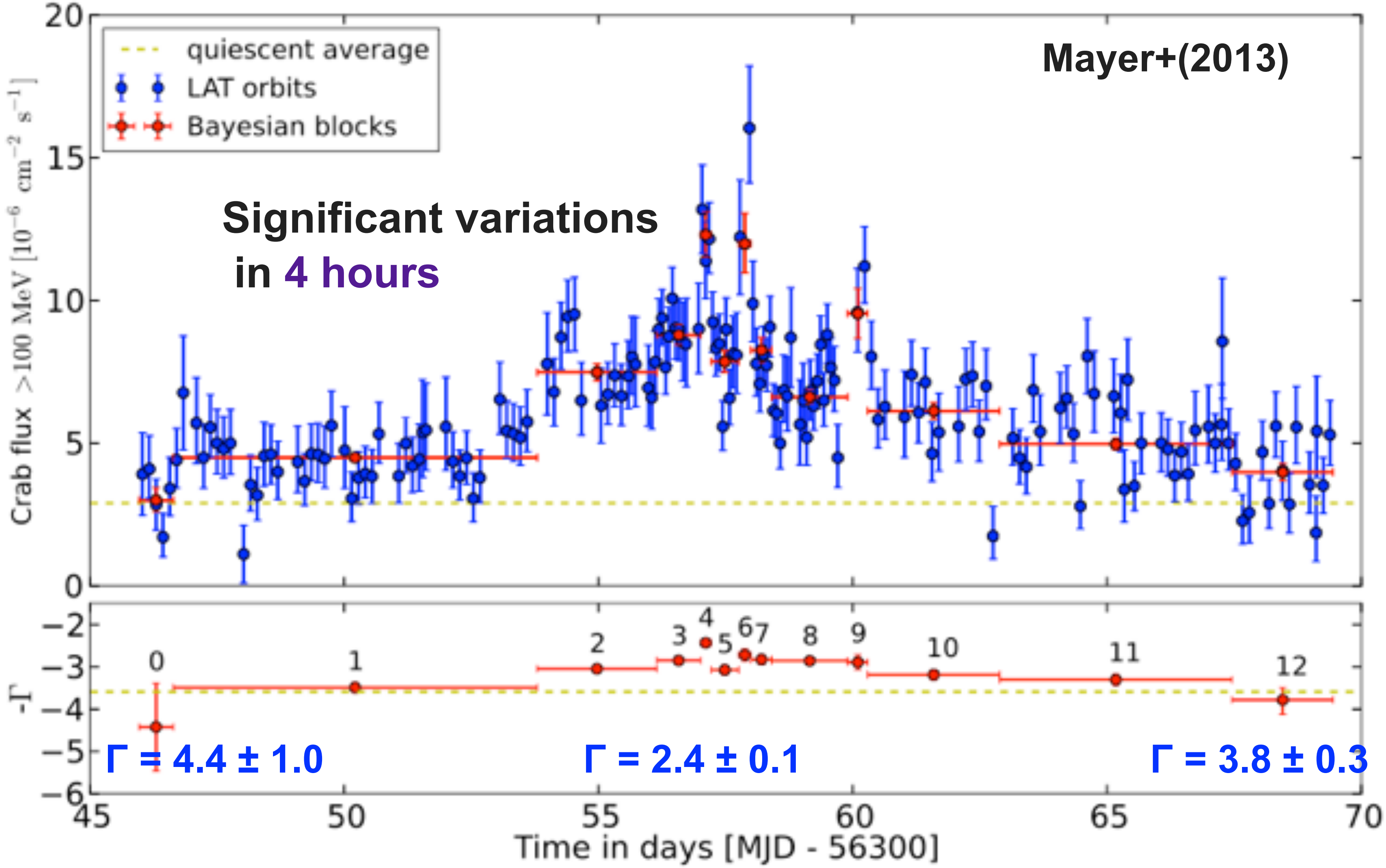

X-ray Images During the Flare

Weisskopf+(2013) inc. Uchiyama

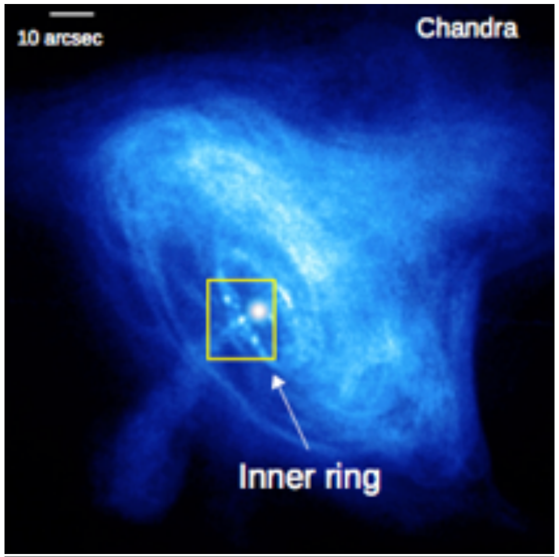

- ✢ Chandra observations during the April 2011 flare
- ✢ No correlated activities in the inner ring region

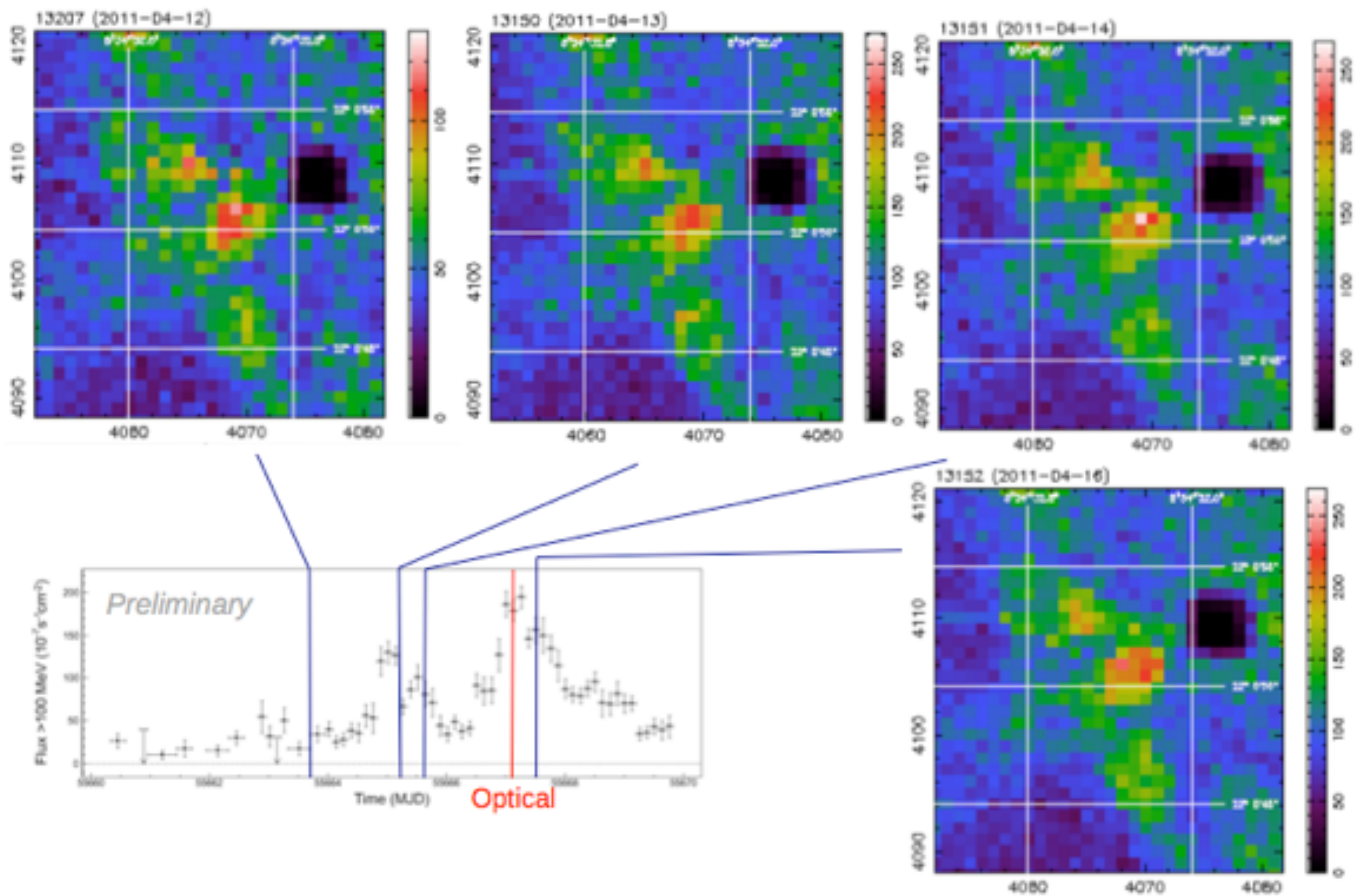

Why Puzzling?

- **Compactness**

  Doubling time t ~ 4-8 hours ➜ Emission region < ct ~ 3×10^{-4} pc

  (Inner ring ~ 0.1 pc)

  Large luminosity (~ 1% of spindown power) from a compact region

- **Spectrum**

  $\Gamma = 1.26 \pm 0.11$: Flare energy is carried by the highest energy electrons

  $\varepsilon_c = 361 \pm 26$ MeV: Appears to violate the radiation reaction limit

  Balance between acceleration (E<B) and synchrotron cooling

  ➜ Cutoff of synchrotron spectrum must be:

  $$\varepsilon_c < (9/4\alpha_F)m_e c^2 = 160\ \text{MeV}$$

At least, relativistic beaming is necessary (δ ~ a few or more)
(But HST/Chandra images show only a mildly relativistic flow of ~0.5c)

Prospect for CTA

Counterpart in the TeV bandpass (IC) would be detectable with CTA

Kohri, Ohira, Ioka (2012)

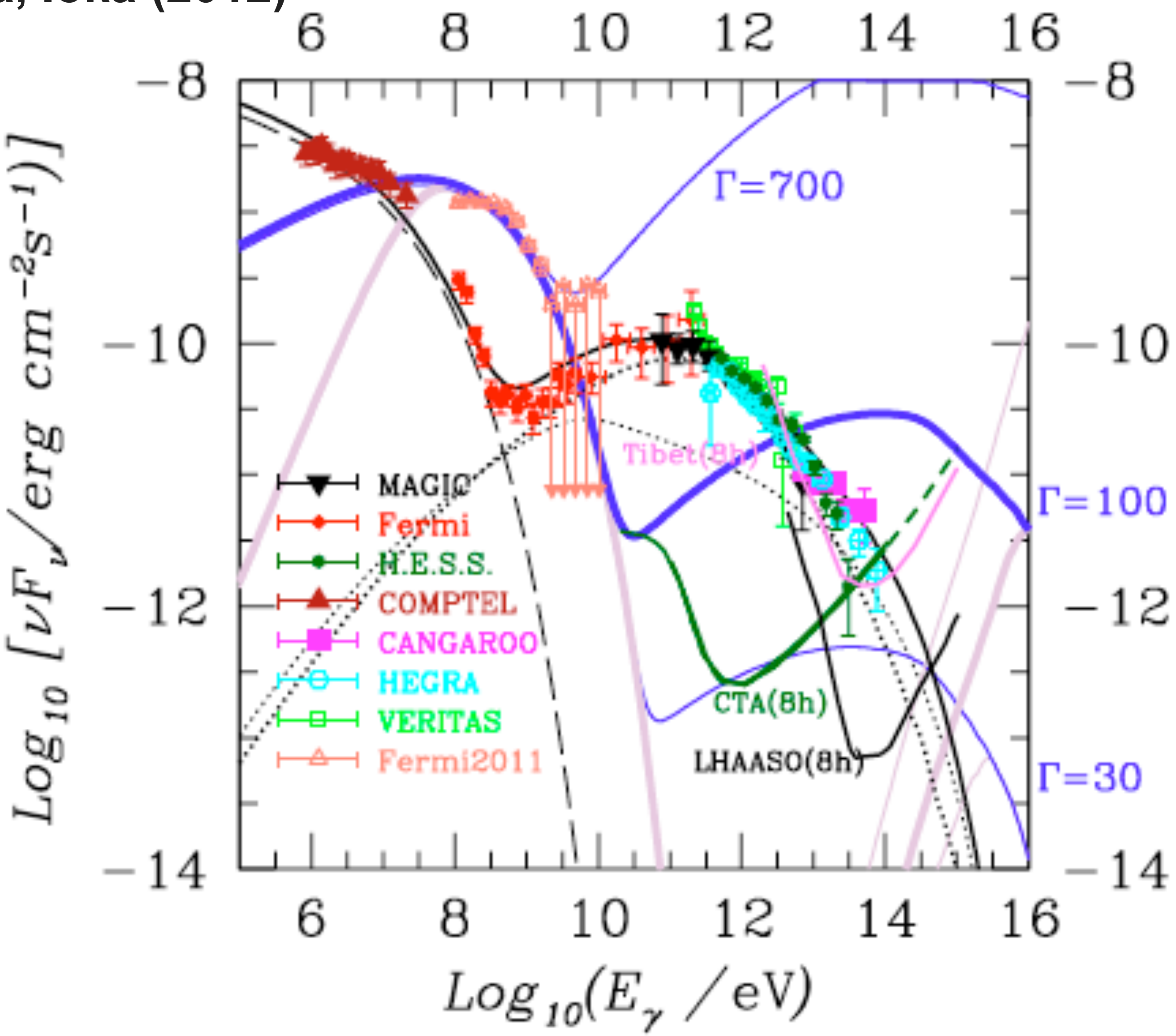

Highly Relativistic Post-shock Flow?

✚ **Komissarov & Lyutikov (2012)**

- **RMHD simulations suggest highly relativistic flows near termination shock (Komissarov & Lyubarsky 04).**
- **High resolution simulations suggest variability of termination shock (Camus+09).**

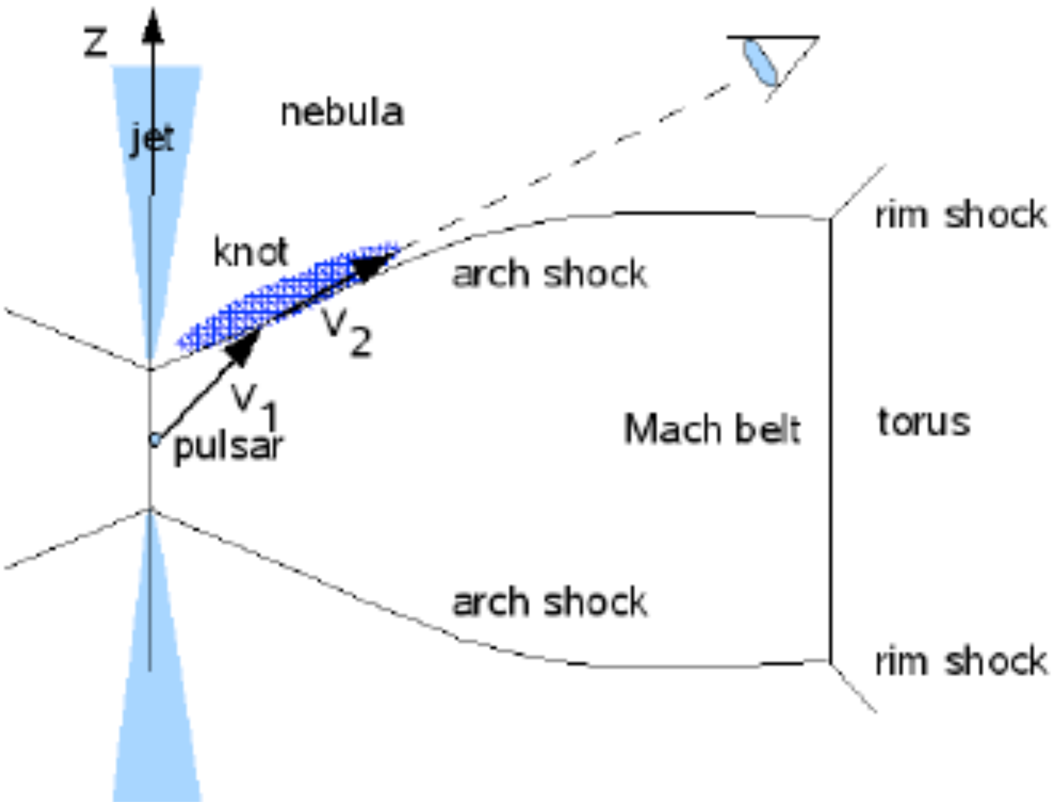

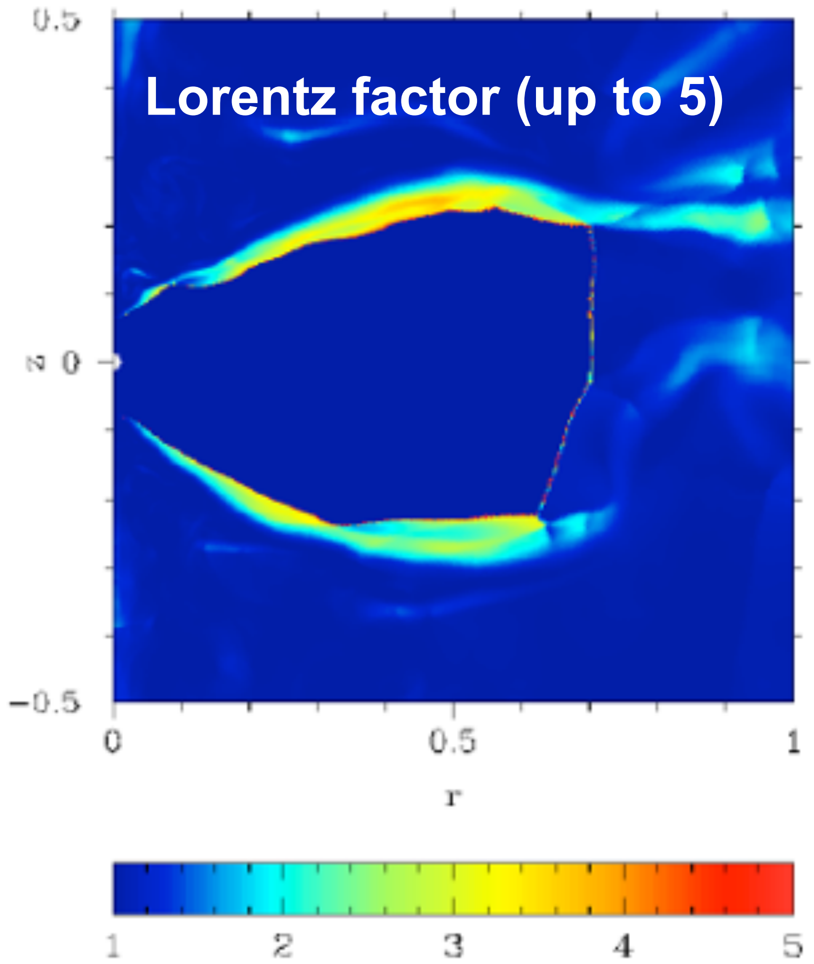

Magnetic Reconnection?

- Cerutti, Uzdensky, & Begelman (2012)

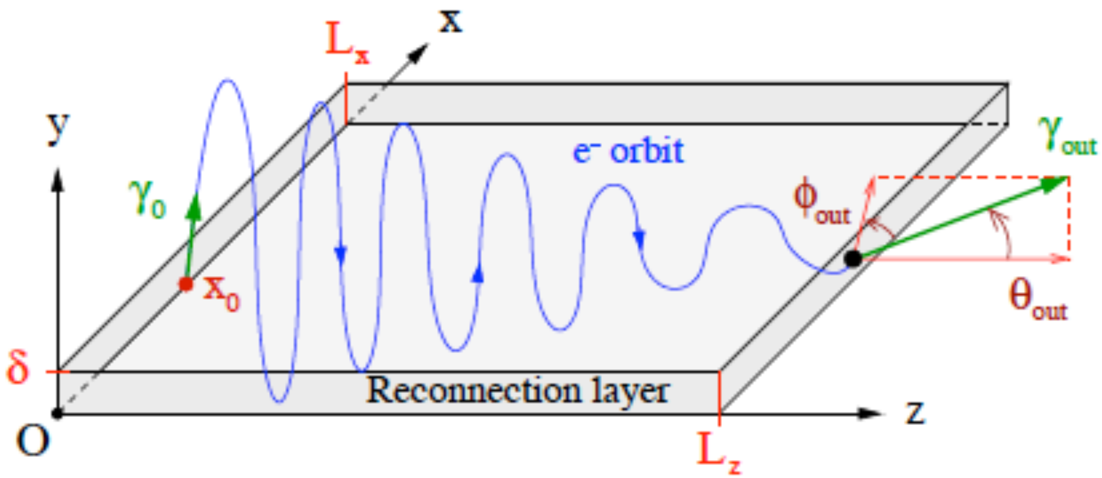

Magnetic reconnection:

- electrons accelerated by reconnection electric field
- focused inside the current layer where B field is small (E>B)
- a beam of PeV electrons

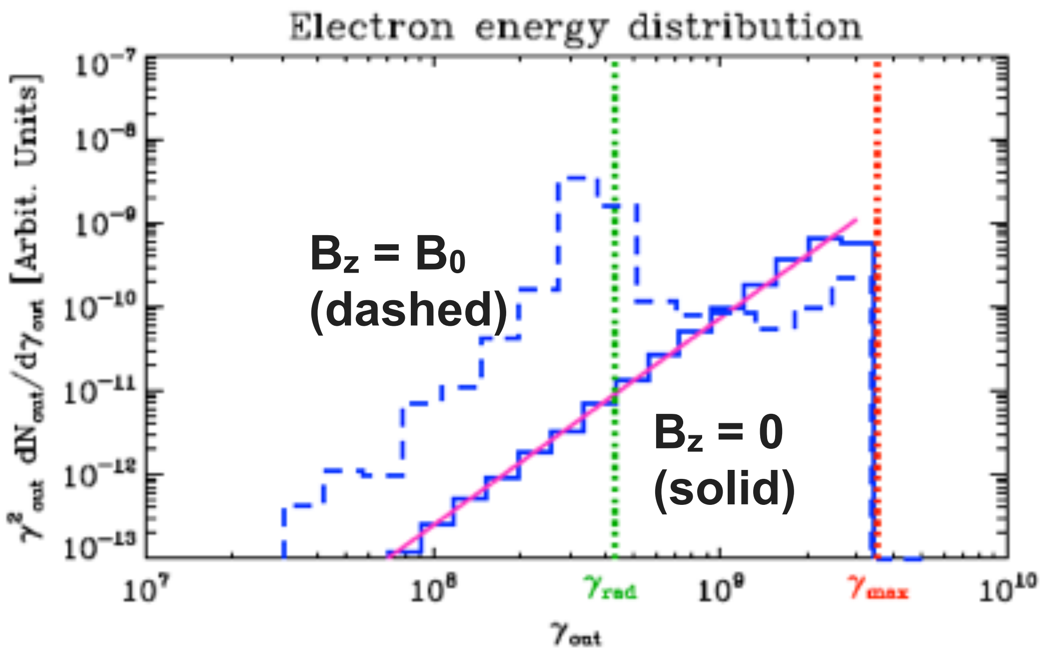

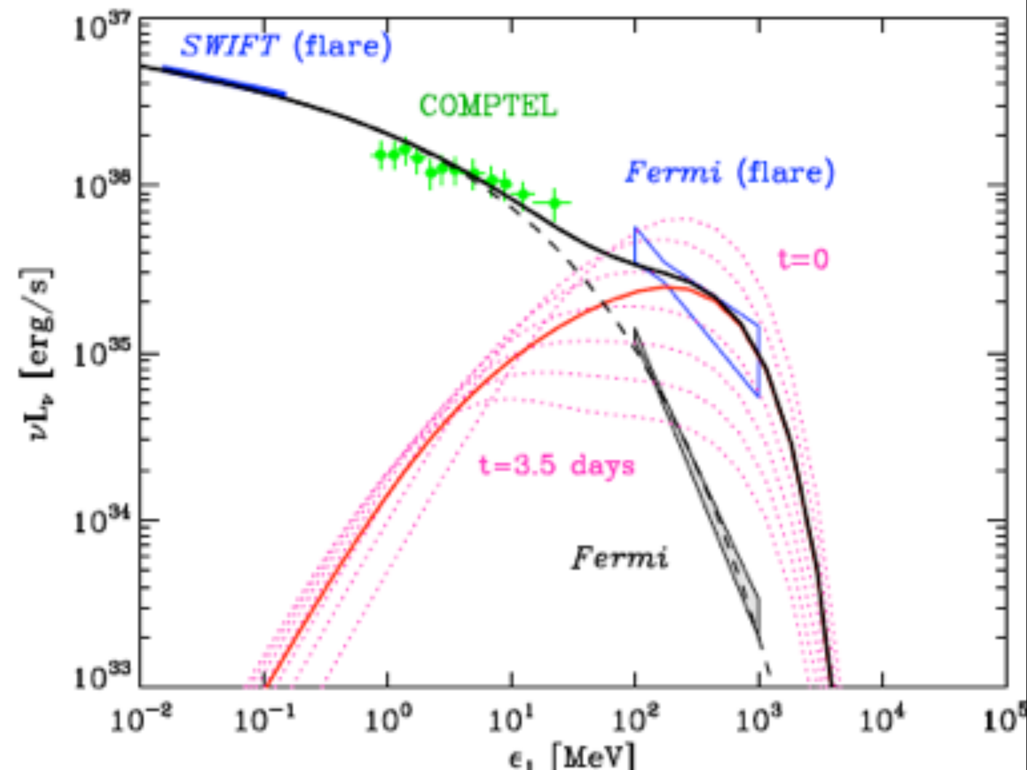

Breakthrough of the Year 2013

Runners Up

Genetic Microsurgery for the Masses

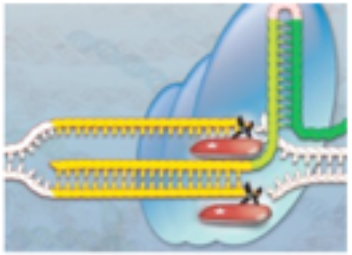

CLARITY Makes It Perfectly Clear

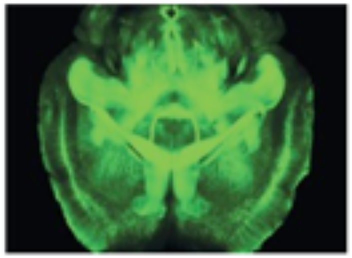

Human Cloning at Last

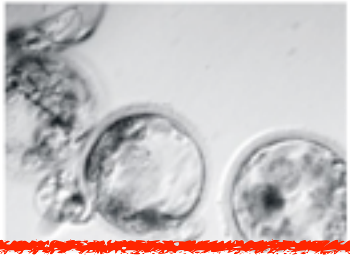

Dishing Up Mini-Organs

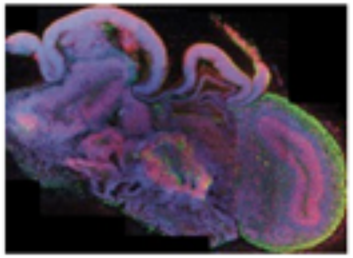

Identification of π^0-decay

Cosmic Particle Accelerators Identified

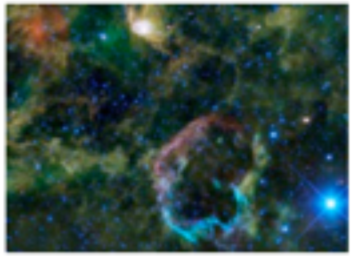

Cosmic Particle Accelerators Identified

Newcomer Juices Up the Race to Harness Sunlight